The zebrafish as a model for tissue regeneration and bone remodelling

Sharif, F.

The Zebrafish as a Model for Tissue Regeneration and Bone Remodelling

Faiza Sharif

To my family, *Ammi, Abbu, Khansa* and *Abdullah*

Faiza Sharif

The Zebrafish as a Model for Tissue Regeneration and Bone Remodelling

Dissertation Leiden University

Cover Figure by Faiza Sharif and Gerda Lamers: A multinucleated osteoclast on Zebrafish scale

Cover design Faiza Sharif and Michael Richardson

The Zebrafish as a Model for Tissue Regeneration and Bone Remodelling

Proefschrift

ter verkrijging van

de graad van Doctor aan de Universiteit Leiden,

op gezag van de Rector Magnificus Prof. Mr. P.F. van der Heijden,

volgens besluit van het College voor Promoties

te verdedigen op Woensdag 12 Oktober 2011

klokke 11:15 uur

door

Faiza Sharif

geboren te Lahore, Pakistan

in 1972

Promotiecommissie

Promotor.	Prof. Dr. Michael K. Richardson
Overig leden.	Prof. Dr. Carel J. ten Cate (Leiden University)
	Prof. Dr. Gert Flik (Radboud University, Nijmegen)
	Prof. Dr. Vincent Everts (University of Amsterdam)
	Prof. Dr. Stefan Schulte-Merker (Hubrecht Institute, Utrecht University and Wageningen University)
	Dr. Annemarie H. Meijer (Leiden University)
	Dr. Danielle L. Champagne (Radboud University, Nijmegen)

This work was supported by the Higher Education Commission of Pakistan and the Smart Mix Programme of the Netherlands Ministry of Economic Affairs and The Netherlands Ministry of Education, Culture and Science.

Contents

Chapter 1

Chapter 1: Introduction

Summary

Bone development and regeneration involves a balance between breakdown and synthesis of bony elements in the skeleton. These two processes are carried out by osteoclasts and osteoblasts, and are influenced by endocrine factors, ageing and drug treatment. The disturbance in this harmonious balance leads to the diseases such as osteoporosis and osteoarthritis. Osteoclasts are of hematopoietic origin while osteoblasts are mesenchymal cells. The process of regeneration allows an organism to regain the function of an organ or structure damaged by injury or disease. Regeneration has interested scientists for centuries. In recent decades this field has gained great attention from biomedical researchers. The main purpose of this interest is to find a way where cells, tissues and structures lost due to mechanical injuries, disease or ageing can be restored through regenerative medicine. Lower animals like urodeles, amphibians and many invertebrates have retained their regenerative capabilities to a remarkable extent throughout evolution, whereas humans and most other vertebrate species seem to have lost much of regenerative abilities for lack of potential mechanism underlying this process. Among other organisms, many species of fish have also retained extensive regenerative capabilities even at adult stages. The zebrafish *Danio rerio*, a teleost, is known to retain regenerative capacity to a great extent in larval and adult stages, and can regenerate heart, notochord, lens, retina and many other organs in addition to scales and fins. Here, I review some key literature concerning bone and tissue regeneration in the vertebrates, with special emphasis on the zebrafish model, and the relevance of these processes to selected diseases in humans.

Zebrafish as an experimental model for developmental biology

Zebrafish or *Danio rerio* is a fresh water teleost fish endemic to the areas of India, Pakistan and Nepal [1]. The total body length at maturity can reach up to 3-4 cm [2]. The presence of black and white stripes on the skin, gives an appearance which is comparable to the zebra hence named as zebrafish [3]. Adult fish has a streamlined laterally compressed body with one dorsal fin, one ventral fin, a notched caudal fin and two pectoral fins which help in swimming. The mouth protrudes outward and dorsally but is devoid of any teeth; however there is a row of pharyngeal teeth in the 5^{th} pharyngeal arch to chew the food [4]. It has long been used as a pet, but its importance as an experimental animal was only realized after initial studies done by Creaser et al [5]. It has a life expectancy of 3-4 yrs. The young fish reach maturity and start to reproduce at about 3 months of age. Zebrafish is known for high fecundity, each female fish can lay around 200-300 eggs per mating, the eggs are fertilized externally. These eggs can be placed in Petri plates until they hatch and reach larval stage where they begin to feed, at around 5 days post fertilization [4].

Zebrafish eggs are highly suitable for developmental research [6]. One of the marvels of nature is that the eggs are virtually transparent and have a very fast rate of development. The most exciting feature for developmental biologists is that all the morphogenetic movements can be easily observed under a dissecting microscope. In contrast to the other experimental animal models the fast rate of development leads to the formation of most of the organs by 38 h post fertilization [3]. The embryos develop inside a transparent external chorion from which they hatch at around 2 -3 dpf and immediately start swimming freely. The embryos at this stage carry all of their nutrients in the form of yolk cells enclosed in a round yolk sac therefore no food is needed for first 5 days. Young larvae at 5 dpf can then be supplied with baby fish food and raised in medium-sized containers with constantly flowing water (for further protocols, see [7]).

The large number of eggs per batch makes it the most appropriate experimental animal for large scale screenings (for examples, see [8,9]) Short generation time that is 3 months, allows the development of transgenic fish

lines. External development of zebrafish embryos without parental care makes it most suitable for behavioural studies [10-13]. Another great advantage of using zebrafish as an experimental model for achieving genetic studies is that the sequence of zebrafish genome is available. In addition, the transparency of embryos and larvae is also ideal for whole mount staining procedures, thus making it possible to analyze in whole mount organism.

The Developmental Biology of Zebrafish Bone

Bone Metabolism

Normal bone development and turnover is a fine balance between bone breakdown (catabolism) and bone formation (anabolism). The chief cells involved in these complementary processes in the vertebrates are as follows [14]:

- **Osteoblasts**, which are derived from the mesenchymal stem cells, and which give rise to bone-depositing osteocytes;
- **Osteoclasts**, derived from mononucleated precursor cells of the haematopoietic lineage, and which fuse to form multinucleated cells.

In human beings, there is a very high rate of bone turnover during childhood, in which formation exceeds resorption. Formation and resorption are in approximate balance in young adulthood, but with ageing there is a net loss of bone [15].

Throughout life, bone Remodelling takes place in foci containing osteoblasts, osteoclasts and their precursors, and the processes are coupled and in the healthy person, are in equilibrium. Both of these cell types arise from distinct cell lineages and maturation processes. Osteoblasts arise from mesenchymal stem cells, while osteoclasts differentiate from hematopoietic monocyte/macrophage precursors [14]. If the balance between the activities of these two cell types is disturbed, this can lead to loss of bone density (osteoporosis) or to increased bone formation (osteopetrosis). Loss of bone is also seen in osteoarthritis and rheumatoid arthritis [16,17].

Studies on osteoclasts in mammals

Osteoclastogenesis is dependent on cytokines, of which two main are RANK-L (receptor activator of nuclear factor-κB ligand) also known as TRANCE (TNF-related activation-inducing cytokine) and MCSF (macrophage colony stimulating factor [18-20]. For a summary of genes involved in bone Remodelling, see Table 1. MCSF (macrophage colony stimulating factor) is considered critical for the proliferation of osteoclast progenitors, whereas RANK L controls the differentiation process directly by activating RANK. It has been established that RANK works in close cooperation with certain other receptors like OSCAR (osteoclast-associated receptor) and TREM 2 (triggering receptor expressed on myeloid cells) [15]. Stimulation of RANK and of the immunoglobulin-like receptors cooperatively phosphorylates ITAM (Immunoreceptor tyrosin based activation motif).

Authors of [21] studied the differentiation of osteoclast precursors into osteoclasts in mice. MCS-F stimulated the proliferation of macrophage precursors and their expression of osteoclast markers (RANK and TRAP; tartarate resistant acid phosphatase) *in vitro*, a macrophage cell line behaved also in this way. During this process the cells changed from spindle-shaped to round (pre-osteoctyes) and finally to multinucleated. The macrophage marker CD14 was simultaneously down regulated. Also down regulated was OPN (osteopontin) which is characteristic of M-CSF dependent cells but this expression weakens after differentiation into pre-osteoclasts. Carbonic anhydrase 2 is expressed in the mature osteoclasts but not in the precursors, its expression is noticed in the cytoplasm and the inner surface of the ruffled border [22]

Studies on osteoclasts in fish

Matrix degradation by osteoclasts is a key process in both normal bone turnover and the bone disease osteoporosis [23]. Osteoclasts are classically described (at least in mammals) as multinucleated giant cells of the myeloid (monocyte-macrophage) lineage [15,24]. They display a characteristic ruffled border where proteases and hydrogen ions are secreted, allowing for bone resorption and formation of ‘resorption pits’ in the bone surface [25]. Osteoclast morphology varies between mammals and teleosts (bony fishes),

and also between different groups of teleosts [24]. In the skeleton of young zebrafish, for example, osteoclast activity is carried out by both mononucleated and multinucleated cells [26]. In fact, there is an ontogenetic progression from mono- towards multinucleated osteoclasts [26]. In juvenile zebrafish, bone resorbing cells in the developing lower jaw are at first mononucleated. In thin skeletal tissues such as the neural arch, mononucleated cells are predominant in adults [26]. In rainbow trout, scale resorption is predominantly carried out by mononucleated osteoclasts [27]. Although in mammals these mononucleated cells are often just regarded as osteoclast precursors, in fish mononucleated osteoclasts are active bone resorbing cells [28,29].

One family of osteoclast proteases are the matrix metalloproteinases (MMPs). They are involved in the breakdown of extracellular matrix by osteoclasts, but also by other cell types like fibroblasts [30]. MMPs are multi-domain enzymes that require zinc as cofactor for proteolytic activity. Extracellular matrix turnover occurs in a wide range of physiological processes, including embryonic development and morphogenesis, bone resorption and tissue regeneration. Moreover, MMP-mediated breakdown of the extracellular matrix has been implicated in disease processes including cartilage destruction in osteoarthritis [31]. The importance of MMPs in bone development is underlined by studies on *mmp-2* and *mmp-9* null mice, which suffer from bone abnormalities, osteoporosis and osteopetrosis respectively [32]. In view of their role in physiological and pathological processes, MMPs are important targets in pharmaceutical research and drug development.

In bone turnover, secreted MMPs participate in the breakdown of collagen, which in turn allows osteoclast attachment [33]. Furthermore, *MMP-9* is associated with osteoclast migration through the collagen matrix [34]. Matrix metalloproteinases may also break down residual collagen left by cathepsin K after the pH rises in the resorption pit [35]. MMP-2 and *MMP-9* (gelatinase A and B, respectively) are particularly active against gelatins (denatured collagens) and intact collagen types I and IV. In the bone of dermal origin, matrix degradation is thought to rely more on MMPs and less on cathepsin K [36]. MMP-2 has also been described to play a crucial role in formation and maintainance of the osteocytic canalicular network whereas MMP-9 is active in early calvarial bone development and in orthodontic tooth movement [37]. Regenerating fins of adult zebrafish express *mmp-2* and regeneration can be

inhibited by the MMP inhibitor GM6001 [38]. More recently, MMPs have also been implicated in angiogenesis and liberation of growth factors [39,40].

TRAP and cathepsin K *in situs* in the newly-hatched medaka (stage 40-44 of [41] show a specific labelling of cells [42]. They found strong scattered expression in the pharyngeal region and teeth. The labelled cells were both mononuclear and multinucleated with typical ruffled borders. Expression of *mmp-9* gene has been studied in different embryonic and adult stages of zebrafish, it is expressed in the myeloid cells [43]

Table 1 Genes expressed by osteoclasts or their precursors

Gene	Expression (any vertebrate)	Ref.	Genbank Accession Number for Zebrafish
TRAP	multinucleated osteoclasts	[21,42,44]	17049327, 10934646, 11148180
CD14	Macrophages (NOT osteoclasts).	[21]	10934646
CD43	pro-osteoclasts	[21]	10934646
Cathepsin K	multinucleated osteoclasts	[21,42,45]	17049327, 10934646, 9028530
RANK/OPGL/TRANCE	Pre osteoclasts	[46-49]	
Oscar	Myeloid cells-Mature DC	[50]	15155468
Calcitonin receptor (ctr)	Inhibits osteoclast activity.	[42,51,52]	17049327, 10704727, 17535751
Carbonic anhydrase II (CAII)	Mature osteoclasts,	[21,22,53]	10934646, 16418777

Mmp-9	Myeloid cells + mono- and multi-nucleated osteoclasts	[21,43] [40,54]	16815100, 10934646,
Vacuolar-type proton ATPase	Pre osteoclasts	[55]	17273786
osteopontin (OPN)	M-CSF dependent bone marrow macrophages	[21]	10934646

Bone turnover and Disease

Parathyroid hormone and menopause

Primary hypothyroidism and hyperthyroidism affects bone turnover. Decreased bone mass and high bone resorption occurs when there is an up-regulation in thyroid hormones and suppression in thyroid stimulating hormone. This effect was observed even in patients with subclinical hyperthyroidism [56].

In women facing menopause, bone turnover is up-regulated with increased activity of osteoclasts and osteoblasts. The net effect of imbalance between bone deposition and resorption is bone loss [57,58] and in most of the cases the primary reason for this imbalance is loss of estrogen. Estrogen deficiency directly or indirectly increases the number of osteoclasts. In a study it is reported that an alternative mean by which TNF alpha modulate post-menopausal osteoporosis may be FSH (follicle stimulating hormone) arising as a powerful inducer of osteoclastic bone resorption [59].

Effects of ageing on bone metabolism

With increasing age the balance between bone deposition by osteoblast and bone resorption by osteoclasts is lost. In childhood there is more bone deposition and less bone resorption, after 20 yrs of age there is a balance between deposition and resorption but later to 25 yrs less deposition and more resorption occurs [15]. As a result of this imbalance there is more bone

resorption, leading to greater incidence of osteoporotic conditions at old age. This weakening of calcified skeleton in elderly population is similar between males and females [58].

Osteoporosis

This group of disorders results in increased fracture risk because of reduced bone mass and poor bone quality [60]. A variety of medical conditions such as diseases or use of certain medications that adversely affect skeletal health leads to secondary osteoporosis. Studies suggest that 20 to 30 % of osteoporotic cases are secondary [61].

There are three main causes of osteoporosis namely ageing, oestrogen deficiency and glucocorticoid use [62,63]. Osteoporosis can be treated by inhibiting resorption using estrogens or bisphosphonates (the latter inhibit osteoclast function) [64]. There is a continuing search for drugs that stimulate bone formation (anabolic agents) or better still, stimulate formation and suppress resorption at the same time. One potential target is Cas-interacting zinc finger protein (CIZ), which inhibits bone formation without affecting resorption. Therefore inhibitors of this gene might be effective therapeutics [60].

Ciz $^{-}/^{-}$ mice have increased bone mass. Calcitonin is also widely accepted as an Osteoclast inhibitor, studies in teleost and mammals suggest that calcitonin suppresses the activity of osteoclasts [51,52].

Glucocorticoid-induced osteoporosis (GIOP) is a major clinical problem given the widespread use of steroids [65]. It is the most common cause of secondary osteoporosis and the association between glucocorticoid use and increased fracture risk is well established. These agents even at low doses, can cause severe reduction in bone formation and can to a lesser extent increase bone resorption [61]. Multiple oral corticosteroid bursts over a period of years can produce a dosage-dependent reduction in bone mineral accretion and increased risk for osteopenia in children with asthma [66].

Osteoporosis also occurs in ageing men but its progress is relatively slower, occurring due to prolonged continuous drop in free serum testosterone. Androgens have a direct effect on the bone cells including osteoclasts [67].

Osteopetrosis

This disease results in a loss of distinction between cortex and trabeculae of the bone. Resorption and skeletal Remodelling are dysfunctional resulting in abnormally shaped bone [68]. The unique feature of this disease is the accumulation of cartilaginous bars surrounded by bone throughout the marrow cavity. This results in a structurally compromised bone explaining the easily breakable bones of osteoporotic patients [69]. Most forms occur due to dysfunctional ion transporting proteins in the osteoclast which results in failure of acidification of the resorptive microenvironment [68].

Pyknodysostosis

Mutation in cathepsin K gene in humans promotes osteoclast dysfunction resulting in a sclerotic bone disease distinct from osteopetrosis. The cathepsin K dysfunction disorder is described by diffuse skeletal sclerosis short stature and distinct cranio-facial abnormalities in addition to the dissolution of terminal phalanges of hands and feet. Pyknodisostotic patients also experience increased fracture risk [70,71].

Silica Nanoparticles for drug delivery

In addition to studying the expression of markers, we also wanted to see whether we could perform functional studies for manipulating cell differentiation. For this purpose, we chose Mesoporous silica nanoparticles (MSNPs) as new drug delivery system (DDS) to deliver osteoclastogenic compounds such as MCSF and RANK-L in zebrafish embryos. These were already under development in our research consortium, and so this provided an interesting opportunity to incorporate them into this study. They have been used for cell culture studies [72], but testing their suitability in zebrafish provided us with an interesting possibility to develop an *in vivo* delivery system. MSNPs are a new DDS the toxicity of which in the zebrafish embryos needs to be studied carefully. The immunotoxicity of MSNPs is not known in zebrafish embryos previously. Therefore in order to use as DDS we needed to carefully determine the toxicity and then use them to deliver compounds into zebrafish embryo model.

Nanoparticles are being synthesized as a next generation of materials used for a variety of applications such as electronic devices, clothes, sunscreens and cosmetics [73]. There is variety of nanomaterials such as metal nanoparticles, nanoshells, Fullerenes, quantum dots, polymer nanoparticles, dendrimer, liposomes [74-84]. In future, nanomaterials may be applied for disease diagnosis and for drug delivery targeted at specific sites for example useful to treat cancer cells [85].

Nanomaterials in Cell culture

Studies of uptake of hydrophobic silica nanoparticles on human breast cancer cells (MCF-7) and rat neural stem cells (NSCs; [72] elucidate the capacity to carry proteins unchanged into the cytosol. *In vitro* studies with HeLa cells has demonstrated the uptake efficiency and uptake mechanism of mesoporous silica nanoparticles (MSNs) can be manipulated by the surface functionalization of nanoparticles [86]. MSNs can be efficiently employed as carriers for intracellular drug delivery in cell cultures [87]. Previous studies have shown that non-phagocytic eukaryotic cells can endocytose latex beads up to 500 nm in size. Particles around 200 nm in size or smaller are taken up with highest efficiency, whereas very little uptake has been observed for particles larger than 1 μm [87].

Toxicity *in vivo* systems

In zebrafish the toxicity assessment of gold and silver nanoparticles shows a higher toxicity of silver compared to gold [88]. The visual inspection of heat map to rank the high content data was ranked for toxicity of nanoparticles as QD1>ZnO.Pt>SiO_2> Ag>AL_2O_3=Au [89]. It is also found that Fullerenes C60 cause oxidative stress in juvenile large mouth bass [90]. Silica nanowires were found to be more toxic as compared to silica nanoparticles in zebrafish embryos when administered in surrounding water [91]. *In vivo* biodistribution and toxicity depends on nanomaterial composition, size surface functionalization and route of exposure [92].

It has been found that toxicity of nanoparticles may vary with size, structure and composition of nanoparticles [93,94]. Mice have also been used for studying nanoparticles biology [95]. Organs that can take up nanostructures in

mice include the spleen, lymph node, and bone marrow [96]. All of these organs contain large concentrations of macrophages, involved in the uptake and metabolism of foreign molecules and particulates [96]. It has been observed that surface-modified nanostructures that are coated with the polymer polyethylene glycol (PEG) are capable of avoiding reticulo-endothelial system uptake [97]. In order to understand the fate and interaction of nanomaterials with the immune cells further studies are needed.

Regeneration in zebrafish

The adult zebrafish as some other teleost fishes possess an ability to regenerate some parts of the body such as heart, liver, fins and scales [2,98]. This ability makes it possible to study various processes involved in regeneration to be useful for regenerative medicine. The purpose is to help understand the mechanisms and establish methods to increase the regenerative capability in humans where it is only found in the form of wound healing.

Osteoclasts on regenerating zebrafish scales

Zebrafish scales have the ability to regenerate quickly when removed from the skin, or damaged by abrasion [99]. Scales can be studied to get a better understanding of the underlying mechanisms of skeletal development, such as matrix formation and degradation, cell differentiation and mineralization [54,99-101].

Elasmoid scales are a component of the dermal skeleton and are composed of a collagen matrix mineralized with hydroxyapatite crystals on the exterior (episquamal) side [102]. Concentric ridges (*circuli*) and grooves (*radii*) radiate from the central *focus* to the edges of the scale giving it the specific form for zebrafish [103]. The scale matrix is synthesized and shaped during ontogeny and regeneration by the scleroblasts [104]. Scleroblasts are subdivided in osteoblasts and osteoclasts, based on their scale forming and resorbing properties, respectively in more recent literature [27].

The external layer is synthesized first, followed by the elasmodine layer which has a similar arrangement to that of mammalian lamellar bone [105,106]. New scale begins to be deposited immediately after the removal of the old one within the scale pocket on the skin [107]. It takes about four weeks to fully

develop the regenerated scale to the original thickness, although there are still some structural differences between the normal and regenerated scales.

Both in mammals and in teleosts, staining of tartarate-resistant acid phosphatase (TRAcP) activity demonstrates bone surfaces that are being actively resorbed or have been resorbed [24]. Indeed, mononuclear and occasional multinuclear osteoclasts, positive for TRAcP but also the osteoclast marker *cathepsin K*, were found on the episquamal side of scales of different fish species [100,108]. Multinucleated osteoclasts resorbing the scale matrix have also been identified by means of electron microscopy in fish [27,107,109].

Adult Zebrafish fin regeneration

Studies have been done to ascertain the process of regeneration in the zebrafish in addition to the generally used regeneration models such as anurans. However, most of the studies are focused on the regeneration of adult tissues in this vertebrate model [2,13,110-118]. The regeneration in the zebrafish caudal fin occurs in two steps; wound healing and blastema formation. Blastema is a tissue critical for appendage regeneration; it consists of proliferative stem cells which lead to the reconstruction of the lost tissue [119,120]. To achieve proper shape, size and structure of a regenerating tissue the blastema is regulated by surrounding influences in teleost species. In adult-amputated zebrafish fins, the blastema develops at the site of each fin ray in turn driving regenerative events [115]. There is some compartmentalization of proliferating and non-proliferating regions in the adult zebrafish regenerating fin tissue. Mesenchymal compartmentalization is found to be critical for regeneration with a role of epidermal influence on the position and size [111,114]. There are eight different cell groups in the regenerating tail of adult zebrafish of which four cell types in the wound epidermis, three cell types in blastema and one is *mmp9* expressing cell type [117].

Caudal fin regeneration in larval zebrafish

It has been previously reported that the molecular mechanisms involving mesenchymal and epithelial cells in the tissue repair are the same in larval and adult fin primordia [121]. Larval fin repair occurs through the formation of blastema and wound epithelium where there are a large number of

proliferative cells present. Cell proliferation leads from the distal to proximal region in embryos as well as adults. It is suggested that neutrophils and macrophages are not deemed essential for regeneration [110]. According to [121] the cells in the regenerates are epidermal or mesodermal.

The normal zebrafish embryonic fin fold extends posteriorly surrounding the dorsal and ventral sides of tail; this morphology is achieved by 28h post fertilisation [121] or between *prim-6* and *prim-16* of [122]. Till 6 dpf the fin is a simple structure composed of epithelial and mesenchymal cells with no cartilage and fin rays differentiated yet. Within three days of amputation the larvae retain the complete form and structure of the lost part of the tail [121].

Glucocorticoids and regeneration

Glucocorticoids (GCs) are the steroid hormones secreted by the adrenal glands under stress conditions, and these hormones are also involved in the regulatory mechanisms of development, bone turnover, cellular apoptosis in general, metabolism, and circadian rhythm regulation [123]. Generally GCs are anti-inflammatory and immuno-suppressive agents widely used clinically to treat autoimmune diseases, allergies, prenatal lung maturation, and transplant rejection [124-126].

The secretion of glucocorticoids is a classic response to stress. It has been found by [127] after reviewing a large data of studies done on the role of glucocorticoids in various mechanisms studied. Depending on physiological endpoint in question glucocorticoid effect falls into different categories with mediating, suppressive or preparative actions. The regulation of actions of GCs is mediated by the glucocorticoid receptor (GR) which belongs to the nuclear receptor superfamily [128]. These genes are known to be highly conserved between species. Zebrafish is known to possess one GR gene. The main endogenous glucocorticoid in rodents is corticosterone while in humans and zebrafish it is cortisol [129] review).

Dexamethasone is a synthetic analogue of the glucocorticoid class of steroid hormones 20 to 30 times more potent than *hydrocortisone* and 4 to 5 times more potent than *Prednisolone* [130-132]. This hormone is commonly used to treat certain inflammatory and autoimmune diseases such as osteoarthritis, to

reduce allergic response, to treat oncologic conditions and high altitude sickness due to neural oedema. Dexamethasone has been found to have some negative effect on wound healing by affecting collagenization, epithelization, and fibroblast content in mice even after single dose of 1 mg/kg [133]. Corticosteroids are known to reduce inflammation, which in turn affects cell migration, proliferation, and angiogenesis [134]. GCs mostly have a suppressive action on the immune and inflammatory response even at basal levels of glucocorticoid concentrations. There is also some evidence of permissive actions of glucocorticoids playing important roles. Therefore it can be assumed that the GCs present already permissively activate the immune response as the first response to a number of stressors, whereas stress induced GCs later suppress increased immune activation later. Corticosteroids are potent drugs that are extensively used for the treatment of inflammatory and autoimmune conditions. Same drugs however are also responsible for causing numerous side effects on many body systems [135].

Genes involved in regeneration of caudal fin

RAR γ

Retinoic acid is a signalling molecule for vertebrate pattern formation both in developing and regenerating tissue [136]. RARγ mRNA is the prominent RAR transcript found in normal regenerating tissue. RARγ is expressed in the distal ends of blastema of regenerating adult fin tissue [112].

Wnt3a

Wnts are secreted glycoprotiens that play an important role in body patterning, cell proliferation, cell differentiation and tumour formation [137]. The function of this protein in body patterning occurs during early embryogenesis. Wnt3a is a ligand shown to activate β-catenin signalling. Wnt3a is a candidate for mediating the function of Wnt /β-catenin signalling during limb regeneration in newt [138]. Wnt 3a has also been shown to have expressed in the fin regenerates in adult zebrafish, found in the regenerating fin epidermis. β-catenin expression thus is most likely important in maintaining fin epidermis and not necessary for regeneration [139]. Wnt signalling plays a role in the maintenance and renewal of stem cells which are cells that help repair the tissue damage [137].

Msxb

Expression of the transcription factor msxb reflects the growth rate of the blastema regulated by cues along proximodistal axis; *msxb* expression may also be required for the higher growth rate of proximal blastema cells [140].

Hoxd11

Transcription factors like *msxb* and *hoxd11* are regeneration-specific in the proximal blastema more than the distal. Mesenchymal cells of the blastema express the genes. It is known that their information on patterning resides in mesenchymal cells rather than the epidermis that covers them [140]. *Msxb* in conjunction with *hoxd11* may be involved in converting positional information into various rates of cell proliferation such that distal blastema grows slower than proximal.

Aims and Scope of this Thesis

This thesis examines the cells, derived from the haematopoietic system, involved in Remodelling and regeneration of various tissues in zebrafish. We hypothesised that precursors for osteoclasts are found in early (5 dpf) embryos. If this hypothesis is proven correct, then it would have the practical benefit of indicating the potential of the zebrafish as an embryonic model for bone Remodelling. As there was no information on any such cells are present in zebrafish embryos that early in development, the first steps were to:

1. Look for the expression of genes known to be expressed in osteoclasts.
2. See whether we could activate expression of these genes with functional studies

In chapter 2 we examined the hypotheses that early zebrafish embryos contain cells expressing osteoclast markers. To do this, we examined the expression patterns of a panel of markers known to be involved in bone Remodelling in other models. To further examine the hypothesis that these cells might be osteoclasts, we examined whether we could activate expression of cathepsin K using vitamin D3 and dexamethasone.

In chapter 3 we activated TRAcP positive cells in zebrafish embryos by injecting MCSF and RANK-L loaded onto Mesoporous Silica Nanoparticles. This was a

further functional test of our hypothesis that cells expressing osteoclasts markers in zebrafish embryos might be osteoclasts.

In chapter 4 we further characterised the cells expressing osteoclast markers by looking at the adult regenerating zebrafish scale model. This was in order to look for similarities between the well-characterised adult osteoclasts and the hypothesised osteoclasts in the embryo.

In chapter 5 we examined whether glucocorticoid exposure in embryonic stages has long lasting effects on wound healing and regeneration. If so, this would support the hypothesis that cells involved in wound healing and regeneration are present in early embryos. Glucocorticoid exposure was used to mimic stress.

Chapter 2: Expression Patterns of Genes Associated with Bone and Tissue Remodelling in Early Zebrafish Embryos

Abstract

Genes involved in bone and tissue Remodelling in the vertebrates include matrix metalloproteinase-9 (*mmp-9*), receptor activator of necrosis factor κ-β (*rank*), *cathepsin K* and tartrate-resistant acid phosphatase (TRAcP). We examine whether these markers are expressed in cells of zebrafish of 1-5 days post fertilization. We also examine adult scales, which are known to contain mature osteoclasts, for comparison. *In situ* hybridisation, histochemistry and serial plastic and paraffin sectioning was used to analyse marker expression. We found that *mmp-9* mRNA, TRAcP enzyme and *cathepsin K* GFP protein were expressed in haematopoietic tissues and in the cells scattered sparsely in the embryo. *Cathepsin K* and *rank* mRNA were both expressed in the branchial skeleton and developing pectoral fin. In these skeletal structures, histology showed that the expressing cells were located around the developing cartilage elements, in the parachondral tissue. In a transgenic zebrafish line with GFP coupled to *cathepsin K* promoter, *cathepsin K* expressing cells were found around pharyngeal skeletal elements. We exposed prim-6 zebrafish embryos to a mixture of 1μM dexamethasone (DEX) and 1μM Vitamin D3. These compounds, which are known to trigger osteoclastogenensis in cell cultures, led to an increase in intensity of *cathepsin K* GFP expression around the skeletal elements as well as in haematopoietic tissue. Our findings suggest that cells expressing a range of osteoclast markers are present in early larvae. If this is confirmed, it could lead to establishing a zebrafish embryonic model for studying bone biology and disease.

Introduction

Bone and tissue Remodelling are normal processes in adult animals, and in developing embryos. The genes involved include enzymes that break down extracellular components, and cell signalling molecules involved in the activation of specialised cells involved in Remodelling [15]. There are two different kinds of cells associated with bone Remodelling, namely osteoclasts and osteoblasts which work in harmony in a normal healthy system [15]. Any irregularity or abnormality in the Remodelling process leads to certain pathological conditions such as osteoporosis [141].

In some previous studies, mature osteoclasts have only been detected in developing zebrafish after 20 days post fertilization (dpf) [26]. These cells are initially mononucleated, although multinucleated osteoclasts are also present in the adult zebrafish [26]. A recent review [142] has shown that the bone of zebrafish is osteocytic or cellular as opposed to the bone of most of the other advanced teleost fishes which are acellular or anosteocytic. Furthermore, those authors concluded that the osteocytes of zebrafish are mesenchymal analogues of the osteoblasts of mammals. The multinucleated osteoclasts of zebrafish display similar features to that of mammalian multinucleated osteoclasts, for example formation of Howship's lacunae and staining positive for TRAcP (tartarate resistant acid phosphatase) enzyme [26]. The presence of two types of active osteoclasts (mono- and multi-nucleated) is not restricted to zebrafish but is common for many other teleost species such as Goldfish (*Carassius auratus*) and Carp (*Cyprinus carpio*).

Resorption by large multinucleated cells is lacunar, whereas resporption by mononucleated cells is shallow and non-lacunar in many teleost species [143,144]. Therefore evidence from humans and other mammalians as well as teleosts suggests that a significant number of active osteoclasts are mononucleated [142,143]. In addition to a number of similarities with human and mammalian bone resorption there are differences in the regulation of mammalian to fish osteoclasts. The calcium homeostasis is based on the gills which are the target organs for calcitonin function and the site of osteoclast origin in teleost fish is not the bone marrow [145], therefore it is considered that osteoclasts are formed in the head kidney and spleen [99,146].

Two molecules which are essential for initiating osteoclastogenesis are macrophage colony-stimulating factor (M-CSF) and receptor for activation of nuclear factor kappa B (NF-κB) RANK ligand (RANK-L). Both of these are expressed by stromal cells related to osteoblasts. RANK is itself expressed on osteoclast precursors [147]. Cathepsin K, *MMP-9*, carbonic anhydrase 2 and calcitonin receptor are expressed strongly in multinucleated osteoclasts and weakly in pre-osteoclasts [21].

Another important enzyme in this context is tartrate resistant acid phosphatase (TRAcP) which is expressed in activated murine and teleost osteoclasts [26]. TRAcP is involved in hydrolysis of various substrates including components of bone matrix [148,149]. Increased levels of TRAcP activity may be detected in clinical disorders involving bone lysis, such as osteoporosis; and also in osteoarthritis and rheumatoid arthritis [150,151].Loss of function studies in mice reveal an important role for TRAcP in skeletogenesis [148]. As is the case with the archetypal multinucleated mammalian osteoclasts, the mono- and multinucleated osteoclasts of teleosts secrete TRAcP at the site of active bone resorption [28,144,152,153]. Thus TRAcP-staining can be specific for osteoclastic bone resorption (and also for sites where osteoclasts were previously active) [26,28,143]. Ballanti et al., [154] regard expression of this marker as one of the best ways to identify osteoclastic cells.

RANK (also known as TNFRSF11A, TRANCE-R) is a member of TNF receptor super family. Together with its ligand, the TNF-family molecule RANK-L (TRANCE, or osteoclast differentiation factor, ODF) it is a key regulator of bone Remodelling, and is essential for the development and activation of osteoclasts [46]. RANK is expressed by osteoclast progenitors, mature osteoclasts, chondrocytes and mammary gland epithelial cells [47,48]. Mice with a genetic mutation of RANK have a complete block in osteoclast development, but after the administration of RANK the osteoclasts develop normally in those mice [49]. It is therefore established that the RANK-L expressed by osteoblasts and its receptor RANK expressed in osteoclast precursors are essential for osteoclastogenesis.

Cathepsin K a cysteine protease expressed by osteoclasts and synovial fibroblasts is responsible for removing the organic matrix, mainly fibrilar type-1 collagen, and solubilisation of the inorganic component (hydroxyapatite) [155].

Cathepsin K is released as a pro-enzyme in the resorption pit having an acidic pH. Inhibition of cathepsin K by specific inhibitors results in the accumulation of undigested collagen fibrils in lysosomes within osteoclasts [155]. Cathepsin K expression is elevated in the synovium of rheumatoid arthritis patients [156]. Expression of cathepsin K is also localized within a range of cells at the site of cartilage erosion in rheumatoid arthritis [156,157].

Members of the matrix metalloproteinase (MMP) family of genes are important for the Remodelling of the extracellular matrix (ECM) in a number of normal biological processes such as embryonic development, morphogenesis, reproduction, tissue resorption and Remodelling [158]. They also perform the same function, i.e. ECM Remodelling in some pathological processes, including cancer metastasis, and rheumatoid arthritis. Finally, MMPs are present in some snake venoms, where they may be involved in lysis of tissue in the prey [159,160].

It is important to understand the processes underlying the Remodelling process, since disease can arise if these are dysregulated. Therefore, as a step towards establishing a zebrafish model for bone diseases, we have characterized the expression of panel of osteoclast-associated markers in early stages of zebrafish development. Early stages are particularly desirable for establishing a model because they are free from the legal restrictions that apply to the use of adults, and are therefore more suited to high throughput assays.

Experimental procedures

Animals

Danio rerio (zebrafish) was used as the animal model for expression profiling of selected genes and proteins. All experimental procedures were conducted in accordance with the Netherlands Experiments on Animals Act that serves as the implementation of" Guidelines on the protection of experimental animals" by the Council of Europe (1986), Directive 86/609/EC, and were performed only after a positive recommendation of the Animal Experiments Committee had been issued to the licensee. Spawning of *Danio rerio* took place at 26^{o}C in aerated 5 litre tanks, in a 10h: 14h light: dark cycle. In each mating setup, two

females and one male fish were placed together. The eggs are usually laid after first light in the morning. They were collected within the first hour, sorted and distributed in Petri dishes, filled with egg water (14 gm 'Instant Ocean®' salt in 100 ml of demi water).

The eggs were cleaned and transferred to 9cm Petri dishes at a concentration of 60 eggs per dish. They were maintained at 28°C in atmospheric air in a climate cell, also with a 10h: 14h light: dark cycle. The Petri dishes were checked 4 h and 8 h for dead and unfertilized eggs which were removed and discarded. After continued incubation in the Petri dishes at 28°C embryos were harvested each morning from day 1 to day 5 and fixed as follows. Eggs were immersed in 4% buffered paraformaldehyde (PFA) at 4°C overnight and then dehydrated in an ascending series of Methanol staring from 25% to 100% and finally stored at -20°C in 100% methanol. One and two day old embryos were dechorionated before fixation.

Cloning of genes and synthesis of probe

The NCBI genbank was searched for homologous sequences with the Blast X algorithm using zebrafish query. Only for cathepsin K (Goldfish, *Carassius auratus*, AB236968) and *MMP-9* (Common carp, *Cyprinus carpio*, AB057407) did we find similar enough sequences for our goal and aligned them with their zebrafish counter parts. These alignments were used to design PCR primers based on conserved regions. The other primers were designed only using, mostly multiple, Zebrafish sequences. Primers are shown in Table 2

Table 2 Nucleotide sequence of primers used for PCR

Primer	Nucleotide sequence 5`-3`	Position
Receptor activator of necrosis factor Kappa B		
RANK F1	TGGCGGAAGGAAAGATTCCTC	157
RANK F2	TGTGGCTCTGACCGCAGTCC	243
RANK R1	CGCAGTCCGGCTGACTCTG	1071
RANK R2	CTGGGACTTTGCTGCAGTAGATGC	1060

Cathepsin K		
CTS K F1	GATGAGGCTTGGGAGAGCTGGAA	180
CTS K F2	GACGATTTGGGAGAAGAACATGCTG	256
CTS K R1	TTTCGGTTACGAGCCATCAGGAC	1013
CTS K R2	CCCTTCTTTCCCCACTCTTCACC	1063
Matrix metalloproteinase 9		
MMP 9 F1	TTCGTGACGTTTCCTGGAGATGTG	207
MMP 9 F2	CACAGCTAGCGGATGAGTATCTGAAGC	253
MMP 9 R1	TGGCTCTCCTTCTGAGTTTCCACC	1120
MMP 9 R2	AATGGAAAATGGCATGGCTCTCC	1135

The PCR parameters consisted of 5 min of denaturation, followed by 40 cycles of denaturation 95^{o} C, 10 sec, annealing (10 sec), and extension 60 second ending with 10 min of extension at 72^{o}C. The PCR products chosen for cloning had the following primer combinations: CTSK F1 & R2, *MMP-9* F2 & R2 and RANK F2 & R2.The PCR products were cleaned using Wizard SV Gel and PCR Cleanup system (Promega: Leiden, the Netherlands).

The ligation, cloning and transformation of plasmids in competent cells were done with the TOPOTA PCRII kit from Invitrogen (Breda, the Netherlands). White colonies of transformed cells were grown and checked by PCR. Samples were then sent for sequencing to Macrogen. All the sequence analysis showed a strong homology with the reference sequences. Linearization of template was done with restriction enzymes XbaI, XhoI, HindIII or BamHI, depending on the direction of the gene and potential restriction sites present in the product, and cleaned with Wizard SV Promega columns. T7 or SP6 RNA-polymerases (Roche) were used to synthesis the digoxigenin labelled RNA probes. The probes were

stored at -20^{o}C. Also sense probes were prepared for all of the genes, and used as negative control in *in situ* hybridization (ISH). The genbank accession numbers of our PCR products are shown in Table 3.

Table 3 Genbank accession numbers of the genes cloned and used for *in situ* hybridization in this study.

Gene	Genbank accession number
MMP-9	HM239640
CTS-K	HM239643
CTS-K-1b	HM239644
Rank	HM239645
TRACP	HM239646

In Situ Hybridization (ISH)

Fixed and dehydrated embryos (see above) were rehydrated from methanol by passing through descending concentration of methanol, namely 75%, 50%, and 25% methanol. They were then washed twice in 1x phosphate buffered saline (PBS) with 0.2% Tween 20 (PBST) for 10 min each. In some cases, embryos of 2-5 dpf were then bleached at room temperature with hydrogen peroxide until pigmentation had completely disappeared (10 to 12 min). One day old embryos were found to be too delicate for bleaching. Then they were washed twice in PBST for 5 min. Embryos were treated with Proteinase-K (10 µmg/ml) for incubation time that was varied according to the stage 1 dpf 10 min, 2 dpf 15 min 3 dpf 20 min 4 and 5 dpf 40 min. Further processing of embryos was conducted, with minor modifications, according to Xu Q and D.G.Wilkinson [161].

Adult fish scales

We fixated adult zebrafish skin with scales in 4% PFA at 4°C overnight and stored them in 100% methanol after dehydration. *In situ* hybridization was carried out as described above for embryos except that no bleaching was done and, proteinase-k treatment was done for 10 min.

Transgenic *Cathepsin K* larvae

Cathepsin K transgenic GFP labelled zebrafish published recently [162] were kindly provided by Prof. Stefan Schulte-Merker . The eggs were obtained from one adult pair and were cleaned and sorted as described above (see 'Animals'). At the *prim-6* stage [122] the transgenic embryos were continuously exposed to a mixture of 1µM (DEX) (Sigma Aldrich Switzerland) and 1 µM vitamin D3 (cholecalciferol; SERVA electrophoresis GmbH, Germany) for 4 days. Controls were treated in the same way except that DEX and vitamin D3 were not added. At 5 dpf, control and treated larvae were observed alive under confocal microscope.

TRAcP enzyme staining

Normal zebrafish embryos and adult scales were preserved in 100% methanol after rehydration through a graded series of methanol in PBST. TRAP enzyme kit (Sigma-Aldrich 387A-1KT, Chemie GmbH, Steinheim, Germany) was used for staining the embryos and scales according to the user instructions.

Sectioning

Sections were prepared from the whole mount ISH larvae. The larvae were dehydrated in graded ethanol, and embedded in wax using Histoclear as the intermediate reagent. Some sections were prepared with Technovit embedding after dehydration.

Imaging

Imaging of *in situ* embryos and sections was done using Nikon eclipse E800M equipped with DSF1 camera. For *in vivo* confocal imaging of the transgenic larvae, they were immobilized in 1% low melting-point agarose (SIGMA) after anesthesia (0.04% Tricaine). Imaging was done using a Zeiss observer LSM 500.

Results

In situ hybridization results for *cathepsin K*, *rank* and *mmp-9* are shown in Figs. 1-9.

Cathepsin K

Hybridization patterns of *cathepsin K* are illustrated in Figs. 1 A-H and Figs. 2 A-D. Embryos hybridized with sense probe showed no specific signal (Figs.1 B). With antisense probe (Figs. 1 A, C-H and Figs. 2 A-D), there was expression as follows. At 1 dpf, hybridization was seen in a longitudinal stripe of adaxial mesoderm cells along each side of the trunk (Figs. 1 A), the stripe being interrupted at intersomitic boundaries (Fig. 1 C). Histological sections (Fig. 2 A) showed that this staining was paranotochordal, extending laterally from the notochord towards the epidermis. Hybridization was also seen in the pectoral fin buds (Fig. 1 A).

At 2 dpf, specific expression in whole mounts gave an appearance of skeletal elements in the head, (trabeculae cranii, branchial arches, and lower jaw) and in the cleithrum and pectoral fin buds (Fig. 1 D, E, and F). Histological sections showed that expression was perichondrial (Fig. 2 B). By 3 dpf the expression in the pectoral fin was reduced and by 4 dpf was faint (Figs. 1 G and H). At 5 dpf, expression in the branchial arches was indistinct in whole mounts but was still visible in histological sections (Fig. 2 B), where specific expression was again seen in what we assume to be the perichondrium of the branchial arches. However, as with the pectoral fin and the lower jaw, there was no staining in the cartilage itself.

To confirm the specificity of the probe we examined expression in adult scales. Here, the hybridization was specific and distinct. Large clusters of heavily-stained cells were localized at the margins of the scales (Fig. 2 C). At higher magnifications these clusters could be seen to have many nuclei, the dark staining being localized to the cytoplasm (Fig. 2 D).

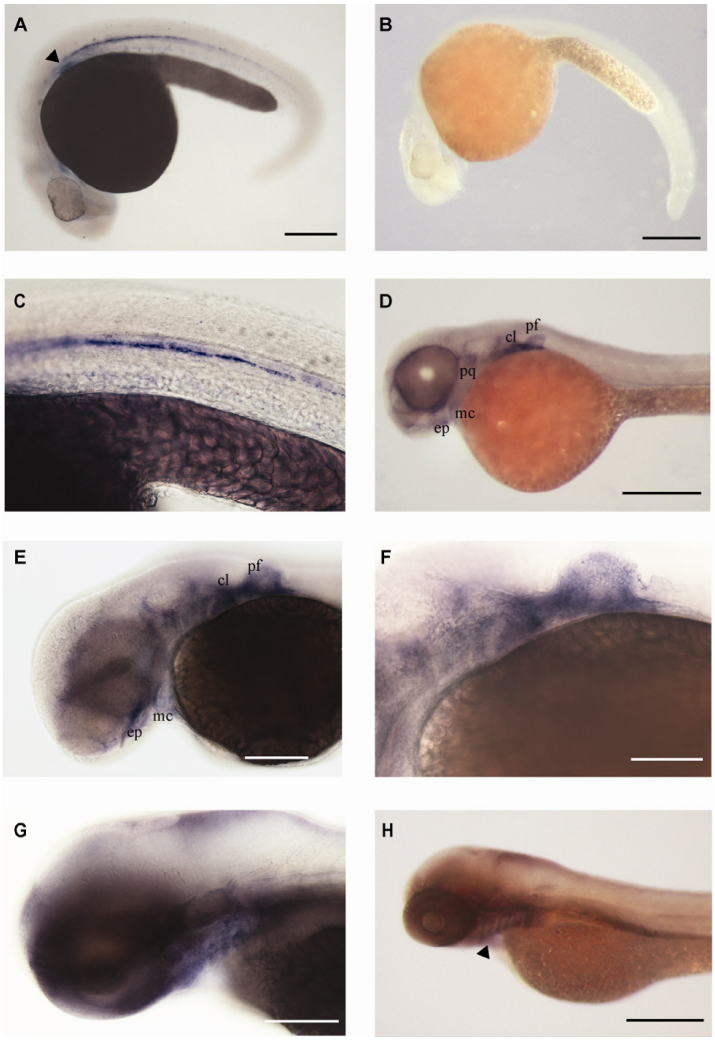

Fig 1 *Cathepsin K* gene expression by *in situ* hybridization in zebrafish embryos, scale bar=200µm unless otherwise mentioned. **A** Expression in rostral blood island, lateral sides of notochord and pectoral fin bud (arrow head), in 1 dpf embryo. **B** Sense control of A with no specific expression. **C** Detail of Fig 1 A showing expression in the lateral region adjacent to the notochord, (arrow heads) scale bar=100 µm. **D** 2 dpf embryo with expression in the Meckel's cartilage (mc), ethmoid plate (ep), cleithrum (cl) palatoquadrate (pq) and pectoral fin bud (pf). **E** Detail of Fig D scale bar=150 µm. **F** Detail of Fig E showing expression in the pectoral girdle and fin bud, scale bar=50 µm. **G** 3 dpf zebrafish embryo showing expression in the pharyngeal arches, scale bar=200 µm. **H** 4 dpf larva with expression in the pharyngeal arches (arrow head).

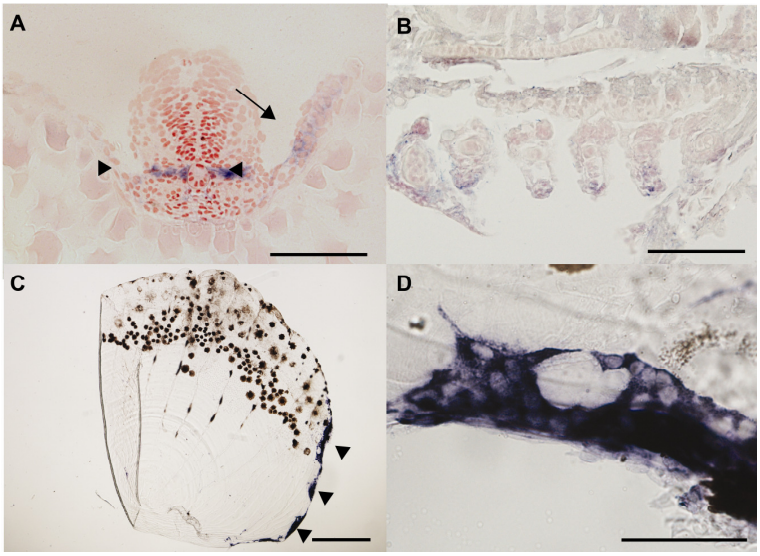

Fig 2 *Cathepsin K* gene expression by *in situ* hybridization in zebrafish larvae and scales. **A**. Histological section through the posterior region of 1 dpf embryo expressing *cathepsin K* gene in the cells of adaxial mesoderm, (arrow heads) and pectoral fin bud (arrow) scale bar=100 µm. **B** Section through pharyngeal arches of 5 dpf larva showing expression around the cartilaginous elements within the arches, scale bar=50 µm. **C** Whole mount adult scale showing expression at the margin, scale bar=300 µm (arrow heads). **D** Putative multinucleated cell expressing *cathepsin K* in the marginal region of a scale, scale bar=20 µm.

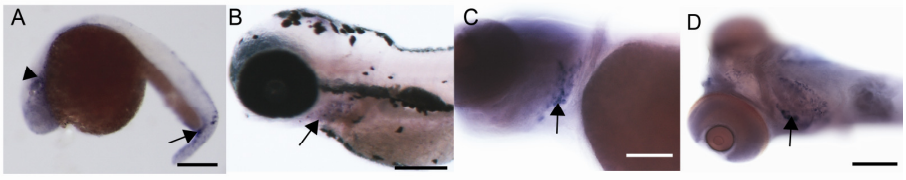

Fig 3 *Rank* gene expression in zebrafish embryos. **A** 1 dpf embryo expressing *rank* gene in the rostral blood island (arrow head) and ventral blood island (arrow) in addition to staining in the jaw region, scale bar=300 µm. **B** 3 dpf larva expressing *rank* in the pharyngeal arches, (arrow) scale bar=150 µm. **C** 4 dpf larva expressing *rank* in the pharyngeal arches (arrow), scale bar= 200 µm. **D** Ventral view of 4 dpf larva with expression in the pharyngeal arches (arrow) and anterior end of the Meckel's cartilage, scale bar= 200 µm.

rank

Hybridization patterns with *rank* antisense (Figs 3 A-D) and sense probes (Fig. not shown). Sense controls showed no hybridization. At 1 dpf, diffuse expression was observed in the head region, around the yolk sac and in the tail in the region of the ventral blood island (Fig. 3 A) where *mmp-9* and *cathepsin-k* expression was also seen. At 2 dpf expression was observed in the cleithrum and pectoral fin bud. At 3 and 4 dpf *rank* expression was seen in the pectoral fins and the branchial arches (Fig. 3 B and C). At 5 dpf, expression was seen only in the branchial arches (Fig. 3 D). Histological sections through the branchial arches of 5d old larvae confirmed that expression was in the loose mesenchyme but not the cartilage elements (Fig. 4 A), the same being true of the pectoral fin (Fig. 4 B). In adult scales, staining was observed in the edges of the scales only (Fig. 4 C).

mmp-9

Hybridization patterns with *mmp-9* antisense probes are illustrated in Fig. 5. At 1 dpf, hybridization was seen in the ventral blood island (also the site of *rank* and *cathepsin-k* expression. Expression of *mmp-9* was also observed in the posterior extension of yolk sac. At 2 dpf, hybridization was seen in numerous, scattered cells in the head, pharyngeal region, on the yolk sac, near the ventral aorta and around the gut (Fig. 5 A and B). At 3 dpf, there was hybridization in individual cells scattered in the tissue including pharyngeal region and caudal hematopoietic tissue (Fig. 5 C). At 4 and 5 dpf a few cells expressing *mmp-9* were found scattered on the rostral part of the body, but were less numerous than at earlier stages.

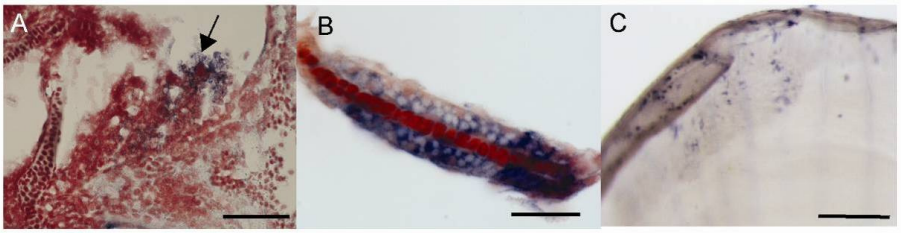

Fig 4 *Rank* gene expression in zebrafish larvae and scales. **A** Histological section through pharyngeal arches showing *rank* expression in the arches (arrow), scale bar=50 µm. **B** Section through pectoral fin of 2 dpf embryo showing *rank* expression in the tissue around the cartilage (red) scale bar= 100 µm. **C** Whole mount adult scale with *rank* expressing cells on the margin, scale bar=100 µm

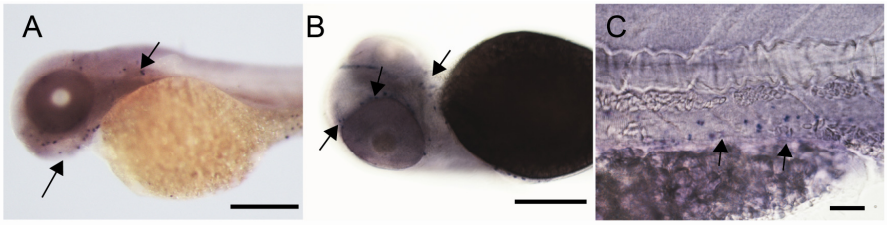

Fig. 5 *mmp-9* gene expression in zebrafish embryos; **A** 2 dpf embryo with numerous cells expressing *mmp-9* gene in the head region (arrows), scale bar=150 µm. **B** 2 dpf embryo, ventral view, scale bar=100 µm. **C** 4 dpf larva with expression in the ventral blood vessel in the posterior region of the body, scale bar=30 µm.

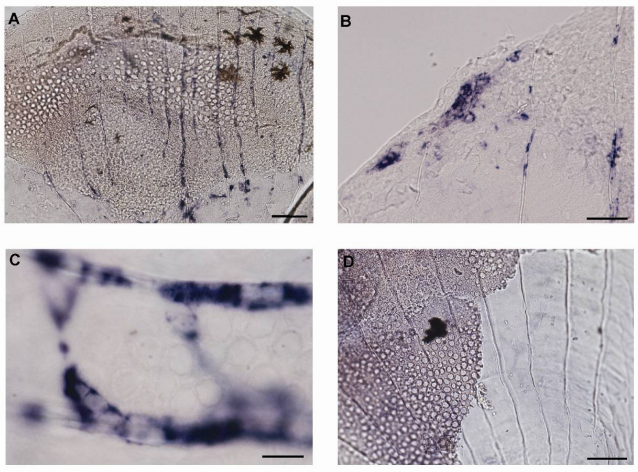

Fig. 6 Whole mount *in situ* hybridization on adult scales with *mmp-9* gene. **A** Expression in the radii of the scale, scale bar=100 µm. **B** *mmp-9* expressing cell aggregates at the margins of a normal scale, scale bar=100 µm. **C** Multinucleated cells expressing *mmp-9* in the radii, scale bar=40 µm. **D** Scale hybridized with sense probe with no specific staining, scale bar=200 µm.

We hybridized adult zebrafish scales as positive controls for *mmp-9* expression. There was expression in the radii of the scales in mono- and multinucleated cells (Fig. 6 A). Specific and strong expression was observed in the margins of the scales similar to that of *cathepsin K* expression (Fig. 6 B). Higher magnification shows expression in the multinucleated cells within the radii (Fig. 6 C). There was no specific expression in the margins or radii of the scales hybridized with the *mmp-9* sense probe (Fig. 6 D).

TRAcP enzyme staining

Immunohistochemical staining with TRAcP enzyme was done on whole mount zebrafish larvae (Fig. 7A-D). In 1 dpf embryos, strong and specific enzyme staining was seen in cells in the ventral blood island. At 2 dpf expression in the cells in the heart and pericardium was visible (data not shown). Stained cells were also present in the ventral fin fold and along the caudal haematopoietic tissue or CHT. In 3 dpf embryos, cells scattered very sparsely over the body expressed TRAcP staining (Fig. 7 A and B). There were numerous cells stained with TRAcP enzyme in the tail region around the notochord. At 4 dpf there was staining at the rostral end of Meckel's cartilage, in the pectoral fin and in the pericardial region. In the posterior region of the body, stained cells were present in the ventral vein. Similar to 4 dpf the expression in 5 dpf larvae was in the Meckels cartilage, pectoral fin (Fig. 7 C) and along the ventral blood vessels and near the somites (Fig. 7 D).

TRAcP enzyme staining was also done on adult zebrafish scales as positive controls. Staining was observed at the lateral margins of the scales (Fig. 8 A) as well as very dense staining in some scales in the mid region along the grooves of normal scales (Fig. 8 B). However no TRAcP staining was seen in the radii of the scales in our specimens. With the same staining multinucleated cells within the mid region of the normal scale were seen (Fig. 8 C).

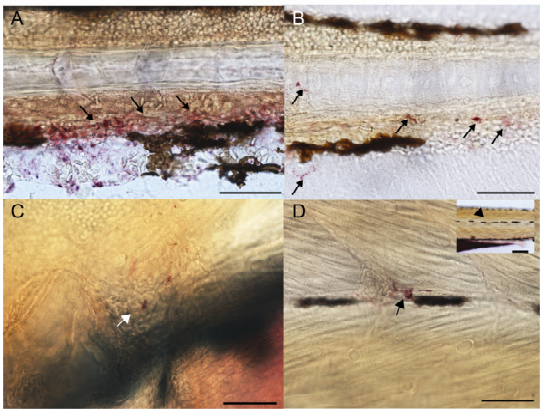

Fig. 7 TRAcP histochemical staining. **A** 3 dpf larva showing expression in the caudal hematopoietic tissue and blood cells (arrows) scale bar 50 µm. **B** Tail region of 4 dpf larva with expression in individual cells (arrows), scale bar 50 µm. **C** 5 dpf larva with expression at the pectoral fin (white arrow). Scale bar = 50 µm. **D** 5 dpf larva expressing TRAcP in a single cell on the left flank of caudal body region (arrow) inset showing D at low magnification. Scale bar = 550 µm

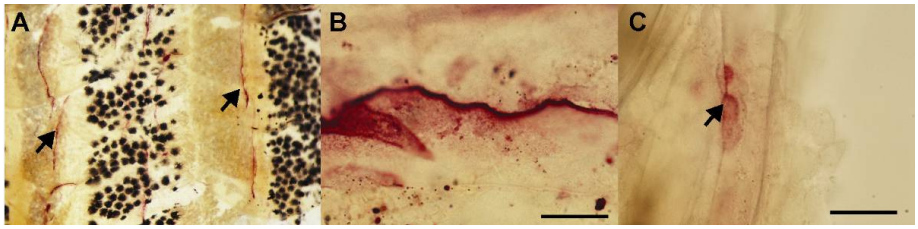

Fig 8 TRAcP histochemical staining on zebrafish scales. **A** Scales on the skin of adult zebrafish expressing staining in the lateral margins (anterior to the top and dorsal to the right), scale bar= 200 µm.**B** Groove on a single scale with TRAcP staining, scale bar=20 µm. **C** Putative multinucleated cell stained with TRAcP enzyme, scale bar=20 µm.

Transgenic Cathepsin K Larvae

GFP labeled *cathepsin K* transgenic zebrafish larvae showed expression in the pharyngeal region in the scattered cells (data not shown). After exposing the embryos continuously with DEX and vitamin D3 for 4 days, the expression was more strongly seen around the pharyngeal skeleton, in np (nasal placode), Mc (Meckels Cartilage), Bh (basihyal), cb (ceratobranchial), pf (pectoral fin) (Fig 9 A-

D) . In the lateral view *cathepsin K* expression was clearly seen in the pharyngeal arches, ceratobranchials, pectoral girdle and pectoral fin. There was also expression around the otic vesicle (Fig 9 C and D). However, a weaker *cathepsin K* expression in the control transgenic larvae was observed (Fig 9 E and F). There was an interesting *cathepsin K* expression in the scattered cells within the ventral vein near the caudal body region of the treated larvae similar to TRAcP and *mmp-9* (Fig 9 G and H).

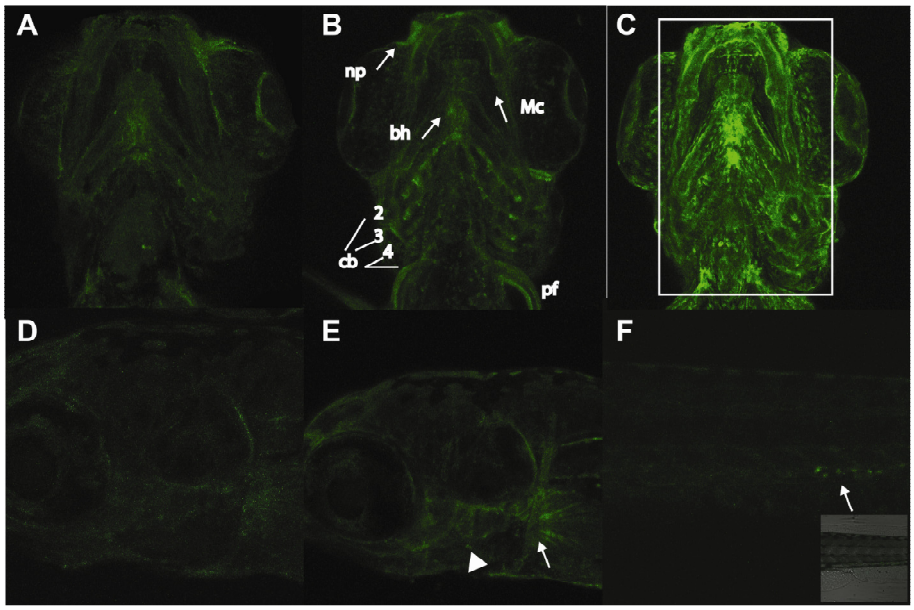

Fig 9 GFP labelled *cathepsin-k* transgenic zebrafish embryos. **A** Confocal image showing 5 dpf larva with expression in pharyngeal skeleton (ventral view, anterior side upwards). **B** DEX and vitamin D3 treated 5 dpf larva showing increased *cathepsin-k* transgenic expression in bh (basihyal), cb (ceratobranchials 2-5), Mc (Meckel's cartilage), np (nasal placode), pf (pectoral fin). **C** DEX and vit D3 treated 5 dpf larva showing increased *cathepsin-k* expression, rectangle shows the area marked for fluorescence intensity assay. **D** Confocal image showing left lateral view (anterior directed to the left) of the 5 dpf control larva with expression around ov (otic vesicle), cb (ceratobranchial), pf (pectoral fin). **E** Lateral view of DEX and vitamin D3 treated larva showing the skeletal elements with strong GFP signal, pharyngeal arches (arrow head) and pectoral girdle (arrow). **F** Caudal region of a treated larva showing the ventral vein with scattered cells expressing GFP *cathepsin-k* (arrows)

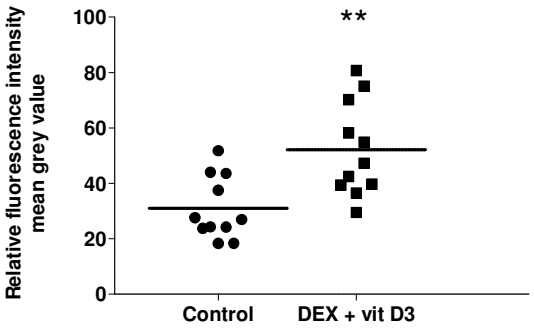

Fig. 10 Measurement of relative fluorescence intensity showing significant increase in case of DEX + vitamin D3. Lines represent standard error mean. Each of the dots represents one control larva, and square represents each treated larva.

Discussion

We studied the expression in zebrafish embryos and larvae of a panel of genes that are associated with bone and tissue Remodelling. Differences in expression were seen between all of the genes and are summarized in Table 4. Similarities in expression were evident between *cathepsin K* and *rank*, on the one hand, and *mmp-9* and TRAcP on the other. *Cathepsin K* transgenic expression in normal embryos was associated with both type of expression as observed in *cathepsin K* and *rank* as well as *mmp-9* and TRAcP.

Table 4 Summary of expression patterns of osteoclast markers in zebrafish development found in this study.

Marker	Expression
cathepsin K	pharyngeal skeleton and pectoral fin, and in CHT in case of (transgenic larvae)
rank	pharyngeal skeleton and pectoral fin
mmp-9	scattered cells on whole body and CHT
TRAcP	scattered cells on whole body and CHT (at 5 dpf in Meckel's cartilage)

Cathepsin K and rank

In 1 dpf embryo hybridized with *cathepsin K* probe, adaxial staining was seen. We cannot say however, whether this expression represents either the slow muscle precursors or sclerotomal elements which are known to occur in this region [163]. *Cathepsin K* and *rank* expression was more restricted to the cells associated with pharyngeal skeleton and pectoral fin skeleton [164,165] in embryos older than 1 dpf. It is known that by 5 dpf osteogenesis occurs where cartilaginous skeleton transforms into calcified tissue [166]. Also this calcification or bone deposition occurs from outside in, that is the exterior part of bone is remodelled to deposit bone [167].

We found expression of *cathepsin K* in the sections around pharyngeal arches, similar to the expression of *osterix* (SP7) in the perichondrium around the cartilage of a 4 dpf zebrafish embryos by (Kimmel et al 2010) [167] Therefore it is possible that this expression of *cathepsin K* mRNA may be due to osteoclasts. It is also important to note here that we found strong similarities in the expression of *cathepsin K* and *rank* genes in the larvae as well as in the adult scales. In the adult zebrafish scales the *cathepsin K* [168] and *rank* genes are both expressed in the marginal regions. This positive expression suggests that same genes are also expressed in the adult tissues which are known to carry osteoclasts [169]. However the scale-margin expression of *cathepsin K*, but not *rank*, was found in multinucleated cells.

Cathepsin K reporter line showed a similar pattern of *cathepsin K* to the *in situs*, with cells scattered along the pharyngeal arches. Further work is being carried out at present to document the expression pattern of GFP *cathepsin K* in detail. When the embryos were exposed at *prim-6* stage with 1µM of DEX and vitamin D3 for 4 days and then observed with *in vivo* confocal microscopy we found that there was much stronger expression of GFP *cathepsin K* gene along the skeletal elements. GFP expression was seen in all the skeletal elements which are known to have developed by this stage, compared to very weak expression in controls.

Initial observations therefore suggest that there was activation in the GFP *cathepsin K* expression in DEX and vitamin D3 treated embryos. It was also found that GFP *cathepsin K* positive cells were present in the tail region along

the ventral blood vessel. This expression in the ventral blood vessel is similar to the expression of TRAcP positive cells as well as *mmp-9* positive cells in normal untreated larvae. It can be therefore concluded that the *mmp-9* mRNA, TRAcP enzyme and GFP *cathepsin K* protein expressing cells are not only found around the skeletal elements but are also found scattered in other parts of body specially blood vessels, which is logical considering hematopoietic origin of osteoclasts.

mmp-9 and TRAcP

In the present study, *mmp-9* and TRAcP enzyme were both expressed in cells sparsely scattered all over the body. Unlike *cathepsin K* and *rank*, *mmp-9* and TRAcP expression was neither specifically associated with the pharyngeal arches nor the pectoral fin. Expression of *mmp-9* has been reported in cells scattered mostly on the head region and the posterio-lateral trunk, in embryos from 2-5 dpf [170,171]. The expression of *rank* in 1 dpf embryos in the ventral blood island and rostral blood island, and *mmp-9* in the ventral blood island is also interesting as this is the site of haematopoiesis in the early embryonic stages of zebrafish development [172].

TRAcP expression was observed in the skeletal structures such as Meckel's cartilage only in 5 dpf larvae, but not in larvae younger than 5 dpf. Previous researchers have argued that TRAcP expression is a definitive marker for active osteoclasts [142]. It is also worth considering here that the enzyme histochemistry does not seem to penetrate deep into the calcified tissue in whole mounts as much as GFP *cathepsin K* expression. Further work is required to determine the nature of the cells expressing the markers characterized here.

In adult scales the *mmp-9, cathepsin K* and TRAcP expression is similar except for additional expression in the radii of the scales in the case of *mmp-9* hybridization. One possibility is that mononucleated cells expressing *mmp-9* in the radii of the scales are non-activated cells of the osteoclast lineage, whereas the multinucleated radial and marginal aggregates are mature osteoclasts. Nonetheless, the fact that marginal, multinucleated cells in the adult scales express *mmp-9*, *cathepsin K* and TRAcP is suggestive of an osteoclastic lineage as we found in other studies recently published for *mmp-9* and TRAcP expression in adult zebrafish scales [42,168,169]. However here we for the first

time present expression of *cathepsin K* in the same cells and *rank* in mononucleated cells.

Conclusions

Our results show that genes associated with osteoclasts are expressed in early zebrafish development and in the multinucleated cells expressing *mmp-9* and *cathepsin K* genes, and TRAcP enzyme, in adult scale osteoclasts. Our data with the transgenic *cathepsin K* larvae suggests an association with the larval pharyngeal skeleton; this is also comparable to our expression data of *cathepsin K* expression with *in situ* hybridisation. The TRAcP enzyme, *mmp-9* mRNA and *cathepsin K* GFP transgenic line also show expression in the blood cells found in the ventral vein. The expression of *cathepsin K* in the reporter line was upregulated by DEX and Vitamin D3 treatment. Together these findings raise the possibility that osteoclast-like cells are present at early stages of zebrafish development. Further work is underway to determine the function of these cells in development.

Chapter 3: Mesoporous silica nanoparticles as a compound delivery system in zebrafish embryos

Abstract

Silica nanoparticles can be efficiently employed as carriers for many drugs *in vitro*. Here, we use zebrafish embryos as a model organism to see whether mesoporous silica nanoparticles (MSNPs) can be used to deliver compounds *in vivo*. We injected 35-40 nl (10mg/ml) of custom-synthesized, fluorescently-tagged 200 nm MSNPs into the left flank, behind the yolk sac extension, of 2 day-old zebrafish embryos. We tracked the distribution and translocation of the MSNPs using confocal laser scanning microscopy. Some of the particles remained localized at the injection site, while others entered the bloodstream and were carried around the body. Embryo development and survival were not significantly affected by MSNP injection. Acridine orange staining revealed that MSNP injections did not induce cell death significantly. We also studied cellular immune responses by means of lysozyme-ds red transgenic embryos. MSNP-injected embryos showed infiltration of the injection site with neutrophils, similar to controls injected with buffer only. In the same embryos, counter-staining with *L-plastin* antibody for leukocytes/macrophages revealed the same amount of cellular infiltration of the injection site in embryos injected with MSNPs or with buffer only. Next, we used MSNPs to deliver two recombinant cytokines (MCSF and RANK-L) to zebrafish embryos. These proteins are known to activate cells involved in bone Remodelling, and this can be detected with the marker tartrate resistant acid phosphatase (TRAcP). Co-injection of these proteins loaded onto MSNPs produced a significant increase in the numbers of TRAcP positive cells after 2-3 days of injection. Our results suggest that MSNPs

can be used to deliver bioactive compounds into zebrafish larvae without producing higher mortality or gross evidence of teratogenicity.

Introduction

Recent years have witnessed an impressive growth of fundamental and applied research in the field of nanoscience and nanotechnology [73]. There is a wide variety of nanomaterials including metal nanoparticles, nanoshells, fullerenes, quantum dots, polymer nanoparticles, dendrimers and liposomes [74-84]. In the future, nanomaterials may be applied in disease diagnostics and for drug delivery targeted at specific sites, for example in the treatment of cancer [85].

The burgeoning field of the nanomaterials brings several advantages to the design of new drug delivery systems (DDSs), as they present very significant properties such as: a high surface area able to incorporate consistent amounts of drug; tunable pore size, shape and diameter; and a chemical surface which can be functionalized to achieve target release [173].

The design of a DDS is crucial for use in medical applications; therefore it has to present some characteristics such as manipulation of biological profiles, such as pharmacokinetics and pharmacodynamics, biodistribution and cellular uptake [86,174] . There are two important challenges in these fields: first, the DDS must protect the cargo from a harsh environment and immune response; second: it has to ensure the delivery to the desired site followed be release of active drug. To meet these challenges, the DDS has to present some prerequisites such as biocompatibility with the biological environment, efficient cellular uptake, and controllable rate of release to achieve an effective local concentration, or concentration gradient [175,176]. Mesoporous silica nanoparticles (MSNPs) can satisfy all these requirements [86].

Previous studies have shown that non-phagocytic eukaryotic cells can endocytose latex beads up to 500 nm in size, and that the efficiency of uptake decreases with increasing particle size [87]. Particles around 200 nm in size or smaller are taken up with highest efficiency, whereas very little uptake is observed for particles larger than 1μm. Therefore MSNPs can be efficiently employed as carriers for intracellular drug delivery [87]. It was found in other

studies that the toxicity of nanoparticles may vary with size, structure and composition [93,94]. Acute toxicity occurs at nanoparticle concentrations in the order of milligrams per litre in the case of the medaka, *Oryzias latipes*, and the largemouth bass, *Micropterus salmoides* [90,177]. Silica nanoparticles were found to be non-toxic to other human and mouse embryonic cells at up to 15 mg/l [178]. In addition silica nanoparticles were not found to have general or overt toxicity between 0.0025 and 200 mg/l [179].

Mice have been used for studying nanoparticle biology [95]. Organs that can take up nanostructures in mice include the spleen, lymph nodes, and bone marrow. All of these are major organs of the immune system and contain large concentrations of phagocytic cells than can ingest the nanostructures. Nanostructures that are coated with polyethylene glycol (PEG), a polymer, have been shown to be more resistant to uptake by phagocytic cells [97].

Zebrafish transgenic lines that express green or red fluorescent proteins (GFP or DsRED2) under a neutrophil-specific promoter, such as the myeloperoxidase (*mpx*) promoter [180,181] or the lysozyme C (*lyz*) promoter [182], provide useful *in vivo* models for real-time imaging and genetic analyses of inflammatory responses. Neutrophils and macrophages in zebrafish larvae can both be visualized by immunolabelling with anti-L-plastin antibody, while the expression of colony stimulating factor 1 receptor *(csf1r*) and the lack of *mpx* and *lyz* expression in macrophages can be used to distinguish them from neutrophils [180,183]. The elongated morphology of the cells expressing these markers further points to a macrophage identity [180]. Both the neutrophil and the macrophage populations are involved in the innate immune response towards infection and injury [180-183]. In order to understand the fate and interaction of nanomaterials with the immune cells, further studies are needed.

Many features of the zebrafish (*Danio rerio*) model make it well-suited for studies of nanomedical applications. It has a short generation time (around three months), and a large clutch size (200-300 eggs), which allows high throughput assays at low cost [4]. Zebrafish embryogenesis is rapid, with most of the internal organs, including the heart, liver, intestine and kidney, developed by 96 h post fertilization (hpf) [3]. The optical transparency of zebrafish embryos, and their fertilization and development outside the mother,

enables an easy and thorough observation of drug effects on internal organs *in vivo*.

The zebrafish is also a very attractive model to study the mechanisms underlying bone formation [184,185] because the key regulators of bone formation are highly conserved between mammals and teleosts, and the corresponding orthologs share significant sequence similarities, and an overlap in expression patterns, when compared to mammals [164,186,187]. Molecules essential to promote osteoclastogenesis [188] include: (i) Macrophage colony-stimulating factor (M-CSF); (ii) receptor for activation of tumour necrosis factor kappa B (TNSF-κB or RANK); and (iii) RANK ligand (RANKL, OPGL or TRANCE).

The aims of this study are: first, to test the toxicity of MSNPs on zebrafish embryos; second: to test the effect of MSNPs on immune cells; and third: to see whether MSNPs can be used to deliver bioactive compounds into zebrafish larvae. For this latter objective, we chose M-CSF and RANK-L because they have a clearly defined biological readout, in the activation of osteoclasts [189].

Materials and Methods

Mesoporous Silica Nanoparticle synthesis

The mesoporous silica nanoparticles (MSNPs) were synthesized via sol-gel chemistry using cetyltrimethylammonium bromide (CTAB) and mesitylene as templates. The surfactant, CTAB, is used as template for the mesoporous structure; while mesitylene is used as pore-expanding agent to increase the pore size. The synthetic procedures were done according to Lin and co-workers [174]. The silica nanoparticles were functionalized with 2-[Methoxy (polyethyleneoxy) propyl] trimethoxysilane in order to create a PEGylate surface (Supporting Information 1.1). For laser confocal microscopy, a different batch of MSNPs were synthesized with the fluorescent label fluorescein isothiocyanate (FITC), the synthesis being done according to Zink et al [175] (Supporting Information). Fourier transform infrared spectroscopy (FT-IR) measurement: effective removal of CTAB was confirmed using a FT-IR Biorad Excalibur Series FTS 4000 (RT) and MSNPs were prepared in a KBr tablet.

Scanning electron microscopy (SEM) and transmission electron microscopy (TEM)

MSNPs were suspended and sonicated in methanol in order to avoid aggregation. 10 µl of suspension was deposited on an aluminium stub and coated with pure carbon with a sputter carbon coater. TEM (transmission electron microscope) was performed with a JEOL 1010 instrument at 60 kV. The sample was prepared as stated above and was deposited on a carbon-coated copper grid, and then air dried for 3 h.

X-Ray Diffraction (XRD)

The XRD was measured with a general powder difractometer with Cu radiation at 40 kV and 30 mA.

Release of FITC-BSA from MSNPs

Release of FITC-bovine serum albumin (FITC-BSA) from MSNPs was measured in 1M phosphate buffered saline (PBS) at pH 7.24, by preparing a suspension of 1 mg/ml of loaded MSNPs. MSNPs were washed twice in PBS to remove excess FITC-BSA. The release was determined by taking aliquots at different times. The aliquots were centrifuged and the UV-VIS absorbance of the FITC-BSA was measured to give quantitative information about the release (Fig. 1 E).

Zebrafish embryos

Maintenance of zebrafish (*Danio rerio*) adults took place at 26^{o}C in aerated 5 litre tanks, in a 10 h: 14 h light: dark cycle. In each mating setup two females and one male fish were present. The eggs were collected within the first hour, cleaned, sorted and transferred to Petri dishes filled with egg water (14 gm 'Instant Ocean®' salt in 100 ml of demi water). Embryos were anesthetized with 0.04% MS-222 (tricaine methanesulfonate) at 2 days post fertilization (dpf) for microinjections.

Mesoporous Silica Nanoparticle Injections

The embryos were divided into two groups: **treatment** (injected with MSNPs in phosphate buffered saline) and **control** (injected with PBS only). The embryos

(2 dpf) were anesthetized and transferred to custom-made agarose gel moulds to hold them in place. The moulds were made with 5% agarose (molecular grade, Bioline Cat. BIO-41025) in PBS, heated to dissolve, and then cooled. Borosilicate glass capillaries (1 mm outer diameter x 0.78 mm inner diameter, Cat. GC100TF-10, Harvard Apparatus, Holliston, MA) were pulled using a needle puller. The resulting flexible, thin, closed tip was snapped off to open the capillary for injecting. Each tip was calibrated for the release of fluid in oil, and the diameter of the droplet in oil recorded. About 35-40nl of MSNP suspension was injected into the left flank of each embryo caudal to the yolk sac extension with an air pulse provided by a Parker Picospritzer 3 (Parker Hannifin, Pneutronics Division, NJ) at a pressure of 30 psi and time 10 µsec. The pulse was delivered immediately after the needle had been pushed through the epidermis.

Human recombinant macrophage colony stimulating factor (MCSF) 40 ng/ml and Receptor for necrosis factor ligand (RANK-L) 400ng/ml in combination were loaded into MSNPs by soaking overnight and then centrifuged the MSNPs and protein suspension. The supernatant was removed and the MSNPs were resuspended in 1 x PBS. Resulting MSNP suspension in PBS was injected into 2 days old embryos, and the embryos were fixated at 1, 2, 3, 4 and 5 days post injection for TRAcP enzyme staining. There was no difference between the results from PEGylated and non Pegylated nanoparticles. Therefore we used PEGylated MSNPs for our studies, to avoid immune response. After injection, the embryos were washed twice with fresh egg water and transferred into Petri dishes (30 embryos per dish) and maintained at 28°C until analysis.

Embryo imaging and analysis

Imaging (including time-lapse recording) was done with confocal microscopy (Zeiss observer LSM 500 inverted microscope), immediately after injection, and 24 h post injection, to assess the uptake and distribution of the fluorescent MSNPs in the body of the living embryo. We recorded mortality, malformations and cell death as described in Supplementary information ‘Analysis of zebrafish embryos’.

Transgenic lysC::DsRED2 embryos for Neutrophils

The transgenic lysC::DsRED2 embryos used in this study have been described previously [182]. The neutrophil-specificity of this line is supported by other studies [190]. Two groups, each consisting of 35 eggs, were injected with or without MSNPs. Embryos were imaged within 2-5 h post injection, at 24 h, 2 d and 3 d post-injection with confocal microscopy.

L-plastin immunostaining

For L-plastin immunostaining, we used the procedure adapted after Cui C, [191]. Incubation was done overnight at 4°C with rabbit anti-*L-plastin* (Mathias *et al.*, 2007) in blocking buffer (1:500 dilution). Embryos were incubated for 2 h at room temperature in Alexa Fluor 405 Goat-anti-Rabbit antibody (Invitrogen, 1:200). They were stored at 4°C and imaged using confocal microscopy.

TRAcP staining

Tartrate resistant acid phosphatase (TRAcP) staining was done with TRAP kit 387A-1KT according to the manufacturer's instructions (Sigma Aldrich Chemie GmbH, Steinheim, Germany).

Quantitative analysis

For *lysC::DsRED2* transgenic embryos and L-plastin immunostaining the quantitative analysis was done by counting the total number of cells present in the area around the injection site (10 embryos/ group) from flattened *z* stacks of confocal images. The total number of TRAcP positive cells was counted manually under a compound microscope from the whole body on both sides (10 embryos/ group). Statistical analysis was done with one way Anova using Bonferroni post hoc test.

Results

Characterisation of MSNPs

We synthesized mesoporous silica nanoparticles via a sol-gel technique with a pore-expanding agent (mesitylene) to a CTAB-templated emulsion system. The template was removed with a methanol acidic wash because CTAB has been demonstrated as a very toxic compound for cells [192] due to its capability to damage biological membranes and cause the release of intracellular enzymes. The effective removal of CTAB was checked via FT-IR (Fig. 1 A and B). The nanoparticle surface was modified with a PEGylated methoxysilane in order to reduce cluster formations in physiological fluids. The nanomaterials thus synthesised present an inner structure comparable to the MCM-41, as previously described [173,193] with a honeycomb arrangement of the channels, as shown by the electron micrographs (Fig. 1 C and D).

The particle size of MSNPs was measured with dynamic light scattering (DLS) in PBS solution (pH 7.2) before and after the PEGylation step. The hydrodynamic diameter of the particles, before the surface functionalisation is 985 nm (PDI $\pm$0.21) indicating an elevated tendency toward aggregation. Nevertheless, after surface modification the diameter measures 255 nm (PDI $\pm$0.198) showing capability of particles to avoid clustering. A sharp peak was detected at, 2.8 theta, showing the presence of a mesoporous structure with a pore size of ca. 8 nm. We used bovine serum albumin (BSA) to study the properties of release and loading capacity of MSNPs. BSA was modified with fluorescein isothiocyanate (FITC) and then used to measure the release profiles of MSNPs. Loading capacity of MSNP-BSA in the supernatant was 65 μg/ml of loaded compound. The release curve shows the concentration of released BSA via UV-VIS in the supernatant (Fig. 1 E). It shows a delay of ca. 1 hour, due mainly to two factors: (i) the steric hindrance of the BSA; and (ii) some ionic interaction between the silica scaffold of the nanoparticles and the positive charges of the amino acids of the chain. Variation of the ζ-potential of the MSNPs and protein loaded MSNPS was measured as a function of pH Fig. 1 F.

Distribution of nanoparticles after injection into embryos

MSNPs conjugated with FITC-dextran were injected into the left flank of zebrafish embryos at 2 dpf, caudal to the yolk sac extension (Fig. 2 A). We found that some nanoparticles were seen circulating in the bloodstream (Fig. 2 A). while others were visible in the tissue at the site of injection, and remained there for the duration of experiment i.e. up to 5 dpf (Fig. 2 B). The earliest time examined was with CLSM was 10 minutes post injection, at which time the particles were already in the circulation.

Toxicity Testing

To see whether nanoparticles had an adverse effect on the development of the embryo we first recorded the cumulative mortality at 5 dpf (Fig. 3 A). Percentage mortality, pericardial oedema and morphological abnormalities are shown in Fig. 3A. Mean mortality in the MSNP-injected group was 5.8% and 4.1% in the control group (PBS only; Fig. 3 A). In the MSNP-injected group, 4.68% of embryos had pericardial oedema and skeletal abnormalities compared with 1.5% of controls. The skeletal abnormalities were of Meckel's cartilage, the pharyngeal arches and the ethmoid plate, as revealed by Alcian blue staining (Figs. 3 B, C). Cell death, as indicated by acridine orange staining (Fig. 3 E), was quantified for the whole embryo at 24 h post injection, and was similar in MSNP-injected and control groups (Fig. 3 D). Statistical analysis showed that there was no significant difference between the MSNP-injected and control (PBS-injected) groups in terms of cell death, mortality or malformations.

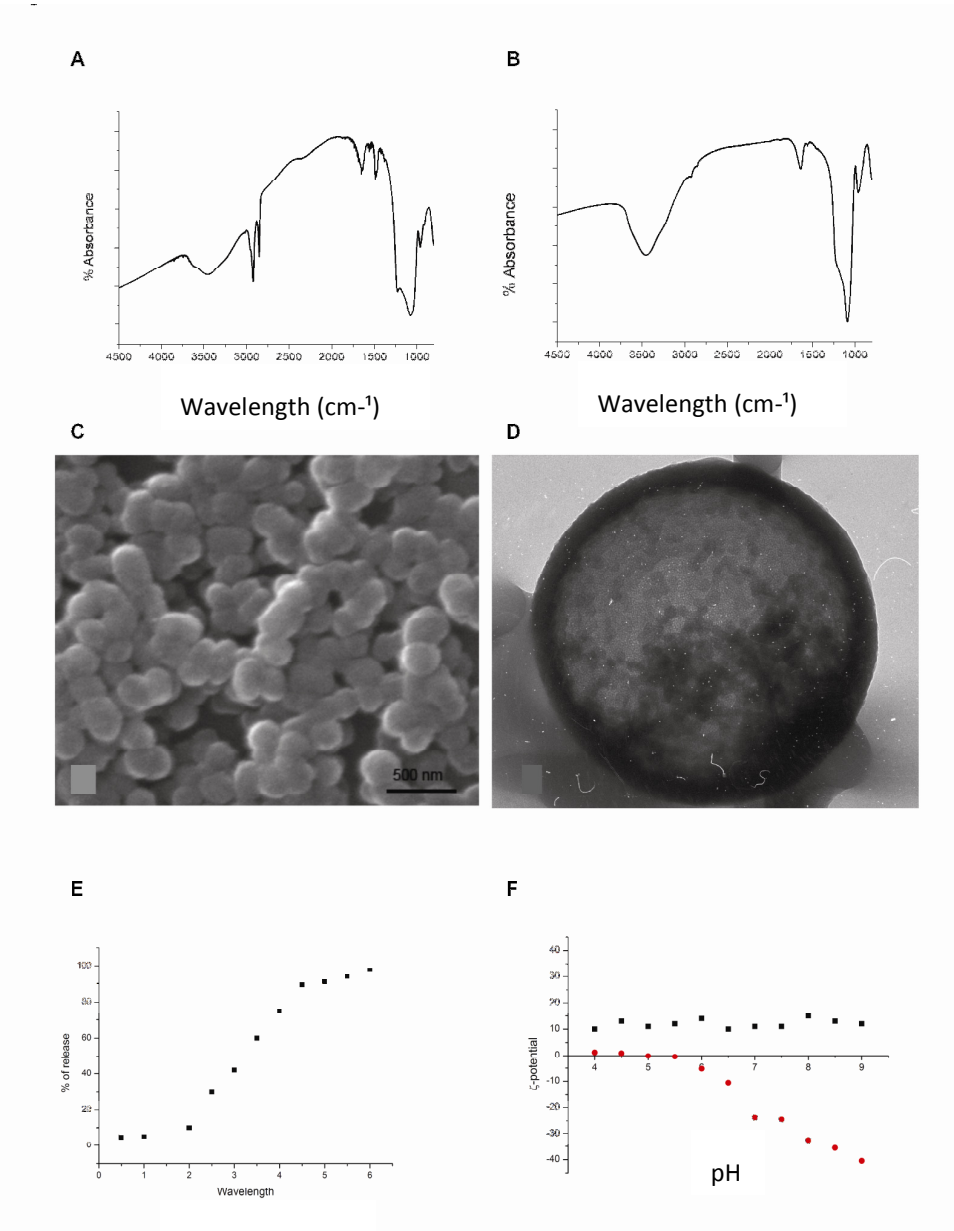

Fig. 1 Characterization of silica nanoparticles. **A** FT-IR of MSNPs before removal of CTAB template, double peak of quaternarium ammonium present at 2750 cm^{-1}. **B** FT-IR of MSNPs after the removal of CTAB template; the double peak at 2750 cm^{-1} is removed with acidic methanol washing. (**C**) SEM image of MSNPs showing the homogeneous

shape and diameter. **D** TEM image of MSNP showing homogeneous displacement of parallel channels. **E** Release of FITC-BSA from MSNPs, a delay of ca. 1.5 h is observed due to the interaction of the BSA with the silica scaffold of the nanoparticle, (y axis shows % of release). **F** Variation of the ζ-potential of the MSNPs (dots) and protein loaded MSNPS (squares) as a function of pH, (Y axis ζ-potential).

Immune cell response to injection

We examined the neutrophil response to the injection of MSNPs or PBS (control) in 2 dpf *lyz::DsRED2* embryos from 2 h until 3 days after injection. At 2 h post injection, the site of injection was already infiltrated by neutrophils (Fig. 4 A, B). Neutrophils were still in the vicinity of the injection site at 24 h and 2 days post injection (Figs. 4 C, D and E), but very few neutrophils remained at the injection site at 3 days post injection (Fig. 4 H).

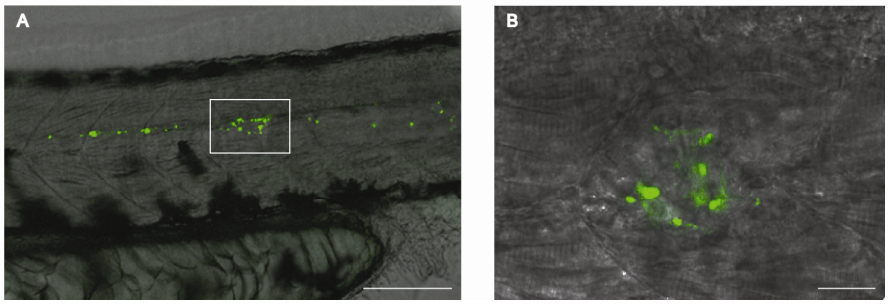

Fig. 2 Fluorescent MSNP injected zebrafish embryos. **A** MSNPs (green) distributed anteriorly and caudally from site of injection (boxed area); the black cells are pigment cells (melanocytes); scale bar, 100 µm. **B** MSNPs aggregated at the site of injection; scale bar 20 µm.

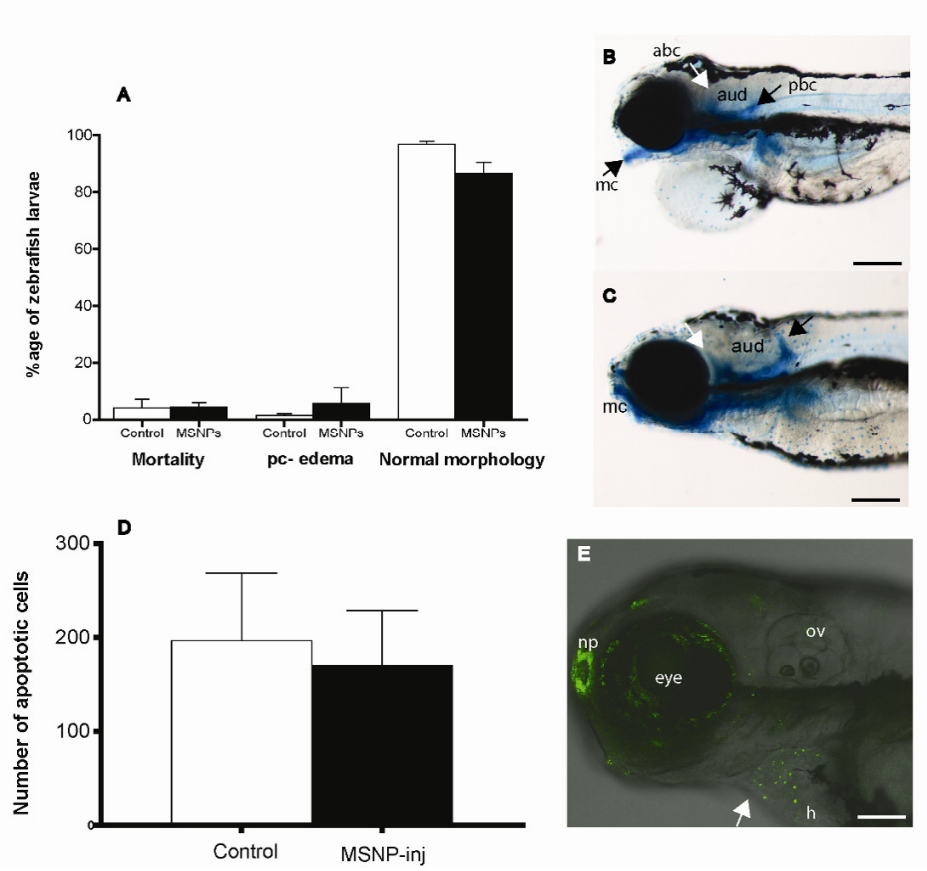

Fig. 3 Toxicity of MSNPs in zebrafish larvae. **A** Graph showing percentage of 1) mortality in larvae injected nanoparticles, 2) larvae affected by pericardial edema 3) normal morphology. The differences between buffer-injected (Control) and MSNP-

injected (MSNP) embryos are not statistically significant. Bars indicate standard error of mean. **B** Embryo injected at 2 dpf with MSNPs and fixed and stained at 5 dpf with Alcian blue; it has a combination of abnormalities as follows: pericardial oedema, a malformed Meckel's cartilage (Mc), anterior brachial cartilage (white arrow), posterior branchial cartilage (black arrow), and auditory capsule (aud). Scale bar, 200 µm. **C** Embryo injected at 2 dpf with buffer only, then fixed at 5 dpf and stained with Alcian blue. This embryo shows a normal pharyngeal skeleton. Scale bar, 200 µm. Although we selected this malformed embryo from the MSNP group, and the normal from the controls, there was no significant difference in the incidence of malformed embryos between buffer-injected and MSNP-injected groups. **D** Quantification of Acridine orange stained cells in control (buffer-injected) and MSNP groups. There was no significant difference after 24 h of injection between the two groups (10 embryos per group). **E** Acridine orange stained embryo with dead cells (green) in the eye, heart (h) and nasal placode (np). Other symbols: ov, otic vesicle. Scale bar, 100 µm.

Large aggregations of neutrophils were seen at the site of injection regardless of whether MSNPs or buffer alone was injected (Fig. 4 A, B). There was no difference between MSNP-injected and PBS-injected embryos in terms of neutrophil infiltration in the larvae 2 days after injection (See supplementary Fig. 1). Additionally, we performed L-plastin immunostaining to image and quantify the accumulation of leukocytes. Like lyz-DsRED2 cells, *L-plastin* positive cells accumulated around the injection sites in both MSNP injected and control larvae (Fig. 4 G, H). Quantitative analysis revealed no significant difference between MSNP and control injections (Supplementary Fig 2).

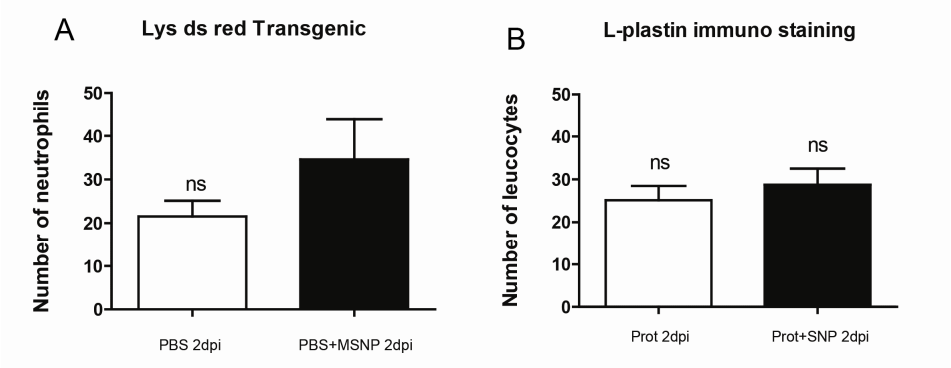

Supplementary Figure 1 Morphometric analysis of immune cells in *lysC::DsRED2* transgenic embryos, (**A)** Number of neutrophils 2 days post injection of PBS (veh) and MSNPs. (**B**) L-plastin positive leucocytes 2 days post injection of PBS (veh) and

MSNPs.

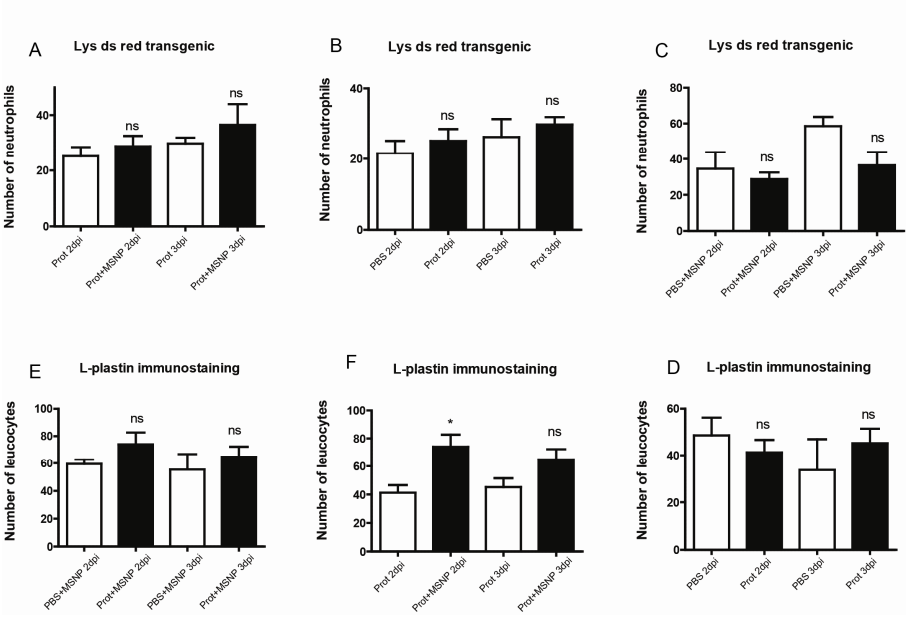

Supplementary Figure 2(A) Number of neutrophils 2 and 3 days post injection with Proteins or [Prot-MSNP]. **(B)** Number of neutrophils 2 and 3 days post injection of [PBS] and [Protein]. **(C)** Number of neutrophils 2 and 3 days post injection of MSNPs with or without proteins. **(D)** Number of total leucocytes 2 or 3 days post injection of [PBS] or [protein]. **(E**) Number of leucocytes 2 or 3 days post injection of [MSNP + PBS] or [Proteins+MSNP]. **(F)** Number of leucocytes 2 or 3 days post injection of protein or prot-MSNPs.

Compound delivery

In embryos injected with MSNPs loaded with a combination of 40 ng/ml of MCSF and 400 ng/ml of RANK-L, and then suspended in buffer, TRAcP positive cells were observed around the injection site (Fig. 5 A) and at many other locations distributed all over the body of the larvae (Fig. 5 A-F). We made a quantitative analysis of the total number of TRAcP positive cells throughout the body of the larvae 1-5 days after the injection of protein-loaded MSNPs. We found a significant increase in the number of TRAcP positive cells from 2 days post injection up to 4 days post injection compared to the controls. This increase in number seems to be transient as it returns to normal after 5 days. There was no significant difference in the number of TRAcP positive cells in the cytokine and cytokine-MSNP injected embryos 2 days and 3 days post injection (supplementary Fig. 2).

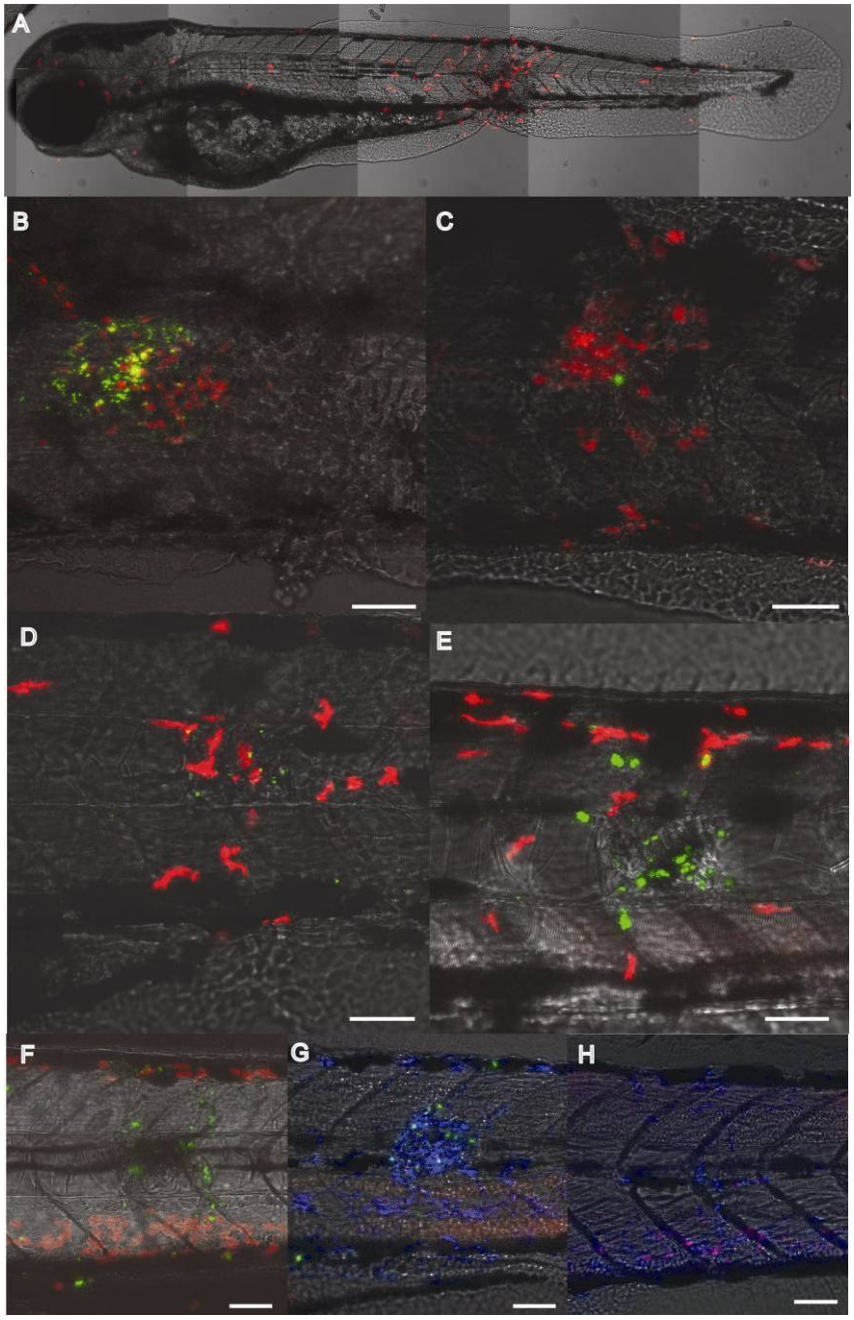

Fig. 4 Confocal images showing injection site of *lysC::DsRED2* transgenic zebrafish embryos/larvae. **A** Buffer-injected 2 dpf embryo 2 h post injection (overlay of tiles with z stacks). Note the neutrophils (red) at the injection site (arrow) and at more remote

sites. **B** An overlay of transmitted and confocal image of a different embryo showing MSNPs (green) Neutrophils (red) at the injection site 2 h post injection. **C** Representative overlay image of a different embryo injected at 2 dpf with MSNPs and analysed at 2 h post injection. This case shows a much smaller accumulation of MSNPs (gree**n**) neutrophils (red) at the injection site than B. **D** MSNP-injected embryo 24 h post injection. MSNPs (green), Neutrophils (red). **E** MSNP-injected embryo, 2 days post injection showing MSNPs (green), Neutrophils (red). **F** MSNP injected 3 days post injection (green), neutrophils (red), leucocytes (blue). **G** MSNPs (green) in 2 days post injection larva, Leucocytes (blue). **H** MSNP injected 2 dpf larva B-H are all to the same scale, bar= 50µm.

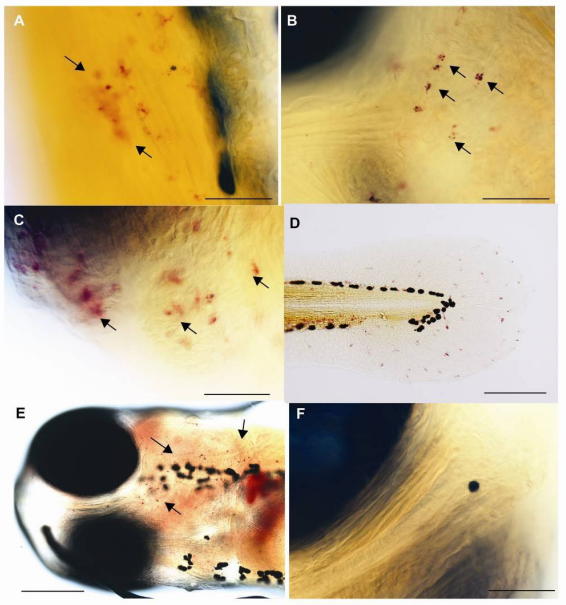

Fig. 5 TRAcP enzyme staining in MSNP injected larvae, **A** TRAcP positive cells at the site of injection in 3 days post injection larva (arrows). **B** TRAcP positive cells in the head region under the eye (arrows) 3days post injection) **C** TRAcP positive cells in the heart region in 3 days post injection embryo (arrows). **D** TRAcP positive cells in caudal fin of a 4 days post injection larva. **E** TRAcP positive cells in ventral side of head of a 4days post injection larva (arrows). **F** PBS injected larva 3 days post injection with no expression below the eye. Scale bar A, B, C, F, H = 50 µm, D 100 µm and E, 200 µm).

There was also the rare presence of apparently multinucleated TRAcP positive cells in cytokine-loaded MSNP injected embryos (Fig. 6 A-D). Hematoxylin and TRAcP double-staining showed 3-5 nuclei in a cell (Fig. 6 B). One of these apparently multinucleated TRAcP positive cells in the somite area of a 3 days

post injection larva in Fig. 6C was counter-stained with (DAPI) to visualise the nuclei (Fig. 6 D boxed area). Quantitative analysis of PEGylated cytokine-loaded MSNPs or buffer-loaded MSNPs in 2 days post injection and 3 days post injection groups showed that the number of TRAcP positive cells significantly increased compared to the buffer-loaded MSNP injected controls (Fig. 6 E).

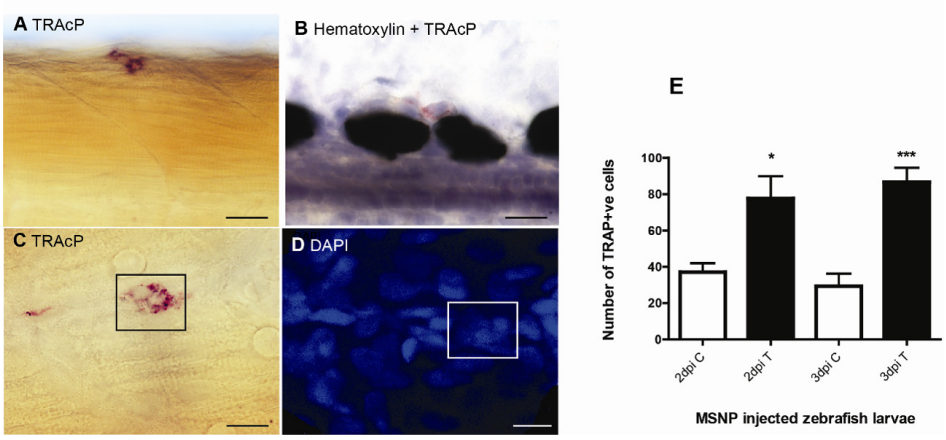

Fig. 6 (**A**) TRAcP expression in the somites of a 3 days post injection larva with apparently multinuclear cell. (**B**) TRAcP positive cells counter stained with Hematoxylin **C** TRAcP positive zebrafish larva showing apparently multinuclear cells (box) **D** TRAcP enzyme stained larva counter stained with DAPI showing 5-6 nuclei in the same area as C (box) Scale bar ABC=12.5 µm and D=12 µm **E** Quantitative analysis of TRAcP positive cells in 2 days or 3 days post injection, 10 larvae/group were studied for the number of TRAcP positive cells, analysis was done with One way analysis of variance * = p< to 0.1,**= $p < 0.01$, *** $p < 0.001$.

Discussion

We have tested the toxicity, and the capacity for controlled drug delivery, of MSNPs injected into living zebrafish embryo. We find that there is no significant difference between the toxicity of MSNP injections, and buffer-only injections, as measured by several parameters (mortality, cell death, gross malformations). Injection of MSNPs led to an influx of immune cells at the site of injection that persisted for 2-3 days. However, the same type of influx was also seen in embryos injected with buffer alone, suggesting that it is not the MSNPs that are

responsible for the immune response, but some aspect of the injection procedure itself (tissue damage, for example). Indeed, it has previously been shown that trauma to zebrafish embryos (e.g. a fin clip or mechanical wounding with an injection needle) causes an influx of macrophages and neutrophils to the wound site [180-183].

In all the studies reported here, we used PEGylated MSNPs because PEGylation is thought to avoid triggering an immune response against the particles [97,194]. With time-lapse imaging it is clear that some MSNPs remain at the site of injury, while others travel in the blood stream from the site of injection. The MSNPs localized at the site of injection were found to be there even after 3 days.

Even though the MSNPs are very small in size with an average diameter of 200nm these particles have a very high surface area that can be used to carry drugs in our case cytokines. This small size helps in fast endocytosis by non-phagocytic cells [96]. In our studies we found no significant toxic effects of injected MSNPs in the living embryos. This means that at low concentrations, MSNPs could be a very good delivery system in the whole organism. Nanomaterials such as fullerenes have been found to be excreted following oral administration or injections in mice [195] while others were shown to be taken up by immune cells. We observed very little co-expression of lyz: DsRED2-labeled cells and MSNPs. This suggests that only a few of the particles are actively phagocytosed by neutrophils. With L-plastin immunolabeling, which stains leucocytes, more overlap with the fluorescent signal of the particles was observed, suggesting that part of the MSNPs may be phagocytosed by immune cells.

Other studies have shown that, in the presence of artificially provided cytokines like MCSF and RANK-L, immune cells are activated into TRAcP+ osteoclasts [196]. We were not able to combine the double staining of fluorescent immune cells with the histochemical staining of TRAcP enzyme activity because the two protocols were not compatible. Using single-labeling, we found a significant increase of TRAcP positive cells in zebrafish larvae injected with MSNP-cytokines, while there was no significant increase in the total number of immune cells in these embryos. Some of these TRAcP positive cells had multiple nuclei, as shown by DAPI staining. By 4-5 days post injection, TRAcP positive

cells appeared to become small and darkly-stained. One possible explanation for these observations is that the TRAcP positive cells were transiently induced by the injected cytokines in the early period (2-4 days) after injection, and returned to a normal level later on.

Further work is required to clarify the differentiation status of the TRAcP positive cells. If it can be confirmed that young larvae have inducible osteoclast-like cells, this would be interesting because zebrafish larvae have not previously been reported to have osteoclasts at the stages studied here. Furthermore, the presence of osteoclast-like cells in zebrafish larvae could lead to a disease model for bone disorders and for the study of effects, for example, of anti osteoporotic drugs. What is clear from our findings is that MSNPs can be used for drug or compound delivery in the zebrafish embryo with no excess of gross toxic effects or immune responses attributable to the nanoparticles themselves.

Chapter 4: Matrix metalloproteinases in osteoclasts of ontogenetic and regenerating zebrafish scales

Sharif F, de Vrieze E, Metz JR, Flik G, Richardson MK.

Published in Bone (2011) 48:704-12

Abstract

Matrix metalloproteinases (MMPs) are key enzymes in the turnover of extracellular matrix in health, disease, development and regeneration. We have studied zebrafish scale regeneration to ascertain the role of MMP-2 and *MMP-9* in these processes. Scales were plucked from the surface of anaesthetised adult male zebrafish, and the scales that regenerated in the scale pocket were recovered at various time points after plucking. Analyses consisted of (i) *mmp-9 in situ* hybridisation; (ii) *MMP-9* + TRAcP double-staining; (iii) qRT-PCR for *mmp-2* and *mmp-9*; (iv) zymography for gelatinolytic activity and (v) a hydroxyproline assay. We found that *mmp-9* positive cells were confined to the episquamal side of the scales. Ontogenetic scales had irregular clusters of mono- and multinucleated *mmp-9* expressing cells along their lateral margins and radii. During regeneration, *mmp-9* positive cells were seen on the scale plate, but not along the lateral margins. Double staining for TRAcP and *MMP-9* revealed the osteoclastic nature of these cells. During early scale regeneration, *mmp-2* and *mmp-9* transcripts increased in abundance in the scale, enzymatic MMP activity increased and collagen degradation was detected by means of hydroxyproline measurements. Near the end of regeneration, all of these parameters returned to the basal values seen in ontogenetic scales. These findings suggest that MMPs play an important role in Remodelling of the scale plate during regeneration, and that this function resides in mononucleated and

multinucleated osteoclasts which co-express TRAcP and *mmp-9*. Our findings suggest that the fish scale regeneration model may be a useful system in which to study the cells and mechanisms responsible for regeneration, development and skeletal Remodelling.

Introduction

The elasmoid scales of zebrafish (*Danio rerio*) can regenerate when removed from the skin, e.g. by abrasion or experiment. Like regenerating fin rays [197], scales can be studied to get a better understanding of the underlying mechanisms of skeletal development, such as matrix formation and degradation, cell differentiation and mineralisation.

Elasmoid scales are a component of the dermal skeleton. They are composed of a collagen matrix that is mineralised on the external (episquamal) side with hydroxyapatite crystals [102].The episquamal side of the scale possesses concentric ridges (*circuli*) and grooves (*radii*) radiating from the central *focus* to the edges of the scale. Each radius is covered by a dermal space with cells and blood vessels embedded within a loose matrix [198]. Scleroblasts synthesise and shape the scale matrix during ontogeny and regeneration [104]. The external layer is synthesised first, followed by the elasmodine layer, composed of type I and V collagen fibres in a plywood-like arrangement [105]. The collagens of the elasmodine layer are similar in arrangement to mammalian lamellar bone [106] and mineralise slowly from the external layer [199]. When a zebrafish scale is plucked from its scale pocket, formation of a new scale is initiated immediately [107]. Already after two days, a new mineralised scale plate can be seen, but it takes up to four weeks for a new scale to grow to the size and thickness of the removed scale. As a consequence of this rapid reformation, the focus of early regenerating scales is less structured than that of ontogenetic scales. The typical grooves and radii appear late in scale regeneration, which is believed to be the result of basal plate Remodelling [101,200]. Note that in this context, the term ‘ontogenetic’ scale is used for the scales that developed during the early ontogeny of the fish, in contrast to the scales that regenerate after plucking.

The scale compartment constitutes a significant, readily accessible calcium source of fish as it can contain up to 20% of the total calcium in the body [201]. Fish withdraw calcium from their scales in periods of high calcium demand, rather than from their axial skeleton as mammals do [202-204]. However, mobilisation of scale calcium demands the same active and controlled mineralisation and demineralization. Scales are covered with a monolayer of cells, originally called scleroblasts, on both the mineralised and un-mineralised side [103]. More recent literature subdivides the scleroblasts in osteoblasts and osteoclasts, based on their scale forming and resorbing properties, respectively [27,205,206].

This is substantiated by the classical osteoblast marker alkaline phosphatase (ALP), found in hyposquamal scleroblasts [108]. Both in mammals and in teleosts, staining of tartrate-resistant acid phosphatase (TRAcP) activity demonstrates bone surfaces that are being actively resorbed or have been resorbed [146]. Indeed, mononuclear and occasional multinuclear osteoclasts, positive for TRAcP but also the osteoclast marker cathepsin K, were found on the episquamal side of scales of different fish species [100,108]. Multinucleated osteoclasts resorbing the scale matrix have also been identified by means of electron microscopy [27,109].

Matrix degradation by osteoclasts is a key process in both normal bone turnover and the bone disease osteoporosis [23]. Osteoclasts are classically described (at least in mammals) as multinucleated giant cells of the myeloid (monoctye -macrophage) lineage [15,146]. They display a characteristic ruffled border where proteases and acid are secreted, allowing for bone resorption and formation of ‘resorption pits’ in the bone surface [25]. Osteoclast morphology varies between mammals and teleosts (bony fishes), and also between different groups of teleosts [146]. In the skeleton of young zebrafish for example, osteoclast activity is carried out by both mononucleated and multinucleated cells [26]. In fact, there is an ontogenetic progression from mono- towards multinucleated osteoclasts. In juvenile zebrafish, bone resorbing cells in the developing lower jaw are at first mononucleated. In thin skeletal tissues such as the neural arch, mononucleated cells are even predominant in adults [26]. In rainbow trout, scale resorption is predominantly carried out by mononucleated osteoclasts [27]. Although in mammals these

mononucleated cells are often just regarded as osteoclast precursors, in fish mononucleated osteoclasts are active bone resorbing cells [28,29].

One family of osteoclast proteases is the matrix metalloproteinases (MMPs). They are involved in the breakdown of extracellular matrix by osteoclasts, but also by other cell types like fibroblasts [30]. MMPs are multi-domain enzymes that require zinc as cofactor for proteolytic activity. Extracellular matrix turnover occurs in a wide range of physiological processes, including embryonic development and morphogenesis, bone resorption and tissue regeneration. Moreover, MMP-mediated breakdown of the extracellular matrix has been implicated in disease processes including cartilage destruction in osteoarthritis [31]. The importance of MMPs in bone development is underlined by studies on *mmp2* and *mmp9* null mice, which suffer from bone abnormalities, osteoporosis and osteopetrosis respectively [32]. In view of their role in physiological and pathological processes, MMPs are important targets in pharmaceutical research and drug development.

In bone turnover, secreted MMPs participate in the breakdown of collagen, which in turn allows osteoclast attachment [35]. Furthermore, *MMP-9* is associated with osteoclast migration through the collagen matrix [34]. Matrix metalloproteinases may also break down residual collagen left by cathepsin K after the pH rises in the resorption pit [35]. MMP-2 and *MMP-9* (gelatinases A and B, respectively) are particularly active against gelatins (denatured collagens) and intact collagen types I and IV. In bone of dermal origin, matrix degradation is thought to rely more on MMPs and less on cathepsin K [36]. MMP-2 has also been described to play a crucial role in formation and maintenance of the osteocytic canalicular network, whereas *MMP-9* is active in early calvarian bone development and in orthodontic tooth movement [37,207,208]. Regenerating fins of adult zebrafish express *mmp-2* and regeneration can be inhibited by the MMP inhibitor GM6001 [38]. More recently, MMPs have also been implicated in angiogenesis and liberation of growth factors [39,40].

Given the involvement of matrix metalloproteinases in bone Remodelling and fin regeneration, we predict the presence of MMP2 and MMP9 in scale cells. We furthermore predict an increased MMP activity in scale regeneration associated with scale matrix Remodelling. In the current study, we investigated

both expression of *mmp* genes and actual activity of MMP enzymes in the process of scale regeneration.

Materials and methods

Animals and scale collection

Experimental procedures were approved by the ethical committee of the Radboud University. Wild type adult male zebrafish (*Danio rerio*) of approximately one year old were kept at 26 °C in 1.5 litre tanks under 12 h light: 12 h dark cycle. Fish were fed twice a day with commercially available food (Tetramin, Tetra, Melle, Germany). Prior to scale harvesting, fish were anesthetised in 0.05% v/v 2-phenoxyethanol. Scales were carefully removed under a microscope from the left side of the body using watchmaker's forceps. When necessary, fish were euthanised using an overdose of 2-phenoxyethanol (0.5% v/v) and then scales or skin were collected.

To induce regeneration, approximately 50 scales were removed under anaesthesia from the left side of a fish. For analysis of gene expression and enzyme activity, ontogenetic (non-plucked) and regenerating scales were taken from the same fish (right and left sides of the body respectively). Fish were sacrificed for scale collection on days 4, 5, 6, 8, 11 and 14 (note that scales before 4 days of regeneration are too small to collect). At these time points, 40 ontogenetic (right side) and 40 regenerating (left side) scales were collected for RNA isolation and zymography. Additional fish were used for *in situ* hybridisation and histological analysis on days 2, 4 and 8 of regeneration.

In situ hybridisation

Primers were designed based on the *Danio rerio mmp-9* sequence (Table 1). The probe sequence was amplified by PCR, cloned in a TOPO vector (Invitrogen, Carlsbad, USA) which was used to transform competent cells. Samples of positive clones were then sent for sequencing to Macrogen Inc. (Seoul, South Korea). Linearization of template was done using enzyme Xho1. The PCR product was cleaned using Wizard SV Gel and PCR Cleanup system (Promega, Leiden, The Netherlands).

Skins samples were fixed overnight in 4% paraformaldehyde in phosphate-buffered saline (PBS, pH 7.4, 4°C). Samples were subsequently dehydrated in a graded series of RNAse-free methanol solutions to 100%, and then stored at -18°C. Prior to hybridisation, the skin samples were cut into 25mm^2 pieces and impaled on Drosophila pins (Watkins & Doncaster, Cranbrook, UK) to prevent the tissue from curling during incubation. The skin pieces were rehydrated through a graded series of methanol and processed for *in situ* hybridisation using standard protocols adapted with minor changes from [161].

Table 5 Sequences of the primers used to quantify relative gene expression levels and develop the in-situ hybridisation probe.

Gene	Accession nr.	Sequence (5'→ 3')
β-actin	AF057040	Fw: CTTGCTCCTTCCACCATGAA
		Rv: CTGCTTGCTGATCCACATCT
40s	AY648802	Fw: GTGTGGTGACCAAGATGAAGATG
		Rv: ACGGTTGTACTTGCGGATGTAA
mmp-2	NM_198067	Fw: GAGAACCAACAGACAAGCCATTG
		Rv: TCTGATCTGGGCTACAGCATCA
mmp-9	NM_213123.1	Fw: CCAGTTGTGCCAACGAAACC
		Rv: GAAGGGACCACCTGAGTTGTG
mmp-9 ISH	NM_213123.1	Fw: CACAGCTAGCGGATGAGTATCTGAAGC (pos. 253)
		Rv: AATGGAAAATGGCATGGCTCTCC (pos. 1135)

Histological sections

After *in situ* hybridisation, the skin pieces were embedded in Technovit 7100 (Heraeus Kulzer GmbH, Wehrheim, Germany), according to the manufacturer's instructions. In some cases, the tissue was first decalcified in Osteosoft® (Merck KGaA, Darmstadt, Germany) for 24 h before embedding. Sections were cut at 5µm, counterstained with neutral red and cover-slipped with Permount™

(Fisher Scientific, Fair Lawn, New Jersey). The imaging was done with Nikon eclipse E800M equipped with DSF1 camera.

Plasma membrane staining

Whole-mount prefixed adult zebrafish scales were stained with Concanavalin A (ConA) FITC conjugate Type 4 (Sigma-Aldrich, St. Louis, USA) for membrane glycoproteins [209]. Scales were incubated in Con A FITC (25 µg/ml) for 10 min and then counterstained with DAPI nuclear stain (5 µg/ml for 2-3 min; Invitrogen, Carlsbad, USA). Confocal imaging was done using a Zeiss observer LSM 500.

Quantitative analysis of *mmp-9* positive cells

The total number of *mmp-9* positive cells was counted in the serial sections of whole mount *in situ* hybridised scales on skin. Each section was 5µm thick and the total number of serial sections selected for counting was the same for each group (control, 2day regenerated and 4day regenerated). The *mmp-9* positive cells were counted under a Nikon eclipse E800M microscope. Cell numbers were expressed relative to ontogenetic scales and statistically tested by means of a Mann-Whitney *U* test.

Anti zf-MMP9 and TRAcP double staining

Ontogenetic and regenerating scales (8 days) were fixed for 30 min in 4% paraformaldehyde in PBS at 4^{o}C and subsequently washed with PBS. Whole scales were incubated for 1 hour with block buffer (1% normal donkey serum in PBS) and subsequently incubated overnight at room temperature with zebrafish anti-*MMP-9* (Anaspec, Fremont, USA) at a dilution of 1:100 in block buffer. Next, scales were rinsed three times with PBS and incubated at room temperature with biotinylated anti-rabbit IgG (Vector Laboratories, Burlingame, USA) in blockbuffer at a dilution of 1:200 for 1 h. Scales were again rinsed three times with PBS and *MMP-9* was visualised with Vectastain ABC kit (Vector Laboratories, Burlingame, USA) according to manufacturer's instructions for staining with nickel-*diaminobenzidine (Ni*-DAB). Scales were subsequently stained for TRAcP activity according to the method described by van de Wijngaert & Burger (1986) [210].Nuclei were stained with haematoxylin.

Dissected skin parts, with scales embedded, were subjected to TRAcP staining only.

qRT-PCR

Total RNA was isolated from regenerating scales and ontogenetic scales using Trizol (Invitrogen, Carlsbad, USA) according to manufacturer's instruction and subsequently treated with DNase I (Invitrogen). cDNA was synthesised using Superscript Reverse Transcriptase II enzyme (Invitrogen) according to manufacturer's instructions. Thus obtained cDNA was 10x diluted in ultrapure water for quantitative PCR.

Quantitative PCR was done according to Gorissen and co-workers [211]. Primer sequences for the different target genes are listed in table 1. The expression levels of the housekeeping genes *β-actin* and *40S* were combined in an index using the software tool *BestKeeper* [212]. Expression of *mmp* genes was corrected for primer efficiency and reference genes, and plotted relative to expression in ontogenetic scales collected on day 0.

Gelatin Zymography

Activity of putative matrix metalloproteinases 2 and 9 was detected with gelatin zymography. Ten ontogenetic and 10 regenerated zebrafish scales were cultured for 20 h in 100 µl MEMα (Invitrogen). Zymography was done according to Bildt and co-workers [213]. Relative MMP activity was calculated from band intensity with Quantity One software (Bio-Rad, Hercules, USA) and related to 2 ng human recombinant proMMP-2.

GM6001 exposure

GM6001 (ilomastat) from Millipore (Billerica, USA) was dissolved in DMSO at a concentration of 1 mg/ml. From two groups of six fish each, approximately 50 scales were removed from the left side of the fish. To specifically investigate MMP activity during scale plate Remodelling, GM6001 exposure (100 nM) was started at day 2 in one group while the other group was exposed to the vehicle. Water was replaced every other day. On day 4 and day 7, three fish from each tank were sacrificed.

Western Blot

Medium from overnight scale cultures was concentrated approximately fivefold by vacuum drying. Samples were loaded on a SDS-PAGE gel according to standard procedures. Proteins were transferred to an Immobilon-P PVDF membrane (Sigma-Aldrich) and used for Western blot with anti-*MMP-9* (Anaspec) at a dilution of 1:1000. Biotinylated anti-rabbit IgG (Vector Laboratories, Burlingame, USA) was used as second antibody at a dilution of 1:1500. The Western blot was developed with Vectastain ABC kit (Vector Laboratories) according to manufacturer's instructions for staining with nickel-*diaminobenzidine* (*Ni*-DAB).

Hydroxyproline assay

Twenty scales (ontogenetic or 6 days regenerating) were taken from 6 fish and cultured overnight in 200 µl MEMα. Collected culture medium was mixed with 400 µl 100% ethanol and allowed to precipitate overnight. Samples were centrifuged 15 min at 1710g and supernatants were collected. Pellets were washed with 200 µl 70% ethanol and supernatants were added to previously obtained supernatants. Samples were dried in a hot stove and then resuspended in 50 µl 2M NaOH. Samples were autoclaved for 30 min and hydroxyproline was measured according to the method described by Reddy and Enwemeka [49].

Results

mmp-9 gene expression in ontogenetic scales

In ontogenetic (non-plucked) scales of adult male zebrafish, *mmp-9* expression was confined to cells on the episquamal side, along the radii and margins of the scale (see Fig. 1 A, B and D for whole-mounts and Fig. 1 C and E for histological sections). Scleroblasts on the hyposquamal side showed no hybridisation; the *mmp-9*-positive cell population was confined mainly to the episquamal surface of the scale and included both mononucleated cells (Fig. 1 C and D) and multinucleated cells (Fig. 1 B, E). Fig. 1 F shows a superimposed confocal image

of plasma membranes stained with concanavalin A FITC conjugate. No separate plasma membranes were seen dividing the cytoplasmic mass of cells similar to the *mmp-9* expressing cell in Fig. 1 B. However, the nuclear membranes of the five nuclei were distinct. The extent and position of these marginal cells varied between individual scales on the same fish, and between scales from different fish, and were absent in some scales. Despite this irregular distribution, the differences in expression as a result of scale regeneration are far more pronounced.

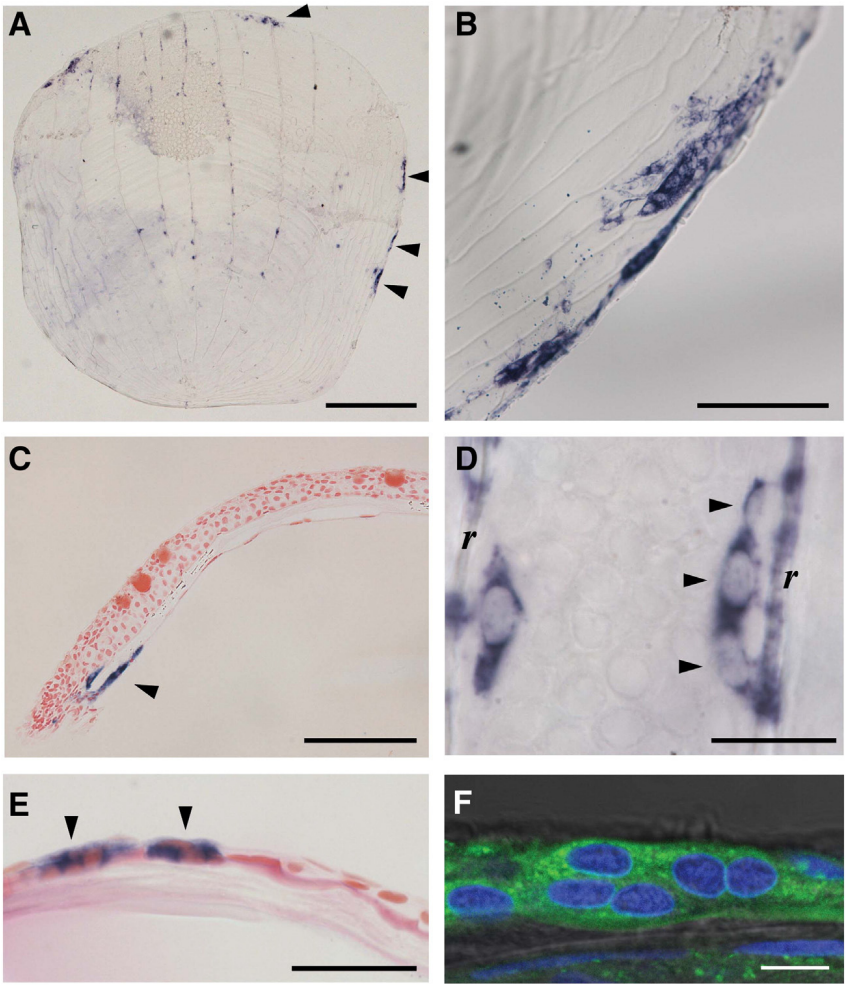

Fig. 1. *In situ* hybridization of zebrafish *mmp-9* on whole ontogenetic scales and in histological sections. **A** whole mount ontogenetic scale, arrowheads indicate the

positive clusters on the scale margins; bar = 300 µm. **B** Another ontogenetic scale showing *mmp-9* positive cells on the margin and radii of the scale; bar = 100µm. **C** Section of an ontogenetic scale, showing the *mmp-9* positive marginal cells (arrowhead); bar = 100 µm. **D** Multinucleated cell(s) expressing *mmp-9* on the radii (*r*) of an ontogenetic scale; bar = 10 µm. **E** Section of an ontogenetic scale with a multinucleated cell (arrowheads) on the episquamal side (towards top of picture); bar = 50 µm. **F** Superimposed Z-stack confocal image of ConA-FITC (green) stained cell on scale margin with nuclei counterstained with DAPI (blue); bar = 10 µm.

mmp-9 gene expression in regenerating scales

In sectioned whole mounts of 2 days regenerated scales, *mmp-9* transcripts were present in cells scattered on the episquamal, mineralised side of the newly-formed scale matrix (Fig. 2 A and B). These cells were predominantly mononucleated. However, after 4 days of regeneration, *mmp-9* expressing cells were more abundant in sections (Fig. 2 C). The 4 days regenerated scales possess aggregates of cells which appear by light microscopic observations to be multinucleated in sections. In the sections of 4 days regenerated scales, the collagenous matrix was thinner than that of ontogenetic scales and radii had not yet formed. In both 2 and 4 days regenerated scales there were no multinucleated marginal aggregates as seen in ontogenetic scales. In the sections of 8 days regenerated scales, *mmp-9* expression was similar to that of 4 day regenerated scales (Fig. 2 D). There were single cells expressing *mmp-9* all over the entire scale. Multinucleated *mmp-9* expressing cells were also present (Fig. 2 E). Quantification of the number of positive cells reveals that there are fewer *mmp-9* positive cells on day 2, but their numbers are increased on day 4 (Fig. 3).

MMP-9 & TRAcP double-staining

Staining on scales embedded in the skin clearly depict TRAcP postive cells along the margins of all scales (Fig. 4 A). Ontogenetic scales show positive staining for TRAcP activity on the episquamal side, predominantly along the radii (Fig. 4 B). At higher magnifications, *MMP-9* positive cells can also be detected (Fig. 4 C and E), some of which were located in close vicinity of resorption pits. Some mononuclear osteoclasts along the the radii show colocalisation of *MMP-9* and TRAcP (Fig. 4 D). On regenerating scales, the TRAcP activity appears increased and irregularly spread compared to ontogenetic scales (Fig. 4 E). Mononuclear

osteoclasts that both express *MMP-9* and secrete TRAcP were seen along the grooves of the scale (Fig. 4 F). At more irregular areas of TRAcP staining, multinuclear osteoclasts with *MMP-9* immunoreactivity appeared to be present as well (Fig. 4 G).

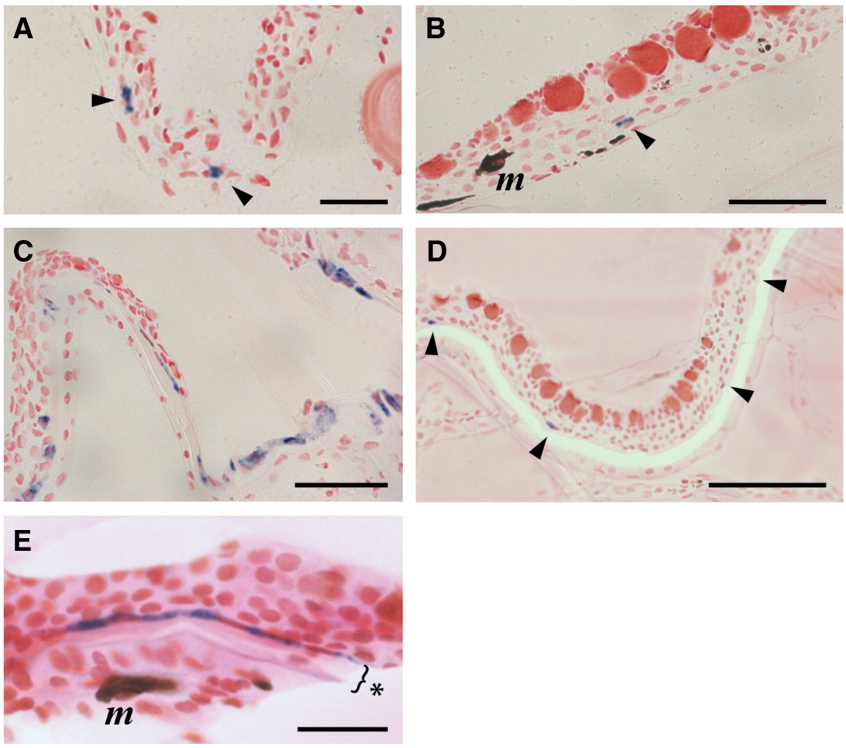

Fig. 2. Regenerating zebrafish scales, hybridised *in situ* as whole mounts with *mmp-9* probe, and then sectioned. **A, B,** Sections through the skin with 2 day regenerating scales. Mononucleated cells positive for *mmp-9* are situated on the newly-deposited matrix (arrowheads); *m* = melanocyte; bars in A and B = 50 µm. **C** Section through the skin and scale at 4 days regeneration. Numerous positive cells are distributed along the whole scale; bar = 100 µm. **D** Section through the skin with an 8 day regenerating scale, showing mononucleated *mmp-9* positive cells (arrowheads) at the radii; bar = 100 µm. **E** Section through 8 day regenerating scale showing *mmp9* positive cells lying on the episquamal surface of the newly-formed scale matrix (indicated by the bracket and asterisk). *m*, melanocyte; bar = 25 µm.

qRT-PCR profiling of mmp-2 and *mmp-9* expression

Expression of the *mmp-2* and *mmp-9* genes in ontogenetic and regenerated scales is illustrated in Fig. 6. Note that scales could not be collected earlier than 4 days of regeneration because of their small size. In 4 day regenerating scales, *mmp-2* expression is increased compared to ontogenetic scales (Fig. 5A). On days 5 and 8 of regeneration, *mmp-2* expression is significantly increased (by as much as fourfold). Expression of *mmp-9* is already up-regulated significantly after 4 days, and remains up-regulated until day 8 (Fig. 5 B). After 2 weeks, expression of both *mmp* genes has returned to levels seen in ontogenetic scales.

Zymographic analysis

The medium from an overnight culture of scales demonstrates the presence of several molecular species with gelatinolytic activity (Fig. 6). To identify the molecular species and normalise the MMP activity, human recombinant MMP-2 and -9 were loaded in lanes 1 and 2, respectively. The largest molecular species secreted by scale cells, can be identified as the inactive pro*MMP-9*, which has been activated after electrophoresis by autocatalysis. The gelatinase with a weight of approximately 77 kDa, has been confirmed to be active *MMP-9* with Western blot (Fig. 6). The other two clear bands are predicted to be MMP-2, the other matrix metalloproteinase with a preference for gelatin. Both the latent form (approximately 67 kDa) and the active form (approximately 59 kDa) of zebrafish MMP-2 are several amino acids smaller than their mammalian counterparts [214]. The faint and heavy bands located around 150 kDa are most likely MMP-dimers, which are normally observed in zymographies [215].

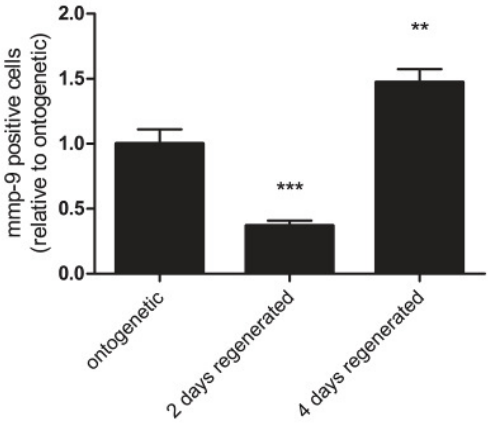

Fig. 3. Analysis of the number of *mmp-9* expressing cells in 2 and 4 days regenerating scales compared to ontogenetic scales. Significance compared to ontogenetic scales was calculated by means of a Mann-Whitney U test. Bars represent the mean value, error bars indicate S.D. (N=68-116, **: P<0,01; ***: P<0,001).

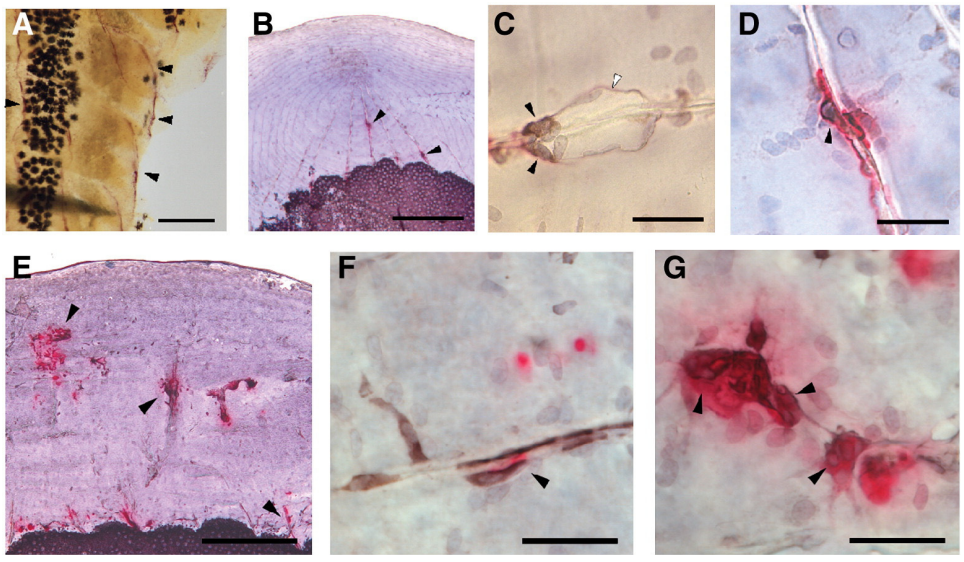

Fig. 4 Whole skin TRAcP staining (A) and *MMP-9*immunocytochemistry (black) combined with enzymatic TRAcP staining (red) in ontogenetic (B, C, D) and 8 day regenerating scales (E, F, G). **A** Overview of ontogenetic scales in the skin with stained for TRAcP. Positive cells are found along the margins (arrow heads), scale bar = 500 µm.

B overview of an ontogenetic scale with TRAcP staining along the radii (arrows); bar = 250 µm **C** *MMP-9* positive cells (black arrows) with minimal TRAcP staining in a typical resorption pit (white arrow) along a radius; bar = 50 µm. **D** mononucleated osteoclast with *MMP-9* immunoreactivity (arrow) along a radius; bar = 50 µm. **E** overview of a regenerating scale with irregularly distributed TRAcP positive areas (arrows); bar = 250 µm **F** Typical *MMP-9* positive cells with TRAcP secreted into the surrounding matrix (arrow) ; bar = 50 µm. **G** Typical multinuclear cells (arrows) positive for TRAcP and *MMP-9*. Note that nuclei are smaller in these cells; bar = 50 µm.

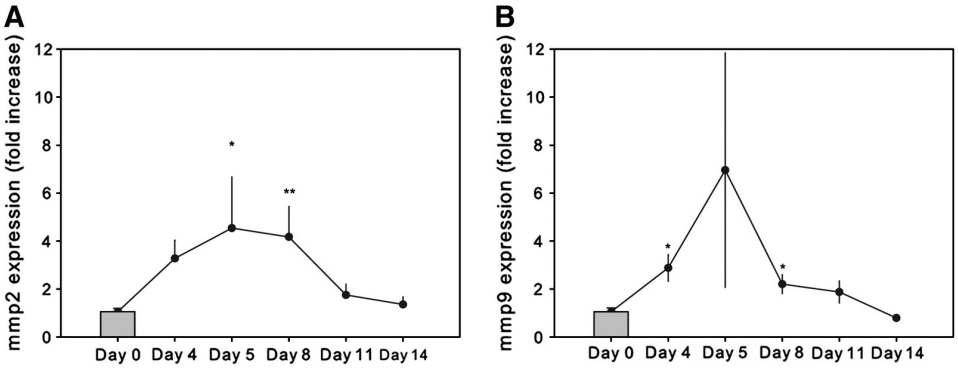

Fig. 5. rtQ-PCR. **A** expression of *mmp-2* in ontogenetic and regenerating scales. **B** expression of *mmp-9* in ontogenetic and regenerating scales. The solid bar represents the expression in ontogenetic scales. Significance was calculated by means of a Mann-Whitney U test. Points represent the mean value, error bars indicate S.E.M. (N=5, *: P<0,05; **: P<0,01).

The total amount of secreted gelatinases is increased in regenerating scales. Especially the activity of the lightest molecular species (active MMP-2) had increased, and the inactive pro*MMP-9* disappeared (Fig. 7A). An analysis of the intensity of the bands sheds more light on the changes in gelatinases expressed in ontogenetic and regenerating scales (Fig. 8). As mentioned above, no bands of 87 kDa could be detected in the regenerating scales. Significantly more of the putative active MMP-2 and *MMP-9* were present in the culture medium of regenerating scales. The amount of latent MMPs remained the same (67 kDa), or decreased (87 kDa).

The zymographic analysis of the scales from fish exposed via the water to GM6001 show clear differences between exposed fish and the control group (Fig. 7B). Although the scales have not been subjected to GM6001 during

culture, the *in vivo* GM6001 exposure resulted in bands of lower intensity compared to the control group.

Hydroxyproline assay

The modified amino acid hydroxyproline was used as a measure of matrix degradation. In culture medium of ontogenetic scales, hydroxyproline could not be detected. However, it could be detected in the culture medium of 6 day regenerating scales at a level of 0,2 ± 0,17 ng hydroxyproline per scale, which indicates increased matrix degradation in regenerating scales.

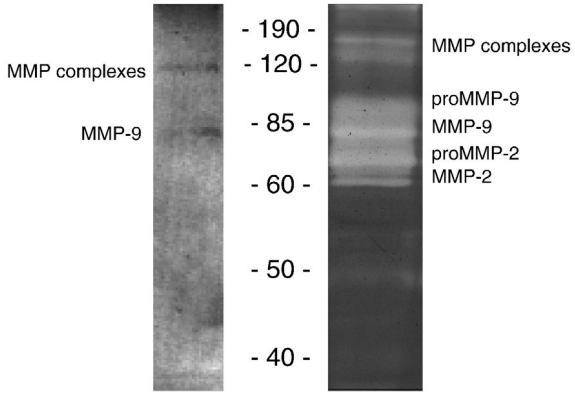

Fig 6. Anti-zf*MMP-9* Western blot (left) and zymogram (right) of the same medium sample from an overnight scale culture. The same band of 77 kDa is observed on the Western blot for *MMP-9* and the zymogram. MMP complexes are also observed.

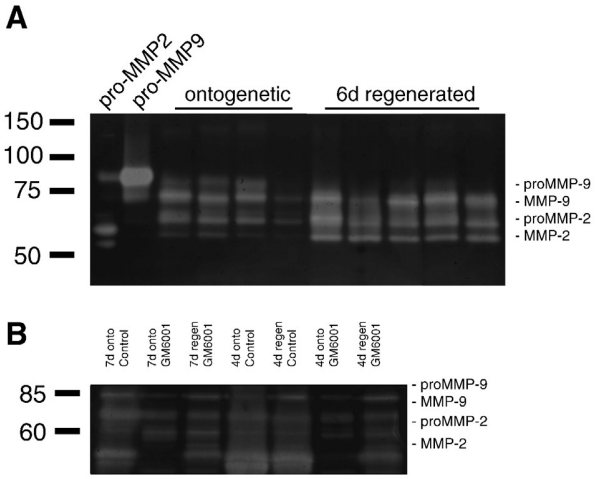

Fig. 7. **A** Zymographic analysis of medium from overnight scale cultures. The positive controls (human recombinant proMMP-2 and pro*MMP-9* are shown in the first two lanes. Lanes 3 to 6 show the gelatinolytic activity of MMPs excreted by ontogenetic scales. Lanes 7 to 11 show an increase in gelatinolytic activity of MMPs secreted by scales after 6 days of regeneration. **B** Zymographic analysis of 4 and 7 day ontogenetic and regenerating scales from fish exposed to GM6001 or vehicle. Gelatinolytic activity was attenuated in all groups of fish exposed to GM6001.

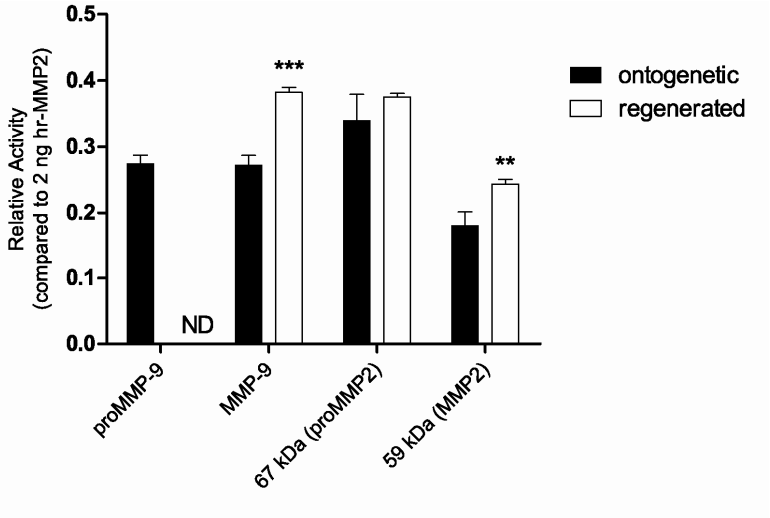

Fig 8. Semi-quantitative analysis of gelatinolytic activity on ontogenetic (closed bars) and regenerating (open bars) zebrafish scales. ND, not detectable. Bars represent mean values, error bars indicate S.E.M. Increase in the putative active MMPs tested for significance by means of a Mann-Whitney U test, N=4-5 (** P<0,01; ***P<0,001).

Discussion

We have shown both by *in situ* hybridisation and immunocytochemistry the presence of mononucleated and multinucleated *mmp-9* positive cells on the episquamal side of adult zebrafish (regenerating) scales. Plasma membrane staining and TRAcP - *MMP-9* double staining identified these cells as osteoclasts. We found an increase in expression of *mmp* genes, cell abundance, activity of MMPs and hydroxyproline levels during scale regeneration. These results combined confirm that MMPs and anticipated osteoclasts play an important role in scale resorption and Remodelling.

Although many other types of cells, such as fibroblasts and macrophages, are known to express *mmp-9* [216], the epidermis that covers the scale is completely devoid of *mmp-9* expressing cells. The wound that results from scale removal closes within two h [101]. This is an important notion as it confirms that gene expression and enzymatic activity reported here is not from inflammatory cells, but exclusively from scale cells.

The *in situ* hybridisation study revealed both mono- and multinucleated cells expressing *mmp-9* transcripts. To provide a better picture of the nature of these cells, scales were stained for plasma membranes and TRAcP. Double staining for TRAcP and *MMP-9* shows that these two osteoclasts markers are usually co-expressed. This is found for both the marginal and episquamal cells and defines these positive cells as osteoclasts. Indeed, mononucleated osteoclasts have been described in other thin zebrafish skeletal elements [26]. Inside the multinucleated aggregates, we did not see plasma membranes which prove that they are indeed multinucleated osteoclasts. They were found on both ontogenetic and regenerating scales. Our finding of mono- and multinucleated osteoclasts, expressing both *MMP-9* and TRAcP, provides further insight into the process of scale regeneration [101,200]. This is significant because TRAcP is considered to be a marker for osteoclasts able to resorb bone, as judged from "resorption pits" seen next to these cells.

The expression of *mmp-9* that we have found in marginal cells of ontogenetic scales is possibly related to the normal growth of scales that continues throughout the fish's growth. The irregular distribution of positive cells along the margins of ontogenetic scales shows that growth does not take place along the entire margin at the same time but is probably confined to different spots. Another explanation for these cells could be that they repair the normal wear-and-tear of individual scales. Cells expressing *mmp-9* transcripts are also found along the radii, where most areas of scale resorption are found. The hypothesis that radii are primary sites of calcium and phosphorus recruitment is supported by the presence of blood vessels above the radii enabling transport of those minerals [198]. Since we found no staining of cells on the hyposquamal surface, it is reasonable to conclude that hyposquamal scleroblasts, which have osteoblast-like characteristics [108], do not express *mmp-9*.

Both *in situ* hybridisation and quantitative PCR show that *mmp* genes are significantly up-regulated in regenerating scales from day 4 onwards. Interestingly, on early regenerating scales (2 days), only a few, mononucleated *mmp-9* positive cells are present on the new scale. At this point in regeneration, the first collagen matrix is deposited and has just started to mineralise (de Vrieze, unpublished data). There are no marginal *mmp-9* positive cells during early regeneration, likely due the complete new-formation of the scale. The increase in *mmp-2* and *mmp-9* expression is at its maximum around day 5. At this time, the scale plate has formed and the focus is already mineralised (de Vrieze, unpublished data). Histology revealed that on day 4 and 8, both mono- and multinucleated osteoclasts are present on the scale matrix. This coincides with the increased *mmp* expression and the initiation of scale plate Remodelling. After 10 to 14 days, expression of the *mmp-2* and *mmp-9* genes declines and returns to levels seen in ontogenetic scales. The scale plate is now formed and mineralised to its full extent, and will be remodelled to its original design [101].

To further establish the role of MMPs in scale regeneration, we investigated here the secretion of these proteins by scale cells. Our results show that the increase in secreted MMP activity in the medium by means of gelatin zymography correlates with the up-regulation in gene expression during scale regeneration. A significant increase is observed in putative active forms of the two gelatinases. The amount of latent proMMP in the medium remains the same or decreases, indicating that more MMPs are activated. The inhibition of MMP activity by *in vivo* exposure to the MMP inhibitor GM6001, further underlines the parallels between zebrafish and mammalian MMPs. The preferred substrates of active MMPs are gelatin, a product of collagen degradation, and to a lesser extent, native collagen. The switch to higher MMP activity indicates an increase in gelatin degradation and thus an increase in scale matrix degradation. As there are other substrates for MMPs [39], additional roles of MMPs in scale regeneration cannot be excluded by our findings. In mammalian bone development, *MMP-9* also regulates bioavailability of growth factors [40]. Nothing is known about the presence of growth factors on scales, but collagen and its degradation products (e.g. gelatin) are present to a large extent in the scale matrix [105]. The release of

hydroxyproline from regenerating scales confirms that the scale matrix is indeed degraded during regeneration as a result of Remodelling. Our data suggest that matrix proteolysis is an important function of matrix metalloproteinases during scale regeneration.

Conclusions

The gelatinases MMP-2 and *MMP-9*, expressed in mono- and multinucleated osteoclasts, play a pivotal role in the regeneration of zebrafish scales. These enzymes are specialised in degradation of extracellular matrix, and are likely to be involved in the Remodelling and organization of the scale surface, probably by shaping the radii and circuli. In mammalian bone of dermal origin, MMPs also function in the osteoclastic degradation of matrix. As a result of these parallels, scales may offer a valuable model to study the underlying mechanisms of osteoclastic bone resorption [217]. Their small size, short regeneration time and possession of cells that express important osteoblast and osteoclast markers, could make them particularly suitable for applications such as high throughput *in vitro* assays.

Chapter 5: Acute exposure to dexamethasone in early-life is associated with enduring effects on wound healing in zebrafish larvae

Abstract

The goal of this study was to assess the impact of an acute but brief DEX exposure in early-life (*prim-6* stage) on the ability to repair damaged tissue following amputation of the caudal fin at later life stages including 5 and 14 dpf in zebrafish larvae. We show that prior history of DEX exposure, that is not concomitant with an injury sustained later in life, significantly impairs wound healing long after DEX has been washed out at both life stages studied. We also show that DEX-induced impairments in wound healing can however be fully restored to normal levels with longer post amputation recovery time.

Analysis of the several outcome measures taken in this study including cell proliferation, cell death (necrosis and apoptosis), gene expression, and leukocyte cell marker (L-plastin) suggest that DEX exerted its effects in the early phase (4 h) of wound healing rather than in the later phases of the tissue repair process. A main event include massive amount of cell death both by necrosis and apoptosis at 4h post amputation, which is not compensated, at least as far as 24 h post amputation. The concomitant significant reduction in the number of L-plastin positive/leukocyte cells observed at 4 h post amputation suggest that these cells may have been among the large amount of cells lost via necrosis and apoptosis. Therefore, it is likely that DEX-induced reduction in the number of L-plastin positive/leukocytes observed in this study may not only have altered the clearance of cell debris but also lowered levels of growth factors and cytokines at the injury site. Such events may simultaneously

contribute to impede the initiation of the blastema formation and its progression, and results in impaired wound healing.

In sum, this study provides evidence that DEX exposure during early sensitive periods of development appears to cause permanent alterations in the cellular/molecular immune processes that are involved in the early phase of wound healing in zebrafish. These findings are consistent with previous studies showing that antenatal course of DEX are associated with immediate and lasting alterations of the immune system in later life in rodents, non-human primates, and humans. Therefore, the findings presented in this study support the use of the larval zebrafish as a valid model to study the impact of stress and stress hormone exposure in immature organisms on health risks in later life.

Introduction

Stress and wound healing

A large core of epidemiological data shows the pervasive effects of both major and minor stressful life events on health including the worsening of existing illnesses [218-221]. One manifestation of this phenomenon is the impact of psychological stress on wound healing in humans. Several studies have clearly demonstrated the slowing of wound healing by psychological stressors including marital conflicts/hostility [221], examination stress [222], and caring for a relative afflicted with a debilitating disease [221]. Complex interplays between the neuroendocrine and immune systems mediate these effects [3][218,223]. One immediate function of the immune system during the early phases of wound healing is to sterilize the wound area and remove dead cells and bacteria. Once the wound has been cleared of debris, cells of the immune system (neutrophils, and leucocytes) play a key role in secreting a wide range of molecules (e.g. TGFα, TGFβ1, TGFβ2, TGFβ3, FGF, PDGF, IL-1,IL-4,IL-8,G-CSF,GM-CSF) that favour subsequent migration and division of cells involved in the proliferative phase of wound healing, just proximal to the injured site, and which results in tissue outgrowth replacing the damaged structure [1] (Table 1).

Progress in the understanding of the interplay between the stress and immune systems revealed that stress, via the stress hormone glucocorticoid (GC)

(cortisol in humans and fish, and corticosterone in rodents), exerts significant detrimental effects in the early phases of the inflammatory response [224]. Specifically, both stress-induced up-regulation of GCs as well as synthetic GC exposure have been shown to impacts the early phase of wound healing (within 4 h) by decreasing the number of immune cell types such as neutrophils, leukocytes, and macrophages recruited at the wound site as well as by down-regulating the expression of their secreted factors such as interleukin 1 (IL-1),interleukin-4 (IL-4),interleukin-5(IL-5), interleukin 8 (IL-8), chemokynes, cytokines and tumour necrosis factor- α (TNF-α) [225,226]. Globally, these GC-mediated events are believed to underlie the slowing of wound healing [218,227]. Conversely the stress-reduction intervention programs have been shown to up-regulate several components of the early immune response, and greatly accelerate wound healing in humans [218], thus confirming the importance of the GC pathway in wound and tissue repair.

Antenatal glucocorticoid exposure and enduring consequences on immunity

In parallel, exposure to various stressors and synthetic CGs in early life also trigger significant and enduring effects on both the neuroendocrine and immune systems [218,228-231]. One prominent example is the clinical practice consisting of administering the synthetic GC dexamethasone (DEX) during late gestation in situations where risks of premature deliveries are elevated [232-237]. This procedure is meant to promote foetal lung maturation and treat inflammatory complications of the respiratory system of newborn infants [238-240]. Though to be safe, this procedure was found to be associated with a host of side effects with far reaching impact on physical and mental health throughout the lifespan [5]. Relevant to the current study, antenatal DEX exposure has been associated with enduring consequences on immunity in two important ways: 1) long-lasting alterations of the stress-regulating system (referred to as the hypothalamic-pituitary-adrenal (HPA) axis leading to conditions of GC resistance (via decreased GC function or GR number and/or function) has been shown to impair immune responses in adulthood [223]. Immediate interference with thymus development leading to enduring changes in the structure of the thymus [241], T cell proliferation [228], cytokine

production [241,242], as well as predisposition to autoimmune disorders [242]. These findings suggest that exposure to stress and GCs during development exerts programming effects on the immune system, which may account to explain individual differences in the ability to deploy adequate immune responses in later life. In the present study, we have investigated the impact of DEX exposure during early development on later ability to repair tissue damage in zebrafish.

A novel model of wound healing in zebrafish: the caudal fin amputation paradigm

Because lower animals like urodeles and amphibians and many invertebrates have retained their regenerative capabilities to a remarkable extent throughout evolution, they have been widely used to deepen our understanding of the processes underlying wound healing and tissue regeneration. This is in sharp contrast with humans and other vertebrate species, which have retained a much less spectacular regenerative capacity, which is mostly restricted to the liver and fingertips [6,7]. One exception is the zebrafish, a vertebrate species endowed with a remarkable capacity to regenerate their fins, optic nerve, scales, heart, and spinal cord [2,243,244]. Over the last decade, the zebrafish has become a model of choice to investigate molecular pathways involved in regeneration and relevant to those of higher vertebrates, including humans [2,197,245]. One of the well-established zebrafish models of tissue regeneration is the caudal fin amputation model. This procedure consists of amputating the caudal fin at the neural keel, without touching the notochord. This procedure is typically performed on 2 day-old embryos [12]. By the third day post amputation (dpa), larval zebrafish can fully regenerate and replace their lost caudal fin including its shape, size, and structure, which become undistinguishable from that of intact larvae of an equivalent life stage [121]. Caudal fin regeneration involves three overlapping steps that are depicted on table 1 and including: 1) wound healing (0–3 h), 2) blastema formation (4–6 h), and regenerative outgrowth, which is divided into an early phase (6-24 h) and late phase (24-48 h). Within 10 min of the wound healing process, epithelial cells begin to migrate over the injured site, where the wound is sealed with actin-purse ring structure. During the blastema stage, cells proximal to the

amputation site initiate a process of dedifferentiation and become momentarily pluripotent cells with the capability to proliferate and differentiate into the various cell types required to regenerate lost tissue [119,120]. The process of cell proliferation and differentiation, gradually leads to tissue outgrowth and eventually to a full recovery of the lost tissue by 3 dpa [121].

It is noteworthy that the caudal fin amputation model can be as reliably performed in both larval and adult zebrafish since the molecular mechanisms of tissue regeneration comprising all cell types (e.g. four cell types in wound epidermis, three cell types in blastema and one *mmp-9* expressing cell type) [117] and key molecules (listed in Table 1), which are strikingly similar between larval and adult zebrafish. These qualities make the larval zebrafish model of caudal fin amputation especially attractive for forward genetic and high-throughput screening of molecules modulating the processes involved in tissue regeneration [121].

Goal of the study

Understanding the mechanisms by which stress and stress hormones slow the wound healing process and delay tissue repair is important. While GCs are known to be potent suppressors of tissue repair in acute exposure regimen concomitant with injury in several animal models [223], relatively little is known about the impact of acute GCs exposure prior (in early-life) but not concomitant with injury (later in life) on the individual's ability to repair damaged tissue. To address this issue, we assessed whether synthetic GCs (i.e. DEX) acutely administered prior but not concomitant with the caudal fin amputation procedure would also impair abilities to repair damaged tissue in the larval zebrafish model. Specifically, we performed the following steps: 1. We assessed the impact of early-life (stage *prim-6*) acute DEX exposure on the subsequent ability to repair damaged tissue following the caudal fin amputation procedure, which was performed later in life at two time points including 3 days

Table 1 Schematic representation of regeneration

schematic	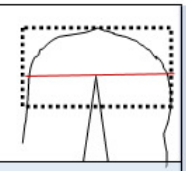	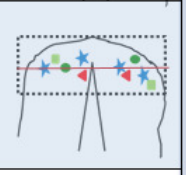	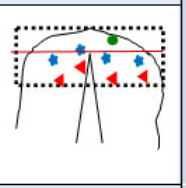	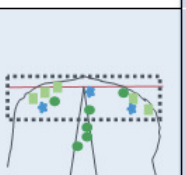	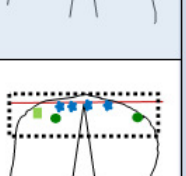
Time point	0-3hpa	4-24hpa	24hpa	48hpa	
Phases	Wound healing	Blastema formation	Early Regenerative outgrowth	Late Regenerative outgrowth	
Genes Involved	*β-catenin, lef1, wnt ligands,apoE (bmp2b), (shh), patched1, msxA and msxD, junb, junb*	**Wound epidermis** *apoE; β-catenin; msxa*[3]; *msxd* [3]*wfgf,fsdf-1a,b, Cxcr4a,b,junbl, junb,dlx5a,wnt3a* **Basal layer of wound epidermis** *apoE; bmp2b*[4]*, lef1; shh*[4]*, ptc1*[4]*, wnt5* **Forming blastema *bmp4***[5]*, eve1*[6]*, evx1*[7]*, evx2*[6]*, fgfr1*[8]*, hoxd11*[5]*, hoxd12*[5]*, msxb*[3 8]*, msxc*[3,8]*, RAR-gamma*[9] *hoxc13a,b*[10] **Differentiating scleroblasts** *bmp2b; ptc1; evx1*	**Wound epidermis** *apoE; -catenin; msxa; msxd; wfgf* [8]*,* dlx4 **Basal layer of wound epidermis** *apoE; bmp2b; lef1; fgfr1; ptc1; shh; wnt3a*[2]*; wnt5* **Blastema** *bmp4; eve1; evx2; fgfr1; hoxd11; hoxd12; lef1; msxb; msxc; RAR-gamma* **Scleroblasts** *bmp2b; evx1; ptc1, col2a1*	
Description	Actin purse ring forms/ Stump surface covers with epithelial cells	Cell proliferation increases, cell death occurs, necrosis occurs, Immune cells arrange at the amputation site	Epithelial cells are tightly packed Proliferation occurs, reduction in necrosis and cell death, immune cells still present		
	Actin purse ring forms/Stump surface covers with epithelial cells	Lesser cell proliferation , more cell death, More necrosis, Immune cells disrupted	Proliferation less than controls, more necrosis, cell death same as control, immune cell count not significantly different from controls		

References: 1, Mannat et al., 1999; 2, Poss et al., 2000a; 3, Akimenko et al., 1995; 4, Laforest et al., 1998; 5, Geraudie et al., 1998; 6, Enulfert et al., 1998; 7, Barday et al., 2001; 8, Poss et al., 2000b; 9, White et al., 1994.10,Ryan Thummel et al 2007

(Experiment 1) and 11 days (Experiment 2) following initial exposure to DEX. In both groups, a 2 day-post amputation recovery period was given after which the extent of tissue damage/repair was measured.

2. We also assessed whether the impairing effects of early-life DEX exposure on tissue repair processes observed in experiment 1 would be restored to levels comparable to that of controls if given longer post amputation recovery period. This was achieved by allowing longer recovery time following caudal fin amputation. In this group the extent of tissue damage/repair was assessed much later following amputation, i.e. 11 days (experiment 3). Note that this experiment could not be performed on individual older than 14 dpf (experiment 2) due to technical difficulties.

3. In order to get insights into the mechanisms underlying the lasting effects of DEX on tissue repair processes observed in experiment 1, we have taken the following endpoint measurements: 1) size of the regenerated area of the caudal fin, 2) analysis of a panel of regeneration-related genes (msxb, wnt3a, rarg, hoxd11, GR and MR) via qRT-PCR, 3) cell death (Tunnel and acridine orange), 4) cell proliferation assay (BrDU), and 5) quantitative analysis of immune cells invasion at the wound site using immunohistochemistry against L-plastin, a macrophage and leukocyte marker.

Materials and Methods

Statement of ethics on animal use

All experimental procedures were conducted in accordance with The Netherlands Experiments on Animals Act that serves as the implementation of "Guidelines on the protection of experimental animals" by the Council of Europe (1986), Directive 86/609/EC, and were performed only after a positive recommendation of the Animal Experiments Committee had been issued to the license holder.

Zebrafish maintenance

Male and female adult zebrafish (*Danio rerio)* of AB wild type were purchased from Selecta Aquarium Speciaalzaak (Leiden, The Netherlands) who obtains

stock from Europet Bernina International BV (Gemert-Bakel, The Netherlands). Fish were kept at a maximum density of 12 individuals in plastic 7.5 L tanks (1145, Tecniplast, Germany) containing a plastic plant as tank enrichment, in a zebrafish recirculation system (Fleuren & Nooijen, Nederweert, The Netherlands) on a 14 h light: 10 h dark cycle (lights on at 7h AM: lights off at 21 h PM). Water and air temperature were maintained at 24 ^{o}C and 23 ^{o}C, respectively. Fish were purchased at the juvenile stage and were allowed to adapt to our facility for at least 2 months before being used as adult breeders. The fish were fed daily with dry food (DuplaRin M, Gelsdorf, Germany) and frozen artemias (Dutch Select Food, Aquadistri BV, The Netherlands).

Zebrafish eggs were obtained by random mating between sexually mature individuals. Briefly, on the day (16h) before eggs were required, a meshed net allowing eggs to pass through but preventing adult fish from accessing/eating them, was introduced in the home tank of a group of 12 adult fish. Each breeding tank was only used once per month to avoid handling stress and ensure optimal eggs quantity and quality.

Selection of the dosage of DEX

The dosage (1 mM) of water soluble DEX (Sigma *Aldrich,* Switzerland) used in the present study was chosen based on a pilot study where four concentrations of DEX, including 100, 250, 500 and 1000 µM were tested on embryos at the life stage 25 hpf (equivalent to the *prim-6* stage [122] for a duration of 6 h. The caudal fin amputation procedure was performed on 3 dpf and assessment of regenerative capacity was done on 5 dpf. We found that dosages of 500 µM ($p< 0.01$) and 1000 µM ($p< 0.001$) of DEX significantly reduced tissue regeneration relative to controls (Fig.1 A). Note that no mortality or morphological abnormalities (Fig.1 B) were observed between the different treatment groups. Therefore, we selected the highest dosage of DEX (1 mM) because of its pharmacological safety and largest impact on tissue regeneration.

DEX Treatment

The eggs were harvested 30 min after the onset of lights at 7 h AM and age was set as dpf 0. This is based on the staging system employed in the zebrafish text book untitled *Zebrafish: practical approach* [43]. Approximately 150 eggs were transferred in 10 cm Petri dishes filled with 50 ml of egg water (0.21 g/l Instant Ocean Sea Salt and 0.0005% (v/v) methyl blue) and housed in a separate climate room maintained at a temperature of 28 °C and 50% humidity and under a light-dark cycle of 14h: 10h (lights on at 7h AM/lights off at 21 h PM). When all embryos reached the stage *prim-6* (25 hpf) they were then transferred to 6-well plate (25 embryos/well) and immediately exposed to an acute pulse of DEX. DEX treatment consisted of exposing the embryos for 6 h to water-soluble DEX (1 mM). At the conclusion of the treatment, the embryos were then washed 3 times with egg water and transferred to new clean 6-well plates (30 embryos/well), where they remained undisturbed for 2 days (experiment 1, see details below) and 11 days (experiment 2, see details below). The control group was treated according to the same procedure as described above except that the DEX exposure step was replaced by egg water only. The larvae were placed in the fish facility at 25°C in large tank in egg water till 7 dpf and later on in regular water as for adult fish. The tanks were cleaned every day. The larvae were fed on baby fish food 2x a day.

Experimental Procedure

The timeline and the experimental steps involved in the caudal fin amputation procedure are depicted in Fig. 2. Also see section 2.6 for details regarding the caudal fin amputation method. In the current study, we have performed three separate experiments, which are described below:

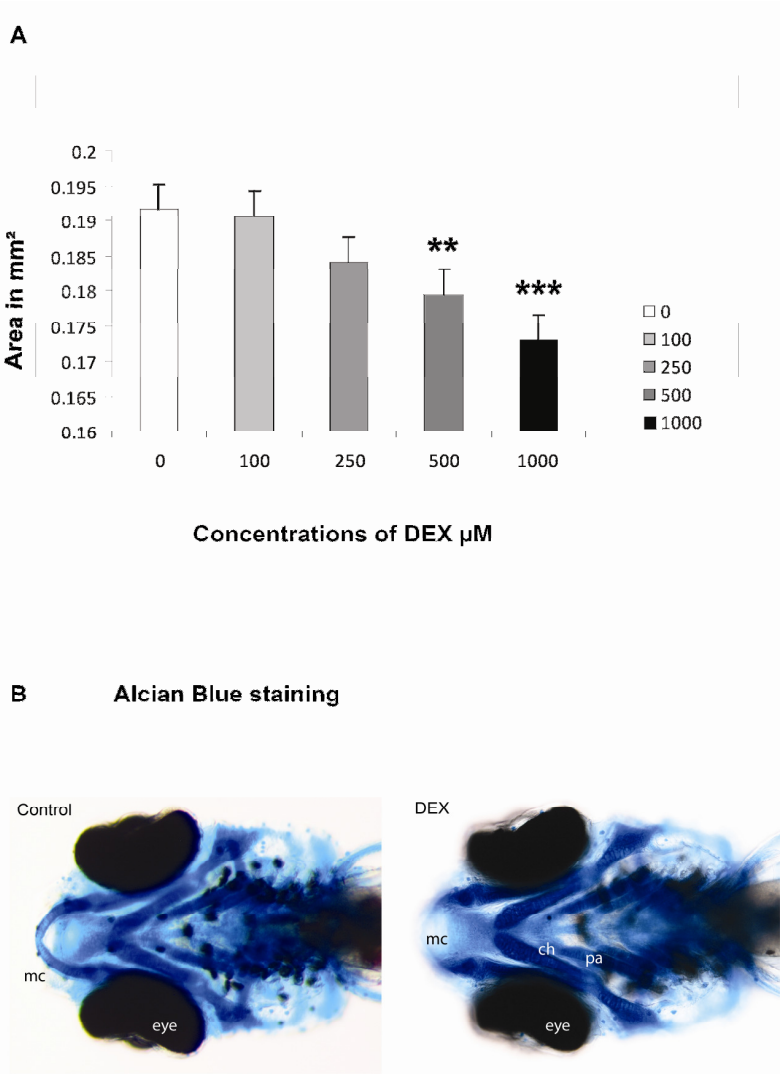

Fig. 1 (A) Effect of varying dosages of dexamethasone (DEX) on tissue regeneration. DEX treatment was administered at the life stage *Prim-6* and lasted 6h. Results show that dosages of 500 µM and 1000 µM significantly affected tissue repair. (**B**) Alcian Blue staining shows that DEX treatment (dose 1000 µM) did not cause any morphological alterations relative to control treatment. All measures presented in panel A and B were performed on 5 dpf larvae. Abbreviations: mc (Meckel's cartilage), ch (ceratohyal) pa (pharyngeal arches), and eye.

Experiment 1: The detailed methodology is presented in Fig. 2A. Briefly, embryos were exposed to DEX (1 mM) at 25 hpf (prim-6) for 6h. On 3 dpf (protruding mouth stage), the embryos were anesthetized with 0.04% Tricaine (MS222, Sigma) after which amputation of the caudal fin posterior to neural keel was performed with a sharp scalpel (see section 2.6). Immediately after amputation larvae were washed 3 times with egg water and then gently transferred to new 6-well plates using a Pasteur pipette. A post amputation recovery period of 2 days was given after which the extent of tissue damage/repair was assessed by measuring a number of outcome measures on 5 dpf-old larvae (see section 2.7).

Experiment 2: The detailed methodology is presented in Fig. 2 B. Embryos were treated exactly according to the procedure described in experiment 1 with the exception that the caudal fin amputation procedure was performed 11 days following DEX exposure (i.e. on 12 dpf-old larvae). Following amputation, larvae were transferred to new tanks (plastic 7.5 L tanks from 1145, Tecniplast, Germany). The post amputation recovery period was the same as in experiment 1, i.e. 2 days. For this experiment, only the size of the regenerated area was measured (see section 2.7.1)

Experiment 3: The detailed methodology is presented in Fig. 2 C. Since findings obtained from experiment 1 showed that acute DEX treatment (1 mM) caused significant reduction in tissue regenerative capacity 2 days post amputation (measured in 5 d old larvae), we assessed whether the impairing effects of DEX on tissue regeneration would recover to a level comparable to that observed in DEX-untreated animals with longer post amputation recovery period. To achieve this goal, larvae were treated exactly as described in experiment 1 with the exception that a longer post amputation recovery period was given, i.e. 11 days. For this experiment, only the size of the regenerated area was measured on 14 dpf-old larvae.

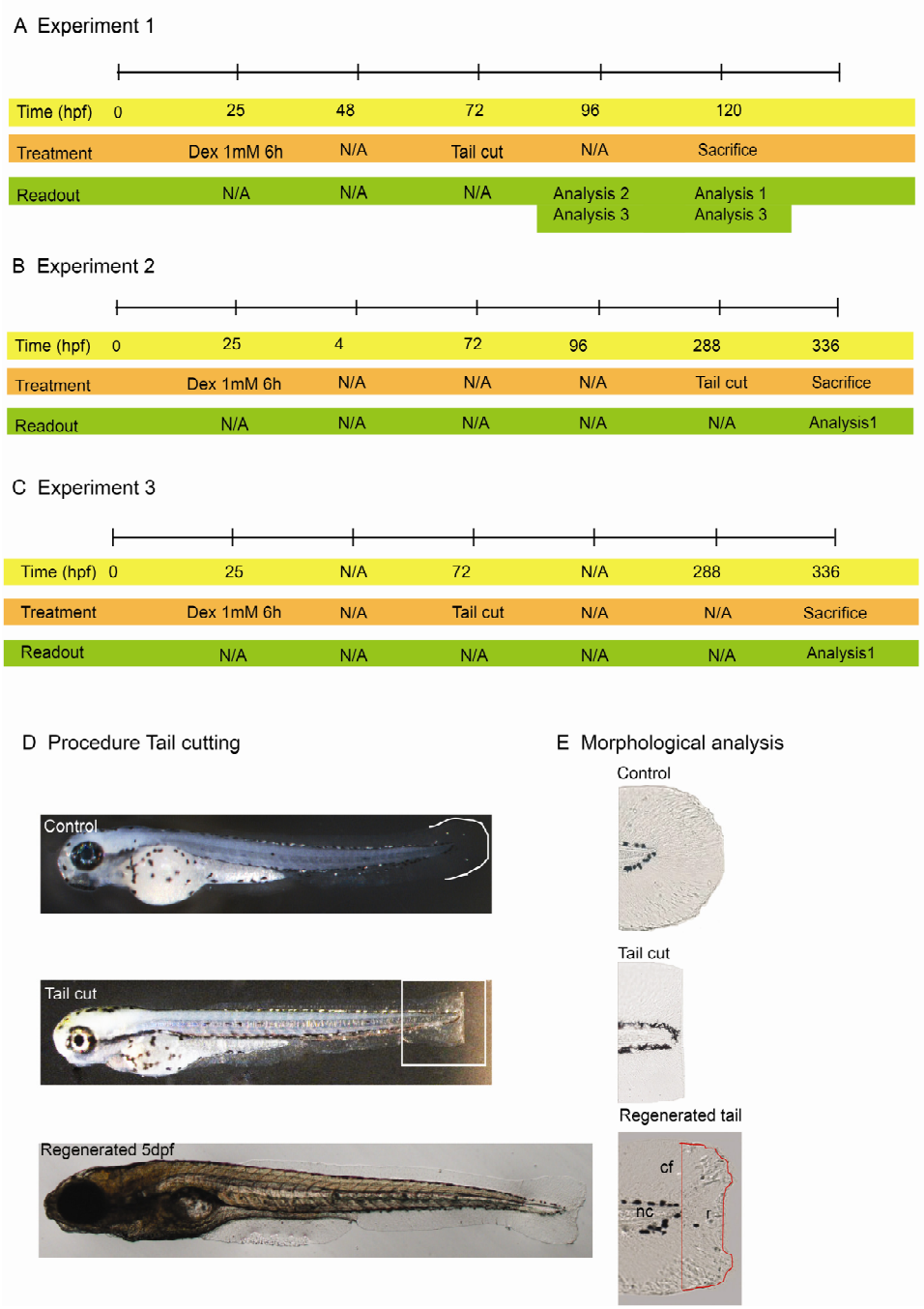

Fig. 2: Overview of the experimental procedure: **(A)** Time line of the experimental procedures performed in experiment 1. The procedures include DEX (1 mM) treatment

at 25 hpf, which lasted 6 h, caudal fin amputation at 72 hpf and termination of the experiment at 120 hpf. Analyses 2 and 3 were performed on 96 hpf while analyses 1 and 3 were done at 120 hpf. **(B)** Time line of experiment 2 is identical to that of experiment 1 with the exception that the caudal fin amputation was performed later on 288 hpf. Termination of the experiment occurred at 336 hpf. Note that only analysis 1 was performed at this time point. **(C)** Time line of experimental 3 was similar to the time line of experiment 1 with the exception that the end of the experiment and analysis 1 were performed later, i.e. at 336 hpf. (**D**) Caudal fin amputation procedure. The top photograph (control) depicts a typical larva with an intact caudal fin while the photograph (tail cut) below depicts a representative example of a larva, which underwent the caudal fin amputation procedure. Note that both larvae are 3 dpf. The amputation plane was kept near the caudal end of neural keel (boxed area). (**E**) Morphological analysis. The top photograph (Control) depicts a high magnification image of normal tail while the middle photograph (Tail cut) depicts a high magnification image of the amputated caudal fin. The bottom photograph depicts a representative example of a regenerated caudal fin at 5 dpf. Analysis of the regenerated tail was performed by outlining the area of the regenerated caudal fin as shown in the photograph (see red line). This area is referred to area 'r'. Measurement of the volume of the regenerated area 'r' was automatically calculated using image J. Analysis 1 includes the measurement of regenerated area of amputated caudal fin with image J. Analysis 2 includes the necrosis, cell proliferation, and apoptosis assays. Analysis 3 includes qRT PCR analysis for expression of GR, MR, hoxd11, msxb, wnt3a and RARγ. Abbreviations: DEX: dexamethasone, GR: glucocorticoid receptor, MR: mineralocorticoid receptor, nc: notochord, cf: caudal fin, N/A: not applicable, hpf: h post fertilization.

Caudal Fin Amputation Procedure

Caudal fin of 3dpf zebrafish embryos were amputated after anesthetising with 0.04% MS-222 (tricaine methanesulfonate). The embryos were placed in the 9cm Petri dish filled with egg water on their lateral side. With a sharp scalpel the caudal fin was carefully cut off under a dissecting microscope along the amputation plane depicted in Fig 2 C and D. After amputation the embryos were transferred 2 x through fresh egg water in separate Petri dishes and then to 6well plate till outcome was measured until 5 dpf (experiment 1) and 14 dpf (experiment 2 and 3), where the experiment was terminated. The larvae were sacrificed by an overdose of anesthesia (tricaine), and were fixated in 4% PFA at 4°C overnight.

Outcome Measures

Assessment of Tissue Repair Capacity

In order to prepare the tissue for morphological analyses, larvae were anesthetized with tricaine and then fixed in chilled 4% PFA over night. This procedure was equivalently performed for experiments 1 and 2 but at different time points depending on the specifics of the experiment, i.e., at 5 dpf (experiment 1), and 14 dpf (experiments 1 and 2). Following fixation, the area of the caudal fin was imaged under a Nikon eclipse E800M equipped with DSF1 camera. (Fig.2D). Area of the regenerated caudal fin was outlined as performed in Fig. 2D and referred to area 'r'. Measurement of the regenerated area 'r' was automatically calculated using image J (National institute of health. See: http://rsbweb.nih.gov/ij/).

Cell Proliferation

To perform a quantitative assessment of cell proliferation, we used the well-established cell proliferation marker BrDU [246]. Briefly, larvae were treated with BrDU beginning 24 h post amputation until 30 h post amputation according to a protocol described previously [121]. At the conclusion of the 6h-BrDU treatment, larvae were immediately fixed in 4% PFA at 4 ^{o}C over night. The tissue was prepared for confocal imaging by undergoing a series of washes with phosphate buffers and dehydration steps with methanol (25%, 50%, 75%, and 100%). Subsequently, the tissue was stored at -20^{o}C until the next day where labelling with fluorescent antibodies was performed. The next day, prior to immunohistochemical staining the larvae were labelled with anti-BrdU antibody (Roche) at a dilution of 1:200 and Alexa flour 534 conjugated anti mouse IgG (Molecular probes Eugene) for 2h at room temperature. Tissue was maintained at 4^{o}C while confocal images were taken for morphological assessments. All samples (Veh n=25 and DEX-treated n=25) were processed within the same day.

Necrosis

For quantitative assessment of necrotic cell death induced by caudal fin amputation and/or antenatal exposure of DEX, acridine orange staining was

performed to label necrotic cells at 4 h and 24 h post amputation in both control and DEX-treated groups. Acridine orange staining consisted of soaking living larvae in a freshly prepared solution of acridine orange stain (200 µM/L distilled water) (Schmid and Co, Stuttgart-Unterturkheim, Germany) for 1 hr at 28^{o}C. After several washes with egg water, living larvae were placed into a cavity glass slide and covered with a thin cover slip, and then imaged under a Zeiss Observer LSM 500. Since acridine orange is fluorescent, necrotic cells were visible at an excitation wavelength of 488 nm. Total number of fluorescent cells was counted with image J.

Apotosis

For assessment of cell death by apoptosis, terminal deoxy-nucleotidyl-transferase-dUTP nick end labelling (TUNEL) was used. The staining procedure consisted of taking fixed (4% PFA) larvae and rehydrating them through graded series of methanol, including 75%, 50%, 25% and phosphate buffer (15 min/solution). Embryos were further washed for 3 time 5 min in phosphate buffer (pH 7.4). We used a commercially available TUNEL labelling kit (TACS® TdT *in situ* – Fluorescein, R&D Systems, Inc. 614 McKinley Place NE) and followed the manufacturer's instructions. Images of the caudal tail area for all larvae were taken using a Zeiss observer LSM 500 microscope using excitation wavelength 488nm. Total number of tunnel-stained cells was counted manually from the images.

Gene Expression

Gene expression levels were measured by qRTPCR [247]. The protocol, methodology and primers (Invitrogen) used for each gene measured in the current study are derived from previous work [10,112,137,140,248] (See Table 1 for sequences).

Table 1. Primer sequences used for qRT-PCR.

Primer	Nucleotide sequence 5`-3`	Reference

wnt3a dr F	TGGGCTCACGCGTGTCATGG	Shimizu et al 2004 [137]
wnt3a dr R	GCGGAGCTGTTTGGGGACCA	
ß-actin F	TGTCCCTGTATGCCTCTGGT	
ß-actin R	AAGTCCAGACGGAGGATGG	Alsop et al 2007 [249]
GR F	ACAGCTTCTTCCAGCCTCAG	Alsop et al 2007 [249]
GR R	CCGGTGTTCTCCTGTTTGAT	
MR F	CCCATTGAGGACCAAATCAC	Alsop et al 2007 [249]
MR R	AGTAGAGCATTTGGGCGTTG	
RARγ F	GCTTGGACCGGGACAGCCAG	White et al 1994 [112]
RARγ R	GAGGTGGCGGGGAAGGGGAA	
Msxb F	GAA TTC TCC TAA GGG ACC C	NM131260 [140]
Msxb R	GATTCAACACTGAACGGGAGG	
Hoxd11 F	AATCCTCCGTTTCAACCTGCGATGG	Van der Hoeven 1995 [248]
Hoxd11 R	GCATCTCTTCTTTCTGGACTTTGTCG	

Total RNA was extracted using Trizol® reagent (Invitrogen Life Technologies, Belgium) according to the manufacturer's protocol. Note that for all genes studies, the cDNA was taken from the amputated tails and not from the whole animal. The following categories of gene were measured: 1) GC receptors (MR and GR mRNA) [129], tissue differentiation markers associated with tissue patterning (wnt3a and RARγ mRNA) [16,17], and cell proliferation markers

(msxb and hoxd11 mRNA) [18]. All genes were measured at two points including 24 h and 48 h post amputation.

Immune Cell Staining

The L-plastin immunostaining procedure used in the current study was derived from a previous study from Cui and colleagues [191]. Briefly, caudal fin tissue was incubated over night at 4°C in blocking buffer containing an antibody directed against L-plastin [final concentration 1:500] [181]. Embryos were incubated for 2 h at RT in Alexa Fluor 405 Goat-anti-Rabbit (Invitrogen) 1:200 and were then stored at 4°C and imaged using Zeiss observer LSM 500.

Statistical Analysis

Statistical analyses and graphs were performed using GraphPad Prism software (version 5.0). One-Way ANOVA analysis was performed to analyze the effects of DEX treatment with varying dosages including 100 µM, 250 µM, 500 µM and 1000 µM on tissue regeneration. A Dunnett's multiple comparison post-hoc test was applied to further decompose group comparisons, where each dosage of DEX was compared to the vehicle treatment (DEX 0 µM/egg water). Student T-tests (two-tailed) were performed to analyze the impact of DEX (1 mM) treatment on tissue regeneration (Experiments 1, 2 and 3) as well as to analyze the impact of DEX (1 mM) on gene expression and cell proliferation (BrdU). Two-Way ANOVA analyses were performed to analyze the data from the acridine orange staining, tunnel staining, and L-plastin immunohistochemistry. Tukey's multiple comparison post-hoc tests were applied to further decompose group comparisons. Data are presented as mean ± SEM, and a probability level of 5% was used as the minimal criterion of significance.

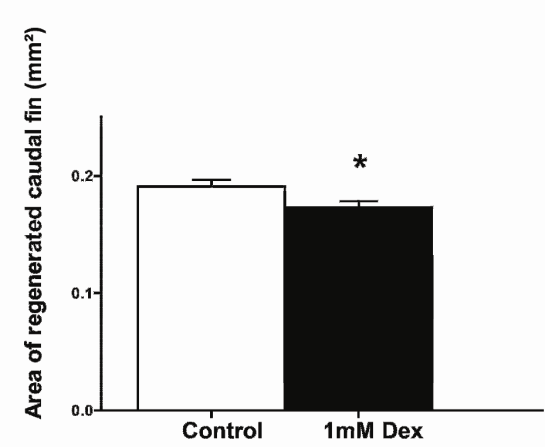

Fig. 3 Area of caudal fin (mm^2) amputated at 3 dpf and regenerated for 48 h. Measurements were done with Image J.

Results

Experiment 1

Relative to the control group, DEX-treated embryos displayed significant decreases in the total area of the regenerated caudal fin tissue at 2 days post amputation (Fig. 3) ($p< 0.05$). In order to gain insights into the possible mechanisms underlying DEX effects, we have measured the following outcome measures including, cell proliferation, necrosis, apoptosis, gene expression, and macrophage markers. The results are presented below:

Cell Proliferation

Relative to controls, we observed a significant reduction in the number of proliferating cells in the regenerating caudal fin in DEX-treated embryos 24 to 30 hrs post amputation (Fig. 4 A) ($p< 0.001$). Confocal images confirm that only the amount and not the appearance and/or distribution of proliferating cells is altered by prior exposure to DEX (Fig. 4 B).

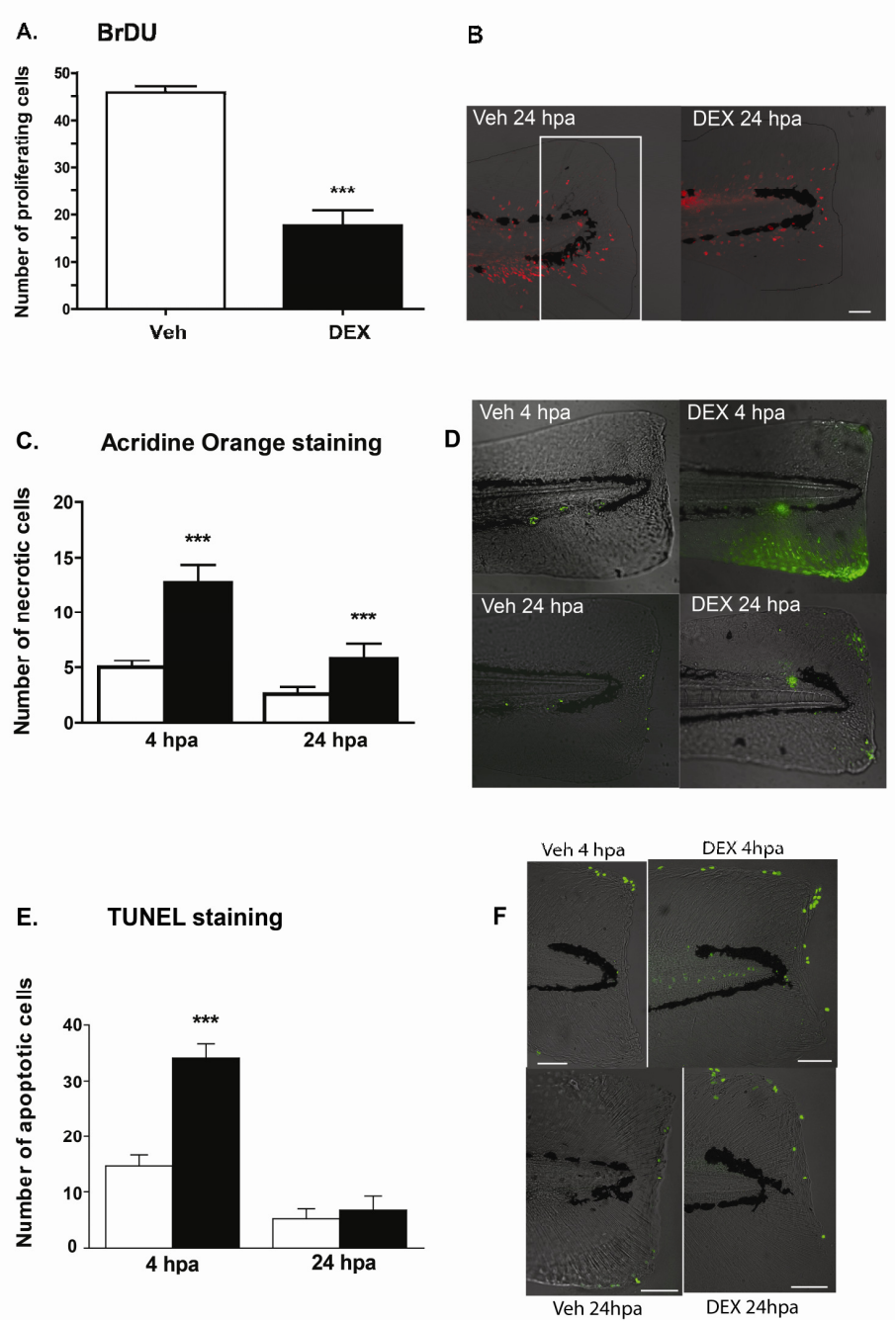

Fig. 4 (**A**) Number of proliferating cells in the regenerated caudal fin after 24-30 hpa is significantly reduced in DEX treated larvae. (**B**) Confocal images showing proliferating

cells (red) in the caudal fin region of the regenerating tails of larvae. Number of the cells was counted within the boxed area. (**C**) Number of necrotic cells labelled with acridine orange staining after 4h and 24h of amputation. The results show a significant increase in cell death in DEX treated larvae as compared to controls. (**D**) Confocal images of (upper left) veh 4hpa and DEX 4hpa (upper right), veh 24hpa (lower left) and DEX 24hpa (lower right) showing necrotic cells (green) in the regenerating tail region in living embryos. (**E**) Number of apoptotic cells labelled with Tunel staining at 4hpa and 24hpa. (**F**) Confocal images of Veh 4hpa (upper left) and DEX 4hpa (upper right), 24hpa Veh (lower left) and 24hpa dex (lower right) dead cells (green).

Cell Death

Analysis of necrotic cell death reveals significantly higher amount of necrotic cells in DEX-treated embryos relative to controls both 4 h ($p< 0.001$) and 24 h ($p< 0.001$) post amputation (Fig. 4 C). Confocal image analysis showed that, for both time points studied, necrotic cells were not aligned within the amputation plane but were rather accumulated at the dorsal and ventral corners of the regenerating fins (Fig. 4 D). Analysis of apoptotic cell death showed significant increases in the number of apoptotic cells at 4 h ($p< 0.001$) but not 24 h post amputation (Fig. 4 E). Confocal image analysis showed that in general the apoptotic cells were aligned with the amputation plane but were also present in the notochord region. Note that this was only observed at 4 h post amputation and appear to have returned to control levels by 24 h post amputation (Fig. 4 F).

Gene Expression

We observed that, while the expression of the GR receptor mRNA (MR and GR) (Fig. 5 A and B) and proliferations markers mRNA (msxb and hoxd11) (Fig. 5C and D) were not significantly altered by prior exposure to DEX, significant changes in the expression levels of genes involved in tissue patterning (wnt3a and RARγ) were observed in DEX-treated embryos relative to controls (Fig. 5E and F). Specifically, we observed a significant up-regulation of wnt3a in DEX-treated embryos relative to controls at 24 h ($p< 0.05$) but not 48 h post amputation (Fig. 5 E). We also observed a significant up-regulation of RARγ mRNA levels in DEX-treated embryos at 24 h post amputation (Fig. 5 F) ($p< 0.05$). We observed an opposite effect of DEX on RARγ mRNA levels at 48 h post amputation, which were significantly down-regulated (Fig not shown).

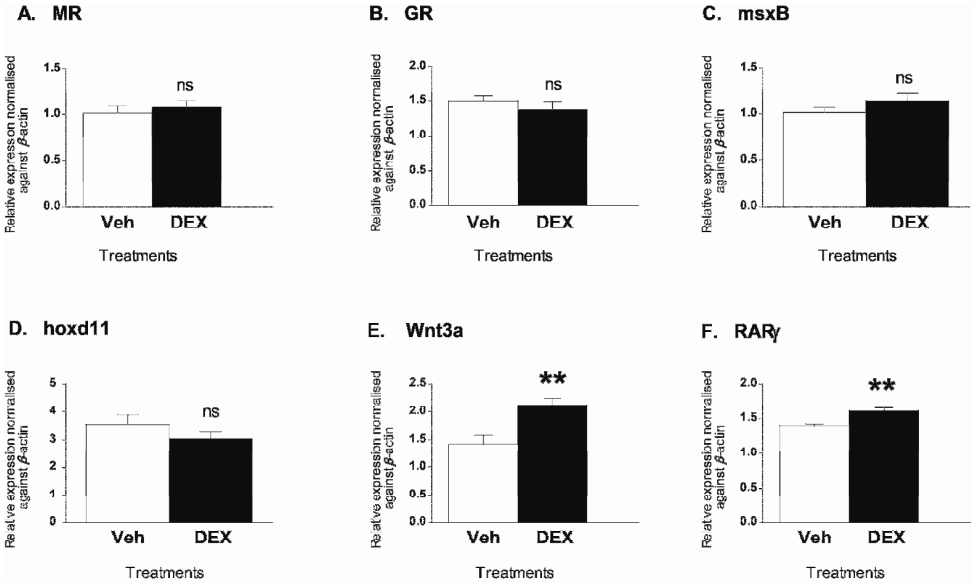

Fig. 5 Column graph showing gene expression relative to β-actin in the regenerated caudal fins of veh and DEX treated zebrafish larvae 24 hpa. Note the significant increase in expression levels of Wnt3a and RARγ in Dex-treated larvae relative to controls.

L-Plastin

We observed a significant decrease in the number of L-plastin positive macrophages/leukocytes in DEX-treated embryos relative to controls at 4 h but not 24 h post amputation (Fig. 6 A) ($p < 0.001$). Interestingly, we also observed that the spatial arrangement of the L-plastin positive cells differed between DEX-treated and control groups at 4 h but not 24 h post amputation. Specifically, confocal image analysis revealed that, while L-plastin positive cells are aligned with the amputation plane in controls, they were rather irregularly distributed across the regenerated area of the caudal fin in DEX-treated embryos (Fig. 6 B).

Experiment 2

To assess if prior history of early-life DEX exposure would also affect tissue repair capacity at later life stages than that tested in experiment 1, we assessed the effect of DEX after initial exposure. Similar to what is observed in

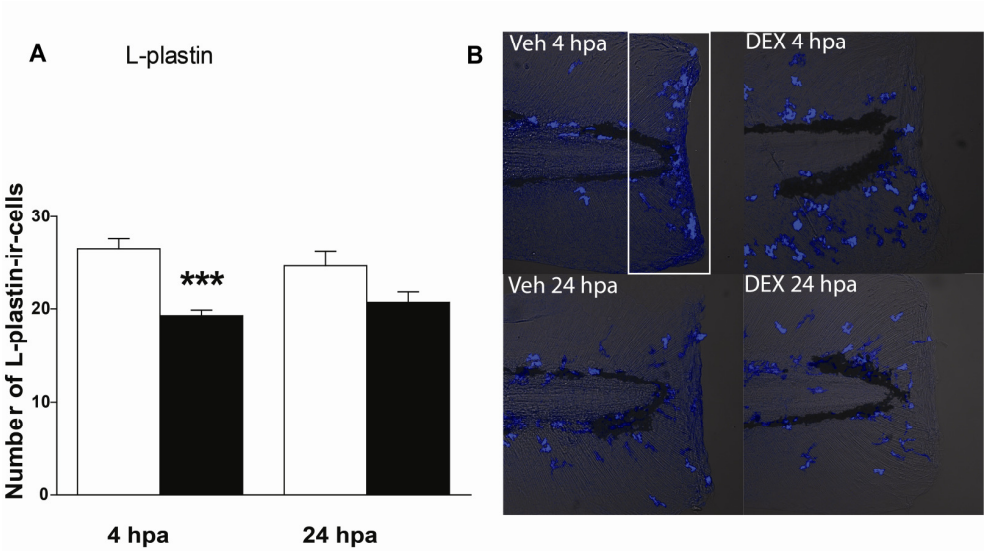

Fig. 6 Graph showing total number of L-plastin immunoreactive (ir) leukocyte cells counted from the area demarcated with a box in panel B. Cells were counted at 4 hpa and 24 hpa in veh and DEX treated larvae. Note the significant decrease in L-plastin positive cell in DEX-treated larvae relative to controls 4hpa but not 24 hpa (although a trend towards a decrease is also observed at 24 hpa). (**B**) Overlay of confocal and transmitted image showing leucocytes (blue cells) in the regenerating caudal fin region in both controls and DEX-treated larvae at both 4 hpa and 24 hpa.

Experiment 1, we also observed that relative to the control group, DEX-treated embryos displayed significant decreases in the total area of the regenerated caudal fin 11 days post exposure to DEX (Fig. 7 A) ($p< 0.5$).

Experiment 3

To assess whether the effects of DEX are permanent or transient, we allowed a longer recovery time following caudal fin amputation and assayed the embryos at 11 days post amputation. We observed that, relative to controls, DEX-treated embryos were no longer significantly different from the control group in terms of size and shape of the total regenerated area of caudal fin at 11 days post amputation (Fig. 7 B).

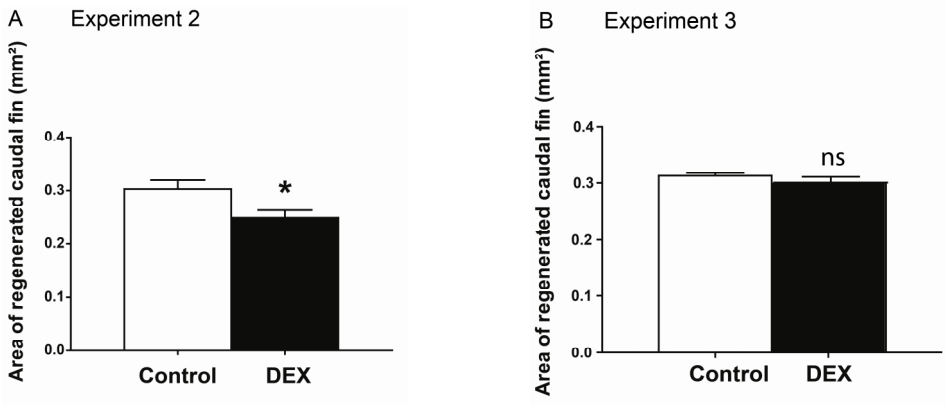

Fig. 7 (**A**) Experiment 2. Graph showing area of regenerated caudal fin in control and DEX-treated larvae amputated after 11 days of initial DEX treatment and allowed to regenerate for 48h. The result show a significant reduction in the are of the regenerated caudal fin in DEX-treated larvae relative to controls. (**B**) Experiment 3. Graph showing the area of the regenerated caudal fin in larvae that were amputated at 3 dpf and allowed to regenerate until 14 dpf. The results show no significant differences in the area of the regenerated caudal fin between controls and DEX-treated larvae suggesting that full recovery occurs despite initial impairment with longer post amputation recovery period.

Discussion

This study investigated the influence of DEX exposure during a sensitive period of development (*prim-6*) on the ability to repair damaged tissue following amputation of the caudal fin in the post-hatching period in larval zebrafish. We report that early-life history of DEX exposure impairs ability to repair and regenerate caudal fin tissue across the first 2 weeks of life, and that significantly longer post-amputation periods are required for full recovery. The possible mechanisms underlying these effects as well as the implication of these results in the field of medicine are discussed below.

Possible mechanisms

The wound healing phase (0-3 hpa)

Analysis of the several outcome measures taken in this study including cell proliferation, cell death (necrosis and apoptosis), gene expression, and

leukocyte cell marker (L-plastin) suggest that DEX exerted its effects in the early phase (4 h) of wound healing rather than in the later phases of the tissue repair process. This is based on our observation of a massive amount of cell death both by necrosis and apoptosis at 4 h post amputation. This cell loss does not appear to have been compensated, at least as far as 24 h post amputation, since cell proliferation was found to be drastically decreased in DEX-treated embryos relative to controls at that time. The large amount of cell death may be responsible for the significant reduction in the number of L-plastin positive/leukocyte cells observed at 4 h but not 24 h post amputation. These results are consistent with previous studies showing significant reductions in immune cell types (e.g. leukocytes) at the injury site few h following acute exposure to synthetic GCs (e.g. DEX) [110,225,226].

Reduction in immune cells at the injury site has important implications for the wound healing phase. Specifically, the invasion of immune cells including leukocytes, macrophages, and neutrophils occurs early (within 4 h) during the wound healing process and is essential for clearance of cell debris and foreign molecules by phagocytosis [250]. It has been shown that alterations in the clearance process may hinder and even prevent subsequent steps to take place (e.g. blastema formation) [251]. Therefore, it is possible that a decrease in the number of immune cell types such as L-plastin positive/leukocytes may have altered the clearance process, which in turn interfered with the initiation of the subsequent steps resulting in impaired tissue repair and regeneration. Following clearance of cell debris, another important function of the immune cells is the secretion of growth factors and cytokines. The presence of sufficient amount of growth factors and cytokines is also essential for the initiation of the blastema formation and its progression [110]. Therefore, it is likely that DEX-induced reduction in the number of L-plastin positive/leukocytes observed in this study may not only have altered the clearance process but also lowered levels of growth factors and cytokines at the injury site. Such events may simultaneously contribute to impede the initiation of the blastema formation and its progression, and results in impaired wound healing.

Interestingly, we also observed an aberrant arrangement (i.e. misalignment with the amputation plane) of the L-plastin positive/leukocytes at the injury site when compared to control situations. These findings suggest that DEX also

affected the migration pattern of immune cells towards the injury site, which may further contribute to delay the initiation of the blastema formation and eventually impair tissue repair. However, the fact that full recovery is possible with longer post amputation period suggests that the molecular components of the immune system are functional but that the natural time course of their actions appears delayed.

The blastema formation (4-24 hpa)

Alterations in gene expression patterns in the early phase of the blastema formation (24 h) reveal that DEX exposure also impedes the natural progression of this phase, although perhaps to a minor extent than the wound healing phase (see above). Specifically, we observed a significant up-regulation of wnt3a and RARγ genes in the DEX treated embryos after 24 h of amputation at the injury site. Both of these genes are actively involved in the Remodelling of the epidermal or blastemal tissue. Retinoic acid is a signalling molecule for vertebrate pattern formation both in developing and regenerating tissue [136]. RARγ mRNA is the prominent RAR transcript found in normal regenerating tissue. RARγ is expressed in the distal ends of blastema of regenerating adult fin tissue [112]. Wnts are secreted glycoprotiens that play an important role in body patterning, cell proliferation, cell differentiation and tumour formation [137]. Wnt signalling plays a role in the maintenance and renewal of stem cells which are cells that help repair the tissue damage [137]. It is possible that up-regulation of these genes may have served the purpose of compensating for the massive cell death and decreased proliferation observed at earlier phases of the wound healing process. However, we did not observed any significant differences between groups in the expression levels for gene coding for cell proliferation marker (msxb and hoxd11). This may be due to our selection of a later time point (24 h) than reported in the literature since a previous study showed an upregulation of these genes at an earlier time point (16-24 h) [117]. Taken together, these findings confirm that the impact of DEX is more prominent in the early phase (4 h) of wound healing and extending to the early phase of the blastema formation (4-24 h) since no further differences were observed between groups in any of the outcome measures studied at 48h post amputation (data not shown).

Possible mediators

A possible mediator of the impairing effects of DEX on the wound healing process may be the immunotoxic properties of DEX on developing organs. For instance, lymphoid organs (spleen and thymus) and lymphocytes have been shown to be particularly sensitive to GCs, especially in immature organisms [230]. A main toxic effect of DEX includes apoptosis of immune cells in thymus and spleen. A significant reduction in the size of both immune organs has been previously reported in response to antenatal DEX exposure in mammal models [229,252]. While both thymus and spleen are not developed before 60 hpf in zebrafish, the caudal hematopoetic tissue (CHT) serves as lymphoid organ in young larvae as early as 24 hpf [253]. Although not measured in the current study, it is possible that a brief exposure to high dose of DEX during early development (*prim-6,* 25 hpf) may have affected the development and/or function of the CHT, which in turn may have impacted the production of immune cells (e.g. macrophages and leukocytes) in the initial phase of wound healing. This possibility is also consistent with our observation of a massive cell death (via apoptosis and necrosis) within 4 h post amputation.

Another possible mediator of the impairing effects of DEX on wound healing may be via DEX effects on GR expression levels. DEX is known (even brief exposure) to cause enhanced activity of the adrenal glands, which causes both lower lymphocytes proliferation response and decrease sensitivity of immune cells to GCs [228-230]. This type of insensitivity is usually related to a down regulation of GR. A reduced sensitivity to GCs has been shown to impair immune processes in several species including humans, and therefore may have contributed to the effects observed in the present study [229,230]. It is noteworthy that GR is expressed on immune cells such as macrophages and leukocytes in fish [110,254]. Since we did not observe any significant changes in both MR and GR expression levels between groups at both 24 h and 48 h post amputation (data not shown), this possibility is unlikely to play a major role in the current study. However, we do not reject the possibility that changes in GR expression levels may exist between groups at the level of certain types of immune cells such as macrophages and leukocytes. This possibility remains to be tested.

Implications

The findings presented here are in agreement with previous studies reporting a link between psychological stress and impaired wound healing in human in adulthood [218,220,221]. Transient psychological stressors, like academic examinations, marital troubles, caring for a sick relative and depression can also slow wound healing [110,218,220,221,228]. Our findings also suggest that not only stress (or stress hormones) experienced in adulthood but also during early-life may influence wound healing at later time points during the lifespan. We provide evidence that DEX exposure during early sensitive periods of development appears to cause permanent alterations in the cellular/molecular immune processes that are involved in the early phase of wound healing in zebrafish. In support to this claim, previous studies have shown that antenatal course of DEX are associated with immediate [255] and lasting alterations of the immune system in later life in rodents, non-human primates, and humans [228-230,256]. The current study extends these findings by showing, for the first time, a similar phenomenon in zebrafish. Our study also provides a demonstration of the immediate functional consequences of a DEX-rendered malfunctioning immune system on tissue repair in the juvenile organisms.

These findings have implications for the field of medicine, especially with regard to the clinical practice consisting of administering antenatal course of DEX to pregnant women at risk for premature delivery. The results obtained in this study contribute to enrich the repertoire of information related to the side effects of such procedure, which are needed by medical authorities to assess the risks/benefits of these extreme intervention methods for the welfare of the developing foetuses and infants.

Future Studies

Further studies are required to assess whether blocking the effect of DEX using pharmacological antagonism or morpholino against GR would have prevented the effects observed in the current study. It may also be possible that the genes selected here may have been up or down-regulated at earlier time than the time points assessed here. Furthermore, whether early-life DEX-induced impairment of wound healing will endure throughout the lifespan remain to be

shown. The results presented in this study argue in favour of this idea since we observed that not only the impairing effects of DEX are observed relatively early (5 dpf) but also at a much later life stage (14 dpf) suggesting that DEX effects on wound healing may endure throughout the lifespan. However, further studies are required to ascertain the last claim.

Concluding Remarks

Our findings are in agreement with the view that GC exposure during early development can influence the embryonic/larval immune system resulting in prolonged effects on the immune response related to functional impairment of tissue repair after hatching. Therefore, similar to other species like rodents and non-human primates, zebrafish larvae also appear particularly sensitive to GC treatment in early development. Therefore, the findings presented in this study support the use of the larval zebrafish as a valid model to study the impact of stress and stress hormone exposure in immature organisms on health risks in later life.

Chapter 6: Summary and Discussion

The aim of this thesis was to investigate the expression, and function of genes associated with Remodelling and regeneration in the zebrafish model species. Since the zebrafish is emerging as a promising low cost and easy to maintain experimental animal model with most of its genome sequence available, it will be very useful to carryout high throughput drug and compound analyses, once specific disease models are established and validated.

Here, we studied the role of cell populations, defined by their expression of markers, in bone regeneration and Remodelling in zebrafish embryos and adult zebrafish scales. We also examined how these processes are disrupted by behavioural stress using the case of zebrafish embryonic caudal fin regeneration. We used mesoporous silica nanoparticles to carry cytokines, known to activate hematopoietic cells into osteoclasts, into tissues of the living embryo. Finally we studied the regeneration of the caudal fin of zebrafish embryos with a special emphasis on the effect of glucocorticoids on regeneration and wound healing. Glucocorticoids in this case mimic stress conditions in the embryos, thus helping understand the effect of early exposure to stress on wound healing and tissue Remodelling.

In chapter 2 we studied the expression of a panel of genes that are associated with bone and tissue Remodelling, namely: *mmp-9*, *cathepsin K, rank* and TRAcP in zebrafish embryos and larvae. Differences in expression were seen between the genes, but there were two identifiable groups based on similarities in expression. The groups were *cathepsin K* and *rank*, on the one hand, and *mmp-9* and TRAcP on the other.

We found strong similarities in the expression of *cathepsin K* and *rank* genes in the larvae as well as in the adult scales. In larvae both these genes were associated with the skeletal structures. In the adult zebrafish scales the *cathepsin K* [168] and *rank* genes are both expressed in the marginal regions. However the scale-margin expression of *cathepsin K*, but not *rank*, was seen in multinucleated cells.

Unlike *cathepsin K* and *rank*, the *mmp-9* and TRAcP expression was neither specifically associated with the pharyngeal arches nor the pectoral fin. The expression of *rank* and *mmp-9* in 1 dpf embryos is interesting as it is found in the site of hematopoietic in the early embryonic stages of zebrafish development such as the ventral blood island and rostral blood island. Previous researchers have argued that TRAcP expression is a definitive marker for active osteoclasts [142]. TRAcP expression was observed in the skeletal structures such as Meckel's cartilage in 5 dpf larvae, but not in larvae younger than this. However, it was strongly expressed in the scattered cells all over the embryos (2-5 dpf) more specifically in the caudal hematopoietic tissue. This TRAcP expression was similar to *mmp-9* expression by *in situ* hybridization in embryos and early larvae.

In cathepsin K GFP transgenic zebrafish embryos, it was found that after a continuous exposure to a combination of dexamethasone (DEX) and vitamin D3, there was a stronger and much clearer expression all over the pharyngeal skeleton in 5 dpf zebrafish embryos, compared to the controls exposed to only egg water. There was also expression in individual scattered cells near the tail region of 5d old embryos. This expression in scattered cells is similar to TRAcP and *mmp-9* expression, and therefore suggests that the TRAcP and *mmp-9* in addition to cathepsin K GFP protein are most probably expressed in the same population of cells which may also be osteoclasts.

In adult scales the *mmp-9,* cathepsin K and TRAcP expression is similar except for additional expression in the radii of the scales in the case of *mmp-9* hybridization. One possibility is that mononucleated cells expressing *mmp-9* in the radii of the scales are non-activated cells of the osteoclast lineage, whereas the multinucleated radial and marginal aggregates are mature osteoclasts. Nonetheless, the fact that marginal, multinucleated cells in the adult scale express *mmp-9*, *cathepsin K* and TRAcP is suggestive of an osteoclastic lineage as we found in other studies recently published for *mmp-9* and TRAcP expression in adult zebrafish scales [42,168,169]. However here we for the first time presented expression of *cathepsin K* in the multinucleated cells and *rank* in the mononucleated cells.

In chapter 3 we used a relatively new drug delivery system (DDS) with the aim of delivering the compounds related to osteoclastogenesis into zebrafish

embryos. We used mesoporous silica nanoparticles (MSNPs) to carry the cytokines MCSF and RANK-L into the living zebrafish embryos. This was to see whether we could activate existing immune cells into TRAcP expressing cells in early larvae, which are not otherwise known to have osteoclasts at that stage.

Before we preceded with osteoclast activation experiments we considered it important to first look at the possible toxicity of MSNPs in the zebrafish embryos, and also to assess the safe concentration of injected particles. Therefore, we tested the toxicity, and capacity for drug delivery, of MSNPs injected into the living zebrafish embryo. We found that there was no significant difference between the toxicity of MSNP injections, and of buffer-only injections, as measured by several parameters (mortality, cell death, gross malformations). Injection of fluorescent MSNPs led to an influx of immune cells at the site of injection that persisted for 2-3 days. However, the same type of influx was also seen in control embryos, suggesting that it is not the MSNPs that are responsible for the immune response, but a reaction of the injection procedure itself. It has previously been shown that trauma to zebrafish embryos (e.g. a fin clip or mechanical wounding with an injection needle) causes an influx of macrophages and neutrophils to the wound site [180-183].

MSNPs are very small in size with a very high surface area, which makes them very attractive systems to carry the drugs. We found no significant toxic effects of injected MSNPs in the living embryos. This means that at low concentrations, MSNPs are very good delivery systems in the whole organism.

We observed very little overlap in expression with confocal imaging of lyz: DsRED2-labeled cells and MSNPs suggesting that very small amount of the particles are actively phagocytosed by neutrophils. With L-plastin immuno-labelling, which stains leucocytes, more overlap with the fluorescent signal of the particles was observed, suggesting that part of the MSNPs may be phagocytosed by immune cells. Other studies have shown that, in the presence of artificially provided essential cytokines like MCSF and RANK-L, immune cells are activated into TRAcP positive osteoclasts [196].

Further work is required to clarify the differentiation status of the TRAcP positive cells. Furthermore, the presence of osteoclast-like cells in zebrafish larvae could lead to a disease model for bone disorders and for the study of

effects, for example, of anti osteoporotic drugs. What is clear from our findings in chapter 3 is that MSNPs can be used for drug or compound delivery in the zebrafish embryo with no excess of gross toxic effects or immune responses attributable to the nanoparticles themselves.

Out of the panel of markers studied in chapter 2 we further investigated the role of genes such as matrix metalloproteinases in chapter 4. These genes are known to be involved in matrix degradation and have been found to be expressed in mammalian osteoclasts. We studied both by *in situ* hybridisation and immunocytochemistry the presence of mononucleated and multinucleated *mmp-9* positive cells on the episquamal side of adult zebrafish (regenerating) scales. Plasma membrane staining and TRAcP–*MMP-9* double staining identified these cells as osteoclasts.

We found an increase in expression of mmp genes, cell abundance, activity of MMPs and hydroxyproline levels during scale regeneration. Together, these results suggest that MMPs and osteoclasts play an important role in scale resorption and Remodelling. It was suggested by our *in situ* hybridisation study that both mono- and multinucleated cells express *mmp-9* transcripts in zebrafish scales. Our finding of mono- and multinucleated osteoclasts, expressing both MMP-9 and TRAcP, provides further insight into the process of scale regeneration.

Our results show that the increase in secreted MMP activity in the medium by means of gelatin zymography correlates with the up-regulation in gene expression during scale regeneration. A significant increase is observed in putative active forms of the two gelatinases. The amount of latent proMMP in the medium remains the same or decreases, indicating that more MMPs are activated.

The inhibition of MMP activity by *in vivo* exposure to the MMP inhibitor GM6001, further underlines the parallels between zebrafish and mammalian MMPs. The release of hydroxyproline from regenerating scales confirms that the scale matrix is indeed degraded during regeneration as a result of Remodelling. Our data suggests that matrix proteolysis is an important function of matrix metalloproteinases during scale regeneration.

In chapter 5 we used a larval zebrafish caudal fin model of generation to investigate the lasting impact of glucocorticoid exposure in early developmental stage on the capacity to regenerate tissue at later time points in life. We report for the first time that a history of glucocorticoid exposure is associated with lasting effects on tissue regenerative capacity in larval zebrafish. These findings are in agreement with previous studies reporting a link between early-life stress and impaired wound healing in human in adulthood.

We found that susceptibility to DEX-induced delay in wound healing/tissue repair is seen not only shortly after injury (i.e. 2 days post caudal fin amputation) but also appear to be an effect that may endure much longer throughout the lifespan, since a similar phenomenon is also observed when injury occurs much later (11 days post caudal fin amputation). Taken together, these findings suggest that DEX exposure during early sensitive periods of development appears to cause permanent alterations in the cellular/molecular immune processes that underlie the early phases of wound healing.

Increased cell death studied by acridine orange and TUNEL labelling suggested that there is significantly higher cell death in the regenerated tissue in the DEX treated larvae as compared to the controls. This increased cell death may be in the immune cells as well as other cells within the blastema tissue. As blastema has pluripotent stem cells in the phases studied here, so it is possible that this aberrant regeneration is a result of increased cell death in the pluripotent stem cells within the blastema. This apoptosis in blastema tissue can be an explanation of restricted tissue regeneration. Future studies are required to assess whether blocking (morpholino or pharmacological antagonism) would have prevented the effects observed here.

Conclusions

- Genes associated with osteoclasts are expressed in early zebrafish embryos (Chapter 2)
- Cells expressing osteoclast markers could be induced by the injection into zebrafish embryos of nanoparticles loaded with cytokines (Chapter 3)

- The same genes are expressed in embryonic, as well as adult contexts (Chapters 2 and 4)
- These cells are involved in adult tissue Remodelling in scale regeneration in zebrafish (Chapter 4)
- Mimicking stress in early life can have a deleterious or delaying effect on the Remodelling or regeneration of tissues in the zebrafish at later stages (Chapter 5)
- The zebrafish could be a useful model for studying the processes involved in bone Remodelling and regeneration (General conclusion from this thesis)

Reference List

1. Spence R, Gerlach G, Lawrence C, Smith C: **The behaviour and ecology of the zebrafish, Danio rerio.** *Biol Rev Camb Philos Soc* 2008, **83:** 13-34.
2. Poss KD, Keating MT, Nechiporuk A: **Tales of regeneration in zebrafish.** *Dev Dyn* 2003, **226:** 202-210.
3. Kimmel CB, Ballard WW, Kimmel SR, Ullmann B, Schilling TF: **Stages of embryonic development of the zebrafish.** *Dev Dyn* 1995, **203:** 253-310.
4. Dahm R, Geisler R: **Learning from small fry: the zebrafish as a genetic model organism for aquaculture fish species.** *Mar Biotechnol (NY)* 2006, **8:** 329-345.
5. Creaser CW: **The technique of handling the zebrafish (*Brachydanio rerio*) for the production of eggs which are favourable for embryological research and are available at any specified time throughout the year.** *Copeia* 1934, **1934:** 159-161.
6. Lieschke GJ, Currie PD: **Animal models of human disease: zebrafish swim into view.** *Nat Rev Genet* 2007, **8:** 353-367.
7. Westerfield M: *The Zebrafish Book, A gude for the laboratory use of zebrafish (Danio rerio)*, 5th edn. Eugen, University of Oregon Press; 2007.
8. Carvalho R, de SJ, Stockhammer OW, Savage ND, Veneman WJ, Ottenhoff TH *et al*.: **A high-throughput screen for tuberculosis progression.** *PLoS One* 2011, **6:** e16779.
9. Wielhouwer EM, Ali S, Al-Afandi A, Blom MT, Olde Riekerink MB, Poelma C *et al*.: **Zebrafish embryo development in a microfluidic flow-through system.** *Lab Chip* 2011, **11:** 1815-1824.
10. Steenbergen PJ, Richardson MK, Champagne DL: **Patterns of avoidance behaviours in the light/dark preference test in young juvenile zebrafish: A pharmacological study.** *Behav Brain Res* 2011, **222:** 15-25.
11. Steenbergen PJ, Richardson MK, Champagne DL: **The use of the zebrafish model in stress research.** *Prog Neuropsychopharmacol Biol Psychiatry* 2010.

12. Champagne DL, Hoefnagels CC, de Kloet RE, Richardson MK: **Translating rodent behavioral repertoire to zebrafish (Danio rerio): relevance for stress research.** *Behav Brain Res* 2010, **214:** 332-342.

13. Brittijn SA, Duivesteijn SJ, Belmamoune M, Bertens LF, Bitter W, de Bruijn JD *et al*.: **Zebrafish development and regeneration: new tools for biomedical research.** *Int J Dev Biol* 2009, **53:** 835-850.

14. Matsuo K, Irie N: **Osteoclast-osteoblast communication.** *Arch Biochem Biophys* 2008, **473:** 201-209.

15. Datta HK, Ng WF, Walker JA, Tuck SP, Varanasi SS: **The cell biology of bone metabolism.** *J Clin Pathol* 2008, **61:** 577-587.

16. Altman R, Asch E, Bloch D, Bole G, Borenstein D, Brandt K *et al*.: **Development of criteria for the classification and reporting of osteoarthritis: Classification of osteoarthritis of the knee.** *Arthritis & Rheumatism* 1986, **29:** 1039-1049.

17. Gough AKS, Emery P, Holder RL, Lilley J, Eyre S: **Generalised bone loss in patients with early rheumatoid arthritis.** *The Lancet* 1994, **344:** 23-27.

18. Yasuda H, Shima N, Nakagawa N, Yamaguchi K, Kinosaki M, Mochizuki S *et al*.: **Osteoclast differentiation factor is a ligand for osteoprotegerin/osteoclastogenesis-inhibitory factor and is identical to TRANCE/RANKL.** *Proc Natl Acad Sci U S A* 1998, **95:** 3597-3602.

19. Lacey DL, Timms E, Tan HL, Kelley MJ, Dunstan CR, Burgess T *et al*.: **Osteoprotegerin ligand is a cytokine that regulates osteoclast differentiation and activation.** *Cell* 1998, **93:** 165-176.

20. Wiktor-Jedrzejczak W, Bartocci A, Ferrante AW, Jr., Ahmed-Ansari A, Sell KW, Pollard JW *et al*.: **Total absence of colony-stimulating factor 1 in the macrophage-deficient osteopetrotic (op/op) mouse.** *Proc Natl Acad Sci U S A* 1990, **87:** 4828-4832.

21. Takeshita S, Kaji K, Kudo A: **Identification and characterization of the new osteoclast progenitor with macrophage phenotypes being able to differentiate into mature osteoclasts.** *J Bone Miner Res* 2000, **15:** 1477-1488.

22. Fujisaki K, Tanabe N, Suzuki N, Kawato T, Takeichi O, Tsuzukibashi O *et al*.: **Receptor activator of NF-kappaB ligand induces the expression of**

carbonic anhydrase II, cathepsin K, and matrix metalloproteinase-9 in osteoclast precursor RAW264.7 cells. *Life Sci* 2007, **80:** 1311-1318.

23. Boyce BF, Yao Z, Xing L: **Osteoclasts have multiple roles in bone in addition to bone resorption.** *Crit Rev Eukaryot Gene Expr* 2009, **19:** 171-180.

24. Witten PE, Huysseune A: **A comparative view on mechanisms and functions of skeletal remodelling in teleost fish, with special emphasis on osteoclasts and their function.** 2009, 315-346.

25. Zelzer E, Olsen BR: **The genetic basis for skeletal diseases.** *Nature* 2003, **423:** 343-348.

26. Witten PE, Hansen A, Hall BK: **Features of mono- and multinucleated bone resorbing cells of the zebrafish Danio rerio and their contribution to skeletal development, Remodelling, and growth.** *J Morphol* 2001, **250:** 197-207.

27. Persson P, Bj+¦rnsson BT, Takagi Y: **Characterization of morphology and physiological actions of scale osteoclasts in the rainbow trout.** *Journal of Fish Biology* 1999, **54:** 669-684.

28. Witten PE, Bendahmane M, bou-Haila A: **Enzyme histochemical characteristics of osteoblasts and mononucleated osteoclasts in a teleost fish with acellular bone (Oreochromis niloticus, Cichlidae).** *Cell Tissue Res* 1997, **287:** 591-599.

29. Lopez E, Mac I, I, Martelly E, Lallier F, Vidal B: **Paradoxical effect of 1,25 dihydroxycholecalciferol on osteoblastic and osteoclastic activity in the skeleton of the eel Anguilla anguilla L.** *Calcif Tissue Int* 1980, **32:** 83-87.

30. Cawston TE, Wilson AJ: **Understanding the role of tissue degrading enzymes and their inhibitors in development and disease.** *Best Pract Res Clin Rheumatol* 2006, **20:** 983-1002.

31. Burrage PS, Brinckerhoff CE: **Molecular Targets in Osteoarthritis: Metalloproteinases and Their Inhibitors.** 2007, **8:** 293-303.

32. Krane SM, Inada M: **Matrix metalloproteinases and bone.** 2008, **43:** 7-18.

33. Everts V, Delaisse JM, Korper W, Niehof A, Vaes G, Beertsen W: **Degradation of collagen in the bone-resorbing compartment**

underlying the osteoclast involves both cysteine-proteinases and matrix metalloproteinases. *J Cell Physiol* 1992, **150:** 221-231.

34. Spessotto P, Rossi FM, Degan M, Di Francia R, Perris R, Colombatti A *et al*.: **Hyaluronan-CD44 interaction hampers migration of osteoclast-like cells by down-regulating MMP-9.** 2002, **158:** 1133-1144.

35. Everts V, Delaisse JM, Korper W, Beertsen W: **Cysteine proteinases and matrix metalloproteinases play distinct roles in the subosteoclastic resorption zone.** *J Bone Miner Res* 1998, **13:** 1420-1430.

36. Everts V, Korper W, Hoeben KA, Jansen ID, Bromme D, Cleutjens KB *et al*.: **Osteoclastic bone degradation and the role of different cysteine proteinases and matrix metalloproteinases: differences between calvaria and long bone.** *J Bone Miner Res* 2006, **21:** 1399-1408.

37. Inoue K, Mikuni-Takagaki Y, Oikawa K, Itoh T, Inada M, Noguchi T *et al*.: **A Crucial Role for Matrix Metalloproteinase 2 in Osteocytic Canalicular Formation and Bone Metabolism.** 2006, **281:** 33814-33824.

38. Bai S, Thummel R, Godwin AR, Nagase H, Itoh Y, Li L *et al*.: **Matrix metalloproteinase expression and function during fin regeneration in zebrafish: Analysis of MT1-MMP, MMP2 and TIMP2.** 2005, **24:** 247-260.

39. McCawley LJ, Matrisian LM: **Matrix metalloproteinases: they're not just for matrix anymore!** 2001, **13:** 534-540.

40. Ortega N, Behonick D, Stickens D, Werb Z: **How Proteases Regulate Bone Morphogenesis.** 2003, **995:** 109-116.

41. Iwamatsu T: **Stages of normal development in the medaka Oryzias latipes.** *Mech Dev* 2004, **121:** 605-618.

42. Nemoto Y, Higuchi K, Baba O, Kudo A, Takano Y: **Multinucleate osteoclasts in medaka as evidence of active bone Remodelling.** *Bone* 2007, **40:** 399-408.

43. Yoong S, O'Connell B, Soanes A, Crowhurst MO, Lieschke GJ, Ward AC: **Characterization of the zebrafish matrix metalloproteinase 9 gene and its developmental expression pattern.** *Gene Expr Patterns* 2007, **7:** 39-46.

44. Janckila AJ, Takahashi K, Sun SZ, Yam LT: **Tartrate-resistant acid phosphatase isoform 5b as serum marker for osteoclastic activity.** *Clin Chem* 2001, **47:** 74-80.

45. Littlewood-Evans A, Kokubo T, Ishibashi O, Inaoka T, Wlodarski B, Gallagher JA *et al*.: **Localization of cathepsin K in human osteoclasts by in situ hybridization and immunohistochemistry.** *Bone* 1997, **20:** 81-86.

46. Theill LE, Boyle WJ, Penninger JM: **RANK-L and RANK: T cells, bone loss, and mammalian evolution.** *Annu Rev Immunol* 2002, **20:** 795-823.

47. Nakashima T, Kobayashi Y, Yamasaki S, Kawakami A, Eguchi K, Sasaki H *et al*.: **Protein expression and functional difference of membrane-bound and soluble receptor activator of NF-kappaB ligand: modulation of the expression by osteotropic factors and cytokines.** *Biochem Biophys Res Commun* 2000, **275:** 768-775.

48. Hsu H, Lacey DL, Dunstan CR, Solovyev I, Colombero A, Timms E *et al*.: **Tumor necrosis factor receptor family member RANK mediates osteoclast differentiation and activation induced by osteoprotegerin ligand.** *Proc Natl Acad Sci U S A* 1999, **96:** 3540-3545.

49. Dougall WC, Glaccum M, Charrier K, Rohrbach K, Brasel K, De ST *et al*.: **RANK is essential for osteoclast and lymph node development.** *Genes Dev* 1999, **13:** 2412-2424.

50. Merck E, Gaillard C, Gorman DM, Montero-Julian F, Durand I, Zurawski SM *et al*.: **OSCAR is an FcRgamma-associated receptor that is expressed by myeloid cells and is involved in antigen presentation and activation of human dendritic cells.** *Blood* 2004, **104:** 1386-1395.

51. Suzuki N, Suzuki T, Kurokawa T: **Suppression of osteoclastic activities by calcitonin in the scales of goldfish (freshwater teleost) and nibbler fish (seawater teleost).** *Peptides* 2000, **21:** 115-124.

52. Yamamoto Y, Yamamoto Y, Udagawa N, Okumura S, Mizoguchi T, Take I *et al*.: **Effects of calcitonin on the function of human osteoclast-like cells formed from CD14-positive monocytes.** *Cell Mol Biol (Noisy -le-grand)* 2006, **52:** 25-31.

53. Katagiri M, Ogasawara T, Hoshi K, Chikazu D, Kimoto A, Noguchi M *et al*.: **Suppression of adjuvant-induced arthritic bone destruction by cyclooxygenase-2 selective agents with and without inhibitory potency against carbonic anhydrase II.** *J Bone Miner Res* 2006, **21:** 219-227.

54. de Vrieze E, Sharif F, Metz JR, Flik G, Richardson MK: **Matrix metalloproteinases in osteoclasts of ontogenetic and regenerating zebrafish scales.** *Bone* **In Press, Corrected Proof**.

55. Kim JM, Min SK, Kim H, Kang HK, Jung SY, Lee SH *et al*.: **Vacuolar-type H+-ATPase-mediated acidosis promotes in vitro osteoclastogenesis via modulation of cell migration.** *Int J Mol Med* 2007, **19:** 393-400.

56. Abe E, Marians RC, Yu W, Wu XB, Ando T, Li Y *et al*.: **TSH is a negative regulator of skeletal Remodelling.** *Cell* 2003, **115:** 151-162.

57. Gates BJ, Das S: **Management of osteoporosis in elderly men.** *Maturitas* 2011.

58. Patsch JM, Deutschmann J, Pietschmann P: **Gender aspects of osteoporosis and bone strength.** *Wien Med Wochenschr* 2011, **161:** 117-123.

59. Sun L, Peng Y, Sharrow AC, Iqbal J, Zhang Z, Papachristou DJ *et al*.: **FSH directly regulates bone mass.** *Cell* 2006, **125:** 247-260.

60. Krane SM: **Identifying genes that regulate bone Remodelling as potential therapeutic targets.** *J Exp Med* 2005, **201:** 841-843.

61. Fitzpatrick LA: **Estrogen therapy for postmenopausal osteoporosis.** *Arq Bras Endocrinol Metabol* 2006, **50:** 705-719.

62. Compston JE: **Sex Steroids and Bone.** *Physiological Reviews* 2001, **81:** 419-447.

63. Rubin MR, Bilezikian JP: **The Role of Parathyroid Hormone in the Pathogenesis of Glucocorticoid-Induced Osteoporosis: A Re-Examination of the Evidence.** *J Clin Endocrinol Metab* 2002, **87:** 4033-4041.

64. Mottaghi P: **Intravenous bisphosphonates for postmenopausal osteoporosis.** *J Res Med Sci* 2010, **15:** 175-184.

65. Barrett R, Chappell C, Quick M, Fleming A: **A rapid, high content, in vivo model of glucocorticoid-induced osteoporosis.** *Biotechnol J* 2006, **1:** 651-655.

66. Kelly HW, Van Natta ML, Covar RA, Tonascia J, Green RP, Strunk RC: **Effect of long-term corticosteroid use on bone mineral density in children: a prospective longitudinal assessment in the childhood Asthma Management Program (CAMP) study.** *Pediatrics* 2008, **122:** e53-e61.

67. Vanderschueren D, Vandenput L, Boonen S, Lindberg MK, Bouillon R, Ohlsson C: **Androgens and bone.** *Endocr Rev* 2004, **25:** 389-425.

68. Tolar J, Teitelbaum SL, Orchard PJ: **Osteopetrosis.** *N Engl J Med* 2004, **351:** 2839-2849.

69. Bollerslev J: **Autosomal dominant osteopetrosis: bone metabolism and epidemiological, clinical, and hormonal aspects.** *Endocr Rev* 1989, **10:** 45-67.

70. Fleming KW, Barest G, Sakai O: **Dental and facial bone abnormalities in pyknodysostosis: CT findings.** *AJNR Am J Neuroradiol* 2007, **28:** 132-134.

71. Edelson JG, Obad S, Geiger R, On A, Artul HJ: **Pycnodysostosis. Orthopedic aspects with a description of 14 new cases.** *Clin Orthop Relat Res* 1992, 263-276.

72. Bale SS, Kwon SJ, Shah DA, Banerjee A, Dordick JS, Kane RS: **Nanoparticle-mediated cytoplasmic delivery of proteins to target cellular machinery.** *ACS Nano* 2010, **4:** 1493-1500.

73. Singh S, Nalwa HS: **Nanotechnology and health safety--toxicity and risk assessments of nanostructured materials on human health.** *J Nanosci Nanotechnol* 2007, **7:** 3048-3070.

74. Medintz IL, Uyeda HT, Goldman ER, Mattoussi H: **Quantum dot bioconjugates for imaging, labelling and sensing.** *Nat Mater* 2005, **4:** 435-446.

75. Caruthers SD, Wickline SA, Lanza GM: **Nanotechnological applications in medicine.** *Curr Opin Biotechnol* 2007, **18:** 26-30.

76. Dobrovolskaia MA, McNeil SE: **Immunological properties of engineered nanomaterials.** *Nat Nanotechnol* 2007, **2:** 469-478.

77. Duncan R, Izzo L: **Dendrimer biocompatibility and toxicity.** *Adv Drug Deliv Rev* 2005, **57:** 2215-2237.

78. Oberdorster G, Oberdorster E, Oberdorster J: **Nanotoxicology: an emerging discipline evolving from studies of ultrafine particles.** *Environ Health Perspect* 2005, **113:** 823-839.

79. Xia T, Kovochich M, Brant J, Hotze M, Sempf J, Oberley T *et al*.: **Comparison of the abilities of ambient and manufactured nanoparticles to induce cellular toxicity according to an oxidative stress paradigm.** *Nano Lett* 2006, **6:** 1794-1807.

80. Smart SK, Cassady AI, Lu GQ, Martin DJ: **The biocompatibility of carbon nanotubes.** *Carbon* 2006, **44:** 1034-1047.

81. Lee HA, Imran M, Monteiro-Riviere NA, Colvin VL, Yu WW, Riviere JE: **Biodistribution of quantum dot nanoparticles in perfused skin: evidence of coating dependency and periodicity in arterial extraction.** *Nano Lett* 2007, **7:** 2865-2870.

82. Reddy GK, Enwemeka CS: **A simplified method for the analysis of hydroxyproline in biological tissues.** *Clin Biochem* 1996, **29:** 225-229.

83. Hardonk MJ, Harms G, Koudstaal J: **Zonal heterogeneity of rat hepatocytes in the in vivo uptake of 17 nm colloidal gold granules.** *Histochemistry* 1985, **83:** 473-477.

84. Renaud G, Hamilton RL, Havel RJ: **Hepatic metabolism of colloidal gold-low-density lipoprotein complexes in the rat: evidence for bulk excretion of lysosomal contents into bile.** *Hepatology* 1989, **9:** 380-392.

85. Nakamura E, Isobe H: **Functionalized fullerenes in water. The first 10 years of their chemistry, biology, and nanoscience.** *Acc Chem Res* 2003, **36:** 807-815.

86. Slowing II, Trewyn BG, Lin VSY: **Mesoporous Silica Nanoparticles for Intracellular Delivery of Membrane-Impermeable Proteins.** *Journal of the American Chemical Society* 2007, **129:** 8845-8849.

87. Rejman J, Oberle V, Zuhorn IS, Hoekstra D: **Size-dependent internalization of particles via the pathways of clathrin- and caveolae-mediated endocytosis.** *Biochem J* 2004, **377:** 159-169.

88. Bar-Ilan O, Albrecht RM, Fako VE, Furgeson DY: **Toxicity assessments of multisized gold and silver nanoparticles in zebrafish embryos.** *Small* 2009, **5:** 1897-1910.

89. George S, Pokhrel S, Xia T, Gilbert B, Ji Z, Schowalter M *et al*.: **Use of a rapid cytotoxicity screening approach to engineer a safer zinc oxide nanoparticle through iron doping.** *ACS Nano* 2010, **4:** 15-29.

90. Oberdorster E: **Manufactured nanomaterials (fullerenes, C60) induce oxidative stress in the brain of juvenile largemouth bass.** *Environ Health Perspect* 2004, **112:** 1058-1062.

91. Nelson SM, Mahmoud T, Beaux M, Shapiro P, McIlroy DN, Stenkamp DL: **Toxic and teratogenic silica nanowires in developing vertebrate embryos.** *Nanomedicine* 2010, **6:** 93-102.

92. Harper S, Usenko C, Hutchison JE, Maddux BLS, Tanguay RL: **In vivo biodistribution and toxicity depends on nanomaterial composition, size, surface functionalisation and route of exposure.** *Journal of Experimental Nanoscience* 2008, **3:** 195-206.

93. Griffitt RJ, Luo J, Gao J, Bonzongo JC, Barber DS: **Effects of particle composition and species on toxicity of metallic nanomaterials in aquatic organisms.** *Environ Toxicol Chem* 2008, **27:** 1972-1978.

94. Klaine SJ, Alvarez PJ, Batley GE, Fernandes TF, Handy RD, Lyon DY *et al*.: **Nanomaterials in the environment: behavior, fate, bioavailability, and effects.** *Environ Toxicol Chem* 2008, **27:** 1825-1851.

95. Akerman ME, Chan WC, Laakkonen P, Bhatia SN, Ruoslahti E: **Nanocrystal targeting in vivo.** *Proc Natl Acad Sci U S A* 2002, **99:** 12617-12621.

96. Saba TM: **Physiology and physiopathology of the reticuloendothelial system.** *Arch Intern Med* 1970, **126:** 1031-1052.

97. Paciotti GF, Myer L, Weinreich D, Goia D, Pavel N, McLaughlin RE *et al*.: **Colloidal gold: a novel nanoparticle vector for tumor directed drug delivery.** *Drug Deliv* 2004, **11:** 169-183.

98. Sadler KC, Krahn KN, Gaur NA, Ukomadu C: **Liver growth in the embryo and during liver regeneration in zebrafish requires the cell cycle regulator, uhrf1.** *Proceedings of the National Academy of Sciences* 2007, **104:** 1570-1575.

99. deVrieze E., Sharif F, Metz JR, Flik G, Richardson MK: **Matrix metalloproteinases in osteoclasts of ontogenetic and regenerating zebrafish scales.** *Bone* 2010.

100. Azuma K, Kobayashi M, Nakamura M, Suzuki N, Yashima S, Iwamuro S *et al*.: **Two osteoclastic markers expressed in multinucleate osteoclasts of goldfish scales.** 2007, **362:** 594-600.

101. Bereiter-Hahn J, Zylberberg L: **Regeneration of teleost fish scale.** 1993, **105A:** 625-641.

102. Bigi A, Burghammer M, Falconi R, Koch MH, Panzavolta S, Riekel C: **Twisted plywood pattern of collagen fibrils in teleost scales: an X-ray diffraction investigation.** *J Struct Biol* 2001, **136:** 137-143.

103. Sire JY, Francoise A, Olivier B, Bourguignon J, Quilhac A: **Scale development in zebrafish (Danio rerio).** 1997, **190:** 545-561.

104. Sire JY, Akimenko M: **Scale development in fish: a review, with description of sonic hedgehog (shh) expression in the zebrafish (Danio rerio).** 2004, **48:** 233-247.

105. Le Guellec D, Zylberberg L: **Expression of Type I and Type V Collagen mRNAs in the Elasmoid Scales of a Teleost Fish as Revealed by In Situ Hybridization.** 1998, **39:** 257-267.

106. Giraud-Guille M: **Twisted plywood architecture of collagen fibrils in human compact bone osteons.** 1988, **42:** 167-180.

107. Sire JY: **The same cell lineage is involved in scale formation and regeneration in the teleost fish Hemichromis bimaculatus.** 1989, **21:** 447-462.

108. de Vrieze E, Metz JR, Hoff JWV, Flik G: **ALP, TRAcP and cathepsin K in elasmoid scales: a role in mineral metabolism?** 2010, **26:** 210-213.

109. Sire JY, Huysseune A, Meunier FJ: **Osteoclasts in teleost fish: Light-and electron-microscopical observations.** *Cell and Tissue Research* 1990, **260:** 85-94.

110. Mathew LK, Sengupta S, Kawakami A, Andreasen EA, Lohr CV, Loynes CA *et al*.: **Unraveling tissue regeneration pathways using chemical genetics.** *J Biol Chem* 2007, **282:** 35202-35210.

111. Poss KD, Nechiporuk A, Hillam AM, Johnson SL, Keating MT: **Mps1 defines a proximal blastemal proliferative compartment essential for zebrafish fin regeneration.** *Development* 2002, **129:** 5141-5149.

112. White JA, Boffa MB, Jones B, Petkovich M: **A zebrafish retinoic acid receptor expressed in the regenerating caudal fin.** *Development* 1994, **120:** 1861-1872.

113. Schebesta M, Lien CL, Engel FB, Keating MT: **Transcriptional profiling of caudal fin regeneration in zebrafish.** *ScientificWorldJournal* 2006, **6 Suppl 1:** 38-54.

114. Lee Y, Grill S, Sanchez A, Murphy-Ryan M, Poss KD: **Fgf signaling instructs position-dependent growth rate during zebrafish fin regeneration.** *Development* 2005, **132:** 5173-5183.

115. Lee Y, Hami D, De VS, Kagermeier-Schenk B, Wills AA, Black BL *et al*.: **Maintenance of blastemal proliferation by functionally diverse epidermis in regenerating zebrafish fins.** *Dev Biol* 2009, **331:** 270-280.

116. Thummel R, Ju M, Sarras MP, Jr., Godwin AR: **Both Hoxc13 orthologs are functionally important for zebrafish tail fin regeneration.** *Dev Genes Evol* 2007, **217:** 413-420.

117. Yoshinari N, Ishida T, Kudo A, Kawakami A: **Gene expression and functional analysis of zebrafish larval fin fold regeneration.** *Dev Biol* 2009, **325:** 71-81.

118. Avaron F, Hoffman L, Guay D, Akimenko MA: **Characterization of two new zebrafish members of the hedgehog family: atypical expression of a zebrafish indian hedgehog gene in skeletal elements of both endochondral and dermal origins.** *Dev Dyn* 2006, **235:** 478-489.

119. Brockes JP, Kumar A: **Appendage regeneration in adult vertebrates and implications for regenerative medicine.** *Science* 2005, **310:** 1919-1923.

120. Stoick-Cooper CL, Moon RT, Weidinger G: **Advances in signaling in vertebrate regeneration as a prelude to regenerative medicine.** *Genes Dev* 2007, **21:** 1292-1315.

121. Kawakami A, Fukazawa T, Takeda H: **Early fin primordia of zebrafish larvae regenerate by a similar growth control mechanism with adult regeneration.** *Dev Dyn* 2004, **231:** 693-699.

122. Kimmel CB, Ballard WW, Kimmel SR, Ullmann B, Schilling TF: **Stages of embryonic development of the zebrafish.** *Dev Dyn* 1995, **203:** 253-310.

123. Donatti TL, Koch VHK, Takayama L, Pereira RMR: **Os glicocorticoides e seus efeitos no crescimento e na mineraliza+º+úo +¦ssea.** *Jornal de Pediatria* 2011, **87:** 4-12.

124. McEwen BS, Biron CA, Brunson KW, Bulloch K, Chambers WH, Dhabhar FS *et al*.: **The role of adrenocorticoids as modulators of immune function in health and disease: neural, endocrine and immune interactions.** *Brain Res Brain Res Rev* 1997, **23:** 79-133.

125. Wick G, Hu YH, Gruber J: **The role of the immunoendocrine interaction via the hypothalamo-pituitary-adrenal axis in autoimmune disease Emphasis on the obese strain chicken model.** *Trends Endocrinol Metab* 1992, **3:** 141-146.

126. Munck A, Naray-Fejes-Toth A: **The ups and downs of glucocorticoid physiology. Permissive and suppressive effects revisited.** *Mol Cell Endocrinol* 1992, **90:** C1-C4.

127. Sapolsky RM: **Stress Hormones: Good and Bad.** *Neurobiology of Disease* 2000, **7:** 540-542.

128. Evans RM: **The Nuclear Receptor Superfamily: A Rosetta Stone for Physiology.** *Mol Endocrinol* 2005, **19:** 1429-1438.

129. Schaaf MJ, Chatzopoulou A, Spaink HP: **The zebrafish as a model system for glucocorticoid receptor research.** *Comp Biochem Physiol A Mol Integr Physiol* 2009, **153:** 75-82.

130. Liapi C CG: **Glucocorticoids.** In *Pediatric Pharmacology*. 2nd edition. Edited by Jaffe SJ AJ. WB Saunders Co, Philadelphia; 1992:466-475.

131. Chrousos GP: **Adrenocorticosteroids and Adrenocortical Antagonists.** In *Basic and Clinical pharmacology*. 10th edition. Edited by Bertram G Katzung. McGraw-Hill Medical; 2007:635-652.

132. Stewart PM: **The adrenal cortex.** In *Williams Textbook of Endocrinology*. 11th edition. Edited by Kronenberg HM MSPKLR. Philadelphia, PA: Saunders; 2008.

133. Durmus M, Karaaslan E, Ozturk E, Gulec M, Iraz M, Edali N *et al*.: **The Effects of Single-Dose Dexamethasone on Wound Healing in Rats.** *Anesthesia & Analgesia* 2003, **97:** 1377-1380.

134. Leibovich SJ, Ross R: **The role of the macrophage in wound repair. A study with hydrocortisone and antimacrophage serum.** *Am J Pathol* 1975, **78:** 71-100.

135. Flammer JR, Rogatsky I: **Minireview: Glucocorticoids in Autoimmunity: Unexpected Targets and Mechanisms.** *Mol Endocrinol* 2011.

136. Kashyap V, Gudas LJ, Brenet F, Funk P, Viale A, Scandura JM: **Epigenomic reorganization of the clustered Hox genes in embryonic stem cells induced by retinoic acid.** *J Biol Chem* 2011, **286:** 3250-3260.

137. Shimizu T, Bae YK, Muraoka O, Hibi M: **Interaction of Wnt and caudal-related genes in zebrafish posterior body formation.** *Dev Biol* 2005, **279:** 125-141.

138. Yokoyama H, Ogino H, Stoick-Cooper CL, Grainger RM, Moon RT: **Wnt/beta-catenin signaling has an essential role in the initiation of limb regeneration.** *Dev Biol* 2007, **306:** 170-178.

139. Poss KD, Shen J, Keating MT: **Induction of lef1 during zebrafish fin regeneration.** *Dev Dyn* 2000, **219:** 282-286.

140. Akimenko MA, Johnson SL, Westerfield M, Ekker M: **Differential induction of four msx homeobox genes during fin development and regeneration in zebrafish.** *Development* 1995, **121:** 347-357.

141. Sims NA, Gooi JH: **Bone Remodelling: Multiple cellular interactions required for coupling of bone formation and resorption.** *Semin Cell Dev Biol* 2008, **19:** 444-451.

142. Witten PE, Huysseune A: **The unobtrusive majority: mononucleated bone resorbing cells in teleost fish and mammals.** *Journal of Applied Ichthyology* 2009, **26:** 225-229.

143. Witten PE, Villwock W: **Bone resorption and bone remodelling in juvenile carp\ Cyprinus carpio L[.** *J[Appl[Ichthyol* 2000, 254-261.

144. Witten PE, Holliday LS, Delling G, Hall BK: **Immunohistochemical identification of a vacuolar proton pump (V-ATPase) in bone-resorbing cells of an advanced teleost species, *Oreochromis niloticus*.** *Journal of Fish Biology* 1999, **55:** 1258-1272.

145. Zapata A, Amemiya CT: **Phylogeny of lower vertebrates and their immunological structures.** *Curr Top Microbiol Immunol* 2000, **248:** 67-107.

146. Witten PE, Huysseune A: **A comparative view on mechanisms and functions of skeletal remodelling in teleost fish, with special emphasis on osteoclasts and their function.** *Biol Rev Camb Philos Soc* 2009, **84:** 315-346.

147. Jilka RL: **Biology of the basic multicellular unit and the pathophysiology of osteoporosis.** *Med Pediatr Oncol* 2003, **41:** 182-185.

148. Hayman AR, Warburton MJ, Pringle JA, Coles B, Chambers TJ: **Purification and characterization of a tartrate-resistant acid**

phosphatase from human osteoclastomas. *Biochem J* 1989, **261:** 601-609.

149. Janckila AJ, Latham MD, Lam KW, Chow KC, Li CY, Yam LT: **Heterogeneity of hairy cell tartrate-resistant acid phosphatase.** *Clin Biochem* 1992, **25:** 437-443.

150. Luukkainen R, Talonen R, Kaarela K, Merilahti-Palo R, Rintala E: **Synovial fluid acid phosphatase in seropositive and seronegative arthritides.** *Clin Exp Rheumatol* 1990, **8:** 63-65.

151. Hayman AR, Bune AJ, Bradley JR, Rashbass J, Cox TM: **Osteoclastic tartrate-resistant acid phosphatase (Acp 5): its localization to dendritic cells and diverse murine tissues.** *J Histochem Cytochem* 2000, **48:** 219-228.

152. Ibbotson KJ, Roodman GD, McManus LM, Mundy GR: **Identification and characterization of osteoclast-like cells and their progenitors in cultures of feline marrow mononuclear cells.** *J Cell Biol* 1984, **99:** 471-480.

153. Baron R, Neff L, Tran VP, Nefussi JR, Vignery A: **Kinetic and cytochemical identification of osteoclast precursors and their differentiation into multinucleated osteoclasts.** *Am J Pathol* 1986, **122:** 363-378.

154. Ballanti P, Minisola S, Pacitti MT, Scarnecchia L, Rosso R, Mazzuoli GF *et al*.: **Tartrate-resistant acid phosphate activity as osteoclastic marker: sensitivity of cytochemical assessment and serum assay in comparison with standardized osteoclast histomorphometry.** *Osteoporos Int* 1997, **7:** 39-43.

155. Zhao Q, Jia Y, Xiao Y: **Cathepsin K: a therapeutic target for bone diseases.** *Biochem Biophys Res Commun* 2009, **380:** 721-723.

156. Hou WS, Li W, Keyszer G, Weber E, Levy R, Klein MJ *et al*.: **Comparison of cathepsins K and S expression within the rheumatoid and osteoarthritic synovium.** *Arthritis Rheum* 2002, **46:** 663-674.

157. Svelander L, Erlandsson-Harris H, Astner L, Grabowska U, Klareskog L, Lindstrom E *et al*.: **Inhibition of cathepsin K reduces bone erosion, cartilage degradation and inflammation evoked by collagen-induced arthritis in mice.** *Eur J Pharmacol* 2009, **613:** 155-162.

158. Ram M, Sherer Y, Shoenfeld Y: **Matrix metalloproteinase-9 and autoimmune diseases.** *J Clin Immunol* 2006, **26:** 299-307.

159. Kini RM, Zhang CY, Tan BK: **Pharmacological activity of the interdomain segment between metalloproteinase and disintegrin domains.** *Toxicon* 1997, **35:** 529-535.

160. Kini RM, Evans HJ: **Structural domains in venom proteins: evidence that metalloproteinases and nonenzymatic platelet aggregation inhibitors (disintegrins) from snake venoms are derived by proteolysis from a common precursor.** *Toxicon* 1992, **30:** 265-293.

161. Wilkinson DG: *In Situ Hybridization: a Practical Approach*. Oxford: Oxford University Press; 1998.

162. Bussmann, Schulte-Merker: **Rapid BAC-selection for Tol2 mediated transgenesis in zebrafish.** *Development* 2011.

163. Germanguz I, Lev D, Waisman T, Kim CH, Gitelman I: **Four twist genes in zebrafish, four expression patterns.** *Dev Dyn* 2007, **236:** 2615-2626.

164. Flores MV, Lam EY, Crosier P, Crosier K: **A hierarchy of Runx transcription factors modulate the onset of chondrogenesis in craniofacial endochondral bones in zebrafish.** *Dev Dyn* 2006, **235:** 3166-3176.

165. Schilling TF, Kimmel CB: **Musculoskeletal patterning in the pharyngeal segments of the zebrafish embryo.** *Development* 1997, **124:** 2945-2960.

166. Du SJ, Frenkel V, Kindschi G, Zohar Y: **Visualizing Normal and Defective Bone Development in Zebrafish Embryos Using the Fluorescent Chromophore Calcein.** *Developmental Biology* 2001, **238:** 239-246.

167. DeLaurier A, Eames BF, Blanco-S+ínchez B, Peng G, He X, Swartz ME *et al*.: **Zebrafish sp7:EGFP: A transgenic for studying otic vesicle formation, skeletogenesis, and bone regeneration.** *genesis* 2010, **48:** 505-511.

168. Azuma K, Kobayashi M, Nakamura M, Suzuki N, Yashima S, Iwamuro S *et al*.: **Two osteoclastic markers expressed in multinucleate osteoclasts of goldfish scales.** 2007, **362:** 594-600.

169. de VE, Sharif F, Metz JR, Flik G, Richardson MK: **Matrix metalloproteinases in osteoclasts of ontogenetic and regenerating zebrafish scales.** *Bone* 2010.

170. Volkman HE, Pozos TC, Zheng J, Davis JM, Rawls JF, Ramakrishnan L: **Tuberculous granuloma induction via interaction of a bacterial secreted protein with host epithelium.** *Science* 2010, **327:** 466-469.

171. Lewis RS, Stephenson SE, Ward AC: **Constitutive activation of zebrafish Stat5 expands hematopoietic cell populations in vivo.** *Exp Hematol* 2006, **34:** 179-187.

172. Warga RM, Kane DA, Ho RK: **Fate mapping embryonic blood in zebrafish: multi- and unipotential lineages are segregated at gastrulation.** *Dev Cell* 2009, **16:** 744-755.

173. Slowing I, Trewyn BG, Lin VS: **Effect of surface functionalization of MCM-41-type mesoporous silica nanoparticles on the endocytosis by human cancer cells.** *J Am Chem Soc* 2006, **128:** 14792-14793.

174. Lin YS, Tsai PJ, Weng MF, Chen YC: **Affinity capture using vancomycin-bound magnetic nanoparticles for the MALDI-MS analysis of bacteria.** *Anal Chem* 2005, **77:** 1753-1760.

175. Lu J, Liong M, Zink J, Tamanoi F: **Mesoporous Silica Nanoparticles as a Delivery System for Hydrophobic Anticancer Drugs.** *Small* 2007, **3:** 1341-1346.

176. Lai CY, Trewyn BG, Jeftinija DM, Jeftinija K, Xu S, Jeftinija S *et al*.: **A mesoporous silica nanosphere-based carrier system with chemically removable CdS nanoparticle caps for stimuli-responsive controlled release of neurotransmitters and drug molecules.** *J Am Chem Soc* 2003, **125:** 4451-4459.

177. Kashiwada S: **Distribution of nanoparticles in the see-through medaka (Oryzias latipes).** *Environ Health Perspect* 2006, **114:** 1697-1702.

178. Brunner TJ, Wick P, Manser P, Spohn P, Grass RN, Limbach LK *et al*.: **In vitro cytotoxicity of oxide nanoparticles: comparison to asbestos, silica, and the effect of particle solubility.** *Environ Sci Technol* 2006, **40:** 4374-4381.

179. Fent K, Weisbrod CJ, Wirth-Heller A, Pieles U: **Assessment of uptake and toxicity of fluorescent silica nanoparticles in zebrafish (Danio rerio) early life stages.** *Aquat Toxicol* 2010, **100:** 218-228.

180. Mathias JR, Dodd ME, Walters KB, Yoo SK, Ranheim EA, Huttenlocher A: **Characterization of zebrafish larval inflammatory macrophages.** *Dev Comp Immunol* 2009, **33:** 1212-1217.

181. Mathias JR, Perrin BJ, Liu TX, Kanki J, Look AT, Huttenlocher A: **Resolution of inflammation by retrograde chemotaxis of neutrophils in transgenic zebrafish.** *J Leukoc Biol* 2006, **80:** 1281-1288.

182. Hall C, Flores MV, Storm T, Crosier K, Crosier P: **The zebrafish lysozyme C promoter drives myeloid-specific expression in transgenic fish.** *BMC Dev Biol* 2007, **7:** 42.

183. Meijer AH, van der Sar AM, Cunha C, Lamers GE, Laplante MA, Kikuta H *et al*.: **Identification and real-time imaging of a myc-expressing neutrophil population involved in inflammation and mycobacterial granuloma formation in zebrafish.** *Dev Comp Immunol* 2008, **32:** 36-49.

184. de Vrieze E, Sharif F, Metz JR, Flik G, Richardson MK: **Matrix metalloproteinases in osteoclasts of ontogenetic and regenerating zebrafish scales.** *Bone* 2010.

185. Spoorendonk KM, Hammond CL, Huitema LFA, Vanoevelen J, Schulte-Merker S: **Zebrafish as a unique model system in bone research: the power of genetics and in vivo imaging.** *Journal of Applied Ichthyology* 2010, **26:** 219-224.

186. Yan YL, Willoughby J, Liu D, Crump JG, Wilson C, Miller CT *et al*.: **A pair of Sox: distinct and overlapping functions of zebrafish sox9 co-orthologs in craniofacial and pectoral fin development.** *Development* 2005, **132:** 1069-1083.

187. Li N, Felber K, Elks P, Croucher P, Roehl HH: **Tracking gene expression during zebrafish osteoblast differentiation.** *Dev Dyn* 2009, **238:** 459-466.

188. Udagawa N, Takahashi N, Akatsu T, Tanaka H, Sasaki T, Nishihara T *et al*.: **Origin of osteoclasts: mature monocytes and macrophages are capable of differentiating into osteoclasts under a suitable microenvironment prepared by bone marrow-derived stromal cells.** *Proc Natl Acad Sci U S A* 1990, **87:** 7260-7264.

189. Collin-Osdoby P, Yu X, Zheng H, Osdoby P: **RANKL-Mediated Osteoclast Formation from Murine RAW 264.7 Cells.** In *Bone Research Protocols*. 80 edition. Edited by Helfrich MH, Ralston SH. Humana Press; 2003:153-166.

190. Ellett F, Pase L, Hayman JW, Andrianopoulos A, Lieschke GJ: **mpeg1 promoter transgenes direct macrophage-lineage expression in zebrafish.** *Blood* 2011, **117:** e49-e56.

191. Cui C BEKZSOvdVMZASHMA: **Infectious disease modeling and innate immune function in zebrafish embryos.** *Methods Cell Biol*, in press.

192. Wang S, Lu W, Tovmachenko O, Rai US, Yu H, Ray PC: **Challenge in understanding size and shape dependent toxicity of gold nanomaterials in human skin keratinocytes.** *Chemical Physics Letters* 2008, **463:** 145-149.

193. Wark M, Ortlam A, Ganschow M, Schulz-Ekloff G, W+¦hrle D: **Monomeric encapsulation of phthalocyanine-dye molecules in the pores of Si-MCM-41 and Ti-MCM-41.** *Berichte der Bunsengesellschaft f++r physikalische Chemie* 1998, **102:** 1548-1553.

194. Fischer HC, Chan WC: **Nanotoxicity: the growing need for in vivo study.** *Curr Opin Biotechnol* 2007, **18:** 565-571.

195. Yamago S, Tokuyama H, Nakamura E, Kikuchi K, Kananishi S, Sueki K *et al*.: **In vivo biological behavior of a water-miscible fullerene: 14C labeling, absorption, distribution, excretion and acute toxicity.** *Chem Biol* 1995, **2:** 385-389.

196. Lorenzo J: **Characterization of osteoclast precursor cells in murine bone marrow.** *J Musculoskelet Neuronal Interact* 2003, **3:** 273-277.

197. Nakatani Y, Kawakami A, Kudo A: **Cellular and molecular processes of regeneration, with special emphasis on fish fins.** 2007, **49:** 145-154.

198. Sire JY, Quilhac A, Bourguignon J, Allizard F: **Evidence for participation of the epidermis in the deposition of superficial layer of scales in zebrafish (Danio rerio): A SEM and TEM study.** 1997, **231:** 161-174.

199. Sire JY, Huysseune A: **Formation of dermal skeletal and dental tissues in fish: a comparative and evolutionary approach.** 2003, **78:** 219-249.

200. OHIRA Y, SHIMIZU M, URA K, Takagi Y: **Scale regeneration and calcification in goldfish Carassius auratus: quantitative and morphological processes.** *Fisheries Science* 2007, **73:** 46-54.

201. Flik G, Fenwick JC, Kolar Z, Mayer-Gostan N, Wendelaar-Bonga SE: **Effects of Low Ambient Calcium Levels on Wholebody Ca2+ Flux Rates and Internal Calcium Pools in the Freshwater Cichlid Teleost, Oreochromis Mossambicus.** 1986, **120:** 249-264.

202. Carragher JF, Sumpter JP: **The mobilization of calcium from calcified tissues of rainbow trout (Oncorhynchus mykiss) induced to synthesize vitellogenin.** 1991, **99:** 169-172.

203. Persson P, Takagi Y, BjÃ¶rnsson BrT: **Tartrate resistant acid phosphatase as a marker for scale resorption in rainbow trout, Oncorhynchus mykiss: effects of estradiol-17Î² treatment and refeeding.** 1995, **14:** 329-339.

204. Mugiya Y, Watabe N: **Studies on fish scale formation and resorption--II. Effect of estradiol on calcium homeostasis and skeletal tissue resorption in the goldfish, Carassius auratus, and the killifish, Fundulus heteroclitus.** *Comparative Biochemistry and Physiology Part A: Physiology* 1977, **57:** 197-202.

205. Suzuki N, Hattori A: **Melatonin suppresses osteoclastic and osteoblastic activities in the scales of goldfish.** 2002, **33:** 253-258.

206. Onozato H, Watabe N: **Studies on fish scale formation and resorption. III. Fine structure and calcification of the fibrillary plates of the scales in Carassius auratus (Cypriniformes: Cyprinidae).** *Cell Tissue Res* 1979, **201:** 409-422.

207. Rice DPC, Kim HJ, Thesleff I: **Detection of gelatinase B expression reveals osteoclastic bone resorption as a feature of early calvarial bone development.** 1997, **21:** 479-486.

208. Takahashi I, Onodera K, Nishimura M, Mitnai H, Sasano Y, Mitani H: **Expression of genes for gelatinases and tissue inhibitors of metalloproteinases in periodontal tissues during orthodontic tooth movement.** 2006, **37:** 333-342.

209. Vaananen KK, Malmi R, Tuukkanen J, Sundquist K, Harkonen P: **Identification of osteoclasts by rhodamine-conjugated peanut agglutinin.** *Calcif Tissue Int* 1986, **39:** 161-165.

210. van de Wijngaert FP, Burger EH: **Demonstration of tartrate-resistant acid phosphatase in un-decalcified, glycolmethacrylate-embedded mouse bone: a possible marker for (pre)osteoclast identification.** *J Histochem Cytochem* 1986, **34:** 1317-1323.

211. Gorissen M, Bernier NJ, Nabuurs SB, Flik G, Huising MO: **Two divergent leptin paralogues in zebrafish (Danio rerio) that originate early in teleostean evolution.** *J Endocrinol* 2009, **201:** 329-339.

212. Pfaffl MW, Tichopad A, Prgomet C, Neuvians TP: **Determination of stable housekeeping genes, differentially regulated target genes and sample integrity: BestKeeper--Excel-based tool using pair-wise correlations.** *Biotechnol Lett* 2004, **26:** 509-515.

213. Bildt MM, Bloemen M, Kuijpers-Jagtman AM, Von den Hoff JW: **Matrix metalloproteinases and tissue inhibitors of metalloproteinases in gingival crevicular fluid during orthodontic tooth movement.** *Eur J Orthod* 2009, **31:** 529-535.

214. Lafleur MA, Hollenberg MD, Atkinson SJ, KnÃ¤uper V, Murphy G, Edwards DR: **Activation of pro-(matrix metalloproteinase-2) (pro-MMP-2) by thrombin is membrane-type-MMP-dependent in human umbilical vein endothelial cells and generates a distinct 63 kDa active species.** 2001, **357:** 107-115.

215. Snoek-van Beurden PA, Von den Hoff JW: **Zymographic techniques for the analysis of matrix metalloproteinases and their inhibitors.** *Biotechniques* 2005, **38:** 73-83.

216. Kessenbrock K, Plaks V, Werb Z: **Matrix Metalloproteinases: Regulators of the Tumor Microenvironment.** 2010, **141:** 52-67.

217. Brittijn SA, Duivesteijn SJ, Belmamoune M, Bertens LF, Bitter W, de Bruijn JD *et al*.: **Zebrafish development and regeneration: new tools for biomedical research.** 2009, **53:** 835-850.

218. Glaser R: **Stress-associated immune dysregulation and its importance for human health: a personal history of psychoneuroimmunology.** *Brain Behav Immun* 2005, **19:** 3-11.

219. Gouin JP, Kiecolt-Glaser JK: **The impact of psychological stress on wound healing: methods and mechanisms.** *Immunol Allergy Clin North Am* 2011, **31:** 81-93.

220. Kiecolt-Glaser JK, Loving TJ, Stowell JR, Malarkey WB, Lemeshow S, Dickinson SL *et al*.: **Hostile marital interactions, proinflammatory cytokine production, and wound healing.** *Arch Gen Psychiatry* 2005, **62:** 1377-1384.

221. Kiecolt-Glaser JK, Marucha PT, Malarkey WB, Mercado AM, Glaser R: **Slowing of wound healing by psychological stress.** *Lancet* 1995, **346:** 1194-1196.

222. Marucha PT, Kiecolt-Glaser JK, Favagehi M: **Mucosal wound healing is impaired by examination stress.** *Psychosom Med* 1998, **60:** 362-365.

223. Godbout JP, Glaser R: **Stress-induced immune dysregulation: implications for wound healing, infectious disease and cancer.** *J Neuroimmune Pharmacol* 2006, **1:** 421-427.

224. Vileikyte L: **Stress and wound healing.** *Clin Dermatol* 2007, **25:** 49-55.

225. Derijk R, Sternberg EM: **Corticosteroid action and neuroendocrine-immune interactions.** *Ann N Y Acad Sci* 1994, **746:** 33-41.

226. Hubner G, Brauchle M, Smola H, Madlener M, Fassler R, Werner S: **Differential regulation of pro-inflammatory cytokines during wound healing in normal and glucocorticoid-treated mice.** *Cytokine* 1996, **8:** 548-556.

227. Lowry SF: **Cytokine mediators of immunity and inflammation.** *Arch Surg* 1993, **128:** 1235-1241.

228. Coe CL, Lubach GR: **Prenatal influences on neuroimmune set points in infancy.** *Ann N Y Acad Sci* 2000, **917:** 468-477.

229. Coe CL, Lubach GR: **Prenatal origins of individual variation in behavior and immunity.** *Neurosci Biobehav Rev* 2005, **29:** 39-49.

230. Coe CL, Lubach GR: **Developmental consequences of antenatal dexamethasone treatment in nonhuman primates.** *Neurosci Biobehav Rev* 2005, **29:** 227-235.

231. Meaney MJ, Szyf M, Seckl JR: **Epigenetic mechanisms of perinatal programming of hypothalamic-pituitary-adrenal function and health.** *Trends Mol Med* 2007, **13:** 269-277.

232. Jobe AH, Soll RF: **Choice and dose of corticosteroid for antenatal treatments.** *Am J Obstet Gynecol* 2004, **190:** 878-881.

233. Trautman PD, Meyer-Bahlburg HF, Postelnek J, New MI: **Effects of early prenatal dexamethasone on the cognitive and behavioral development of young children: results of a pilot study.** *Psychoneuroendocrinology* 1995, **20:** 439-449.

234. Hirvikoski T, Nordenstrom A, Lindholm T, Lindblad F, Ritzen EM, Wedell A *et al*.: **Cognitive functions in children at risk for congenital adrenal hyperplasia treated prenatally with dexamethasone.** *J Clin Endocrinol Metab* 2007, **92:** 542-548.

235. Karemaker R, Karemaker JM, Kavelaars A, Tersteeg-Kamperman M, Baerts W, Veen S *et al*.: **Effects of neonatal dexamethasone treatment on the cardiovascular stress response of children at school age.** *Pediatrics* 2008, **122:** 978-987.

236. Mesquita AR, Wegerich Y, Patchev AV, Oliveira M, Leao P, Sousa N *et al*.: **Glucocorticoids and neuro- and behavioural development.** *Semin Fetal Neonatal Med* 2009, **14:** 130-135.

237. **Effect of corticosteroids for fetal maturation on perinatal outcomes. NIH Consensus Development Panel on the Effect of Corticosteroids for Fetal Maturation on Perinatal Outcomes.** *JAMA* 1995, **273:** 413-418.

238. Yeh TF, Torre JA, Rastogi A, Anyebuno MA, Pildes RS: **Early postnatal dexamethasone therapy in premature infants with severe respiratory distress syndrome: a double-blind, controlled study.** *J Pediatr* 1990, **117:** 273-282.

239. Yeh TF, Lin YJ, Hsieh WS, Lin HC, Lin CH, Chen JY *et al*.: **Early postnatal dexamethasone therapy for the prevention of chronic lung disease in preterm infants with respiratory distress syndrome: a multicenter clinical trial.** *Pediatrics* 1997, **100:** E3.

240. Rastogi A, Akintorin SM, Bez ML, Morales P, Pildes RS: **A controlled trial of dexamethasone to prevent bronchopulmonary dysplasia in surfactant-treated infants.** *Pediatrics* 1996, **98:** 204-210.

241. Dietert RR, Lee JE, Olsen J, Fitch K, Marsh JA: **Developmental immunotoxicity of dexamethasone: comparison of fetal versus adult exposures.** *Toxicology* 2003, **194:** 163-176.

242. Bakker AB, Hoek RM, Cerwenka A, Blom B, Lucian L, McNeil T *et al*.: **DAP12-deficient mice fail to develop autoimmunity due to impaired antigen priming.** *Immunity* 2000, **13:** 345-353.

243. Brockes JP, Kumar A: **Plasticity and reprogramming of differentiated cells in amphibian regeneration.** *Nat Rev Mol Cell Biol* 2002, **3:** 566-574.

244. Akimenko MA, Mari-Beffa M, Becerra J, Geraudie J: **Old questions, new tools, and some answers to the mystery of fin regeneration.** *Dev Dyn* 2003, **226:** 190-201.

245. Shao J, Chen D, Ye Q, Cui J, Li Y, Li L: **Tissue regeneration after injury in adult zebrafish: The regenerative potential of the caudal fin.** *Dev Dyn* 2011.

246. Ohta Y, Ichimura K: **Proliferation markers, proliferating cell nuclear antigen, Ki67, 5-bromo-2'-deoxyuridine, and cyclin D1 in mouse olfactory epithelium.** *Ann Otol Rhinol Laryngol* 2000, **109:** 1046-1048.

247. Etienne W, Meyer MH, Peppers J, Meyer RA, Jr.: **Comparison of mRNA gene expression by RT-PCR and DNA microarray.** *Biotechniques* 2004, **36:** 618-6.

248. van der Hoeven F, Sordino P, Fraudeau N, Izpisua-Belmonte JC, Duboule D: **Teleost HoxD and HoxA genes: comparison with tetrapods and functional evolution of the HOXD complex.** *Mech Dev* 1996, **54:** 9-21.

249. Alsop D, Vijayan MM: **Development of the corticosteroid stress axis and receptor expression in zebrafish.** *Am J Physiol Regul Integr Comp Physiol* 2008, **294:** R711-R719.

250. Xia ZD. Macrophages in degradation of collagen/hydroxylapatite(CHA), beta-tricalcium phosphate ceramics (TCP) artificial bone graft. An in vivo study. Chin.Med.J.(Engl.) 107, 845. 1994.

251. Martin JL, Koodie L, Krishnan AG, Charboneau R, Barke RA, Roy S: **Chronic morphine administration delays wound healing by inhibiting immune cell recruitment to the wound site.** *Am J Pathol* 2010, **176:** 786-799.

252. Sawyer R, Hendrickx A, Osburn B, Terrell T, Anderson J: **Abnormal morphology of the fetal monkey (Macaca mulatta) thymus exposed to a corticosteroid.** *J Med Primatol* 1977, **6:** 145-150.

253. Crowhurst MO, Layton JE, Lieschke GJ: **Developmental biology of zebrafish myeloid cells.** *Int J Dev Biol* 2002, **46:** 483-492.

254. Verburg-van Kemenade BM, Ribeiro CM, Chadzinska M: **Neuroendocrine-immune interaction in fish: Differential regulation of phagocyte activity by neuroendocrine factors.** *Gen Comp Endocrinol* 2011, **172:** 31-38.

255. Zachman RD, Bauer CR, Boehm J, Korones SB, Rigatto H, Rao AV: **Effect of antenatal dexamethasone on neonatal leukocyte count.** *J Perinatol* 1988, **8:** 111-113.

256. Coe CL: **Psychosocial factors and immunity in nonhuman primates: a review.** *Psychosom Med* 1993, **55:** 298-308.

Nederlandse Samenvatting

De levensverwachting van mensen in de Westerse wereld neemt toe en daarmee neemt ook het aantal botziektes zoals osteoporose toe. Door deze toename van botziektes is er onderzoeksgebied ontstaan die oplossingen zoekt om de levensomstandigheden van de patiënten te verbeteren. De studies zijn er meestal op gericht om de botresorptie te verminderen of om de botafzetting te verbeteren. Tijdens deze studies ligt de focus op twee celtypen namelijk de osteoclasten en de osteoblasten. Onder normale en gezonde omstandigheden is er een evenwicht in activiteit van beide celtypen. Ze zorgen beiden voor het behoud van de integriteit van het skelet. Het evenwicht van beide celtypen wordt gedurende het hele leven van een individu instant gehouden door regeneratie van het botweefsel. Wanneer het evenwicht verstoord wordt, kan er boterosie of een overmatige botafzetting plaatsvinden.

Tijdens botontwikkeling en botregeneratie is er een balans tussen botafbraak en botaanmaak. Deze twee processen van botafbraak en botaanmaak worden uitgevoerd door de osteoclasten en de osteoblasten respectievelijk. Tevens staan deze processen onder invloed van verscheidene factoren zoals endocriene hormonen, veroudering en medicatie. Een verstoring in de balans leidt tot botziektes als osteoporosis en osteoarthritits. Al eeuwenlang zijn wetenschappers gefascineerd door het regeneratie vermogen van organismen. Juist in de laatste decennia heeft het vooral aandacht gekregen in de biomedische wereld. Vele vissoorten hebben de mogelijkheid om weefsels en structuren te regenereren zelfs als ze volwassen zijn. De zebravis (Danio rerio) is een beenvis waarvan bekend is dat regeneratie kan plaatsvinden in zowel de larven als in de volwassen vissen. Organen en weefsel van de zebravis die kunnen regenereren zijn onder andere het hart, notochord, lens, retina maar ook structuren als schubben en vinnen.

Wij hebben gedurende deze studie celpopulaties bestudeerd die een rol spelen tijdens botontwikkeling en botregeneratie van de schubben van zebravis embryo’s en volwassen zebravissen. Met behulp van mesoporeuze silica nanodeeltjes konden cytokinen aan verscheidene weefsels van levende embryo’s worden toegediend. Daarnaast hebben we de rol van

metalloproteinases in de osteoclasten bestudeerd tijdens de regeneratie en ontwikkeling van de schubben en vonden dat hun aantal/activiteit was toegenomen tijdens regeneratie. We vonden ook dat er tijdens de ontwikkeling van de schubben multinucleaire osteoclasten aanwezig zijn. Dit in tegenstelling tot de aanwezigheid van mononucleaire cellen tijdens de regeneratie. Als laatste hebben we de effecten van glucocorticosteroiden op de regeneratie van de caudale vin van zebravis embryo's bestudeerd. Hiermee werden stress condities nagebootst in de embryo's waardoor we het effect is van een vroege blootstelling aan stress op de wondgenezing en remodellering van weefsels konden bestuderen.

We hebben laten zien dat genen die geassocieerd zijn met osteoclasten vroeg tot expressie komen tijden de ontwikkeling van zebravis embryo's. Tevens vonden we dat dezelfde genen betrokken zijn bij de remodellering van de schubben tijdens het regeneratie proces van deze schubben. Deze genen komen dus tot expressie in zowel embryo's als in volwassen zebravissen. De expressie van deze osteoclast markers kunnen worden geïnduceerd door injectie van nanodeeltjes geladen met cytokinen. Uit onze observaties kunnen we concluderen dat de zebravis een bruikbaar diermodel is om de processen die betrokken zijn bij botmodellering en botregeneratie te bestuderen. Ook de snelle groei en regeneratie maken dat de zebravis een goed modeldier kan zijn dit in tegenstelling tot de zoogdiermodellen waar dezelfde processen relatief veel langzamer zijn. Het nabootsen van stress gedurende de (vroege) ontwikkeling van de zebravis heeft een schadelijk en vertragend effect op de remodellering en regeneratie van weefsel op latere leeftijd. Echter, meer onderzoek is nodig om te valideren dat zebravis embryo's als diermodel gebruikt kunnen worden om botziektes te bestudere

Acknowledgements

I would like to thank Prof. Dr. Michael K. Richardson for providing this opportunity to conduct PhD research at Leiden University, and for supervising my research during the period of my study. I would also like to thank Dr. Danielle Champagne for her excellent supervision in one of the projects.

I am thankful to the Higher Education Commission of Pakistan (HEC) for providing me this scholarship. I also acknowledge the support of the *SmartMix* Program of the Netherlands Ministry of Economic Affairs and the Netherlands Ministry of Education, Culture and Science.

I am thankful to Dr. P. Crosier (The University of Auckland, Auckland, New Zealand) for providing the Lyz-DsRED2 zebrafish line and Dr. A. Huttenlocher (University of Wisconsin, Madison, USA) for the kind gift of the L-plastin antibody. I am thankful to Dr. Annemarie Meijer for her helpful discussions, and Dr. Alexander Kros for kindly giving us a Tunnel staining kit for use.

I would also like to gratefully acknowledge the unlimited help and support throughout the period of my PhD from Peter Steenbergen, and technical assistance from Merijn de Bakker. I would like to thank Gerda Lamers for her great help and cooperation with confocal imaging. I am thankful to Peter Steenbergen, Davy de Witt and Ulrike Nehldrich, for fish care and maintenance, and their expert technical assistance. I thank Leonie Huitema in Stefan Schulte-Merker's lab for developing the cathepsin K transgenic zebrafish. I also thank Remco de Zwijger for help with imaging, Daisy van der Heijden and Senna van der Heijden for the Western blot, and Hans Von den Hoff for his assistance with MMP zymography and supplying hrMMPs.

I would also like to thank Dr. Nabila Bardine for her company and lunch discussions related to research, Dr Janine Ziermann and Erik Wielhouwer for their helpful discussions, and to the whole group for providing a great working environment.

Acknowledgements

I have no words to express gratitude for my mother Mrs Amtul Rehman for taking extremely good care of my children in Pakistan during the whole period of PhD, and my children Khansa and Abdullah for being so patient and considerate during this temporary, but long term separation from me. I cannot forget the unconditional and endless support of my brother Noaman Sharif and his wife Humaira Noaman. Special thanks to my father Maj. (Retd.) Muhammad Sharif, my elder brother Col. Rizwan Sharif and his wife Faiza Rizwan my dear sister Saema Azhar and her husband Dr M. Jamil Azhar and all of my nephews and nieces for constant support during the whole period of my study. Last but not least I would like to thank my cousin Dr. Faiza Gul for guiding me about doctoral research before I decided to begin my PhD studies.

Curriculum vitae, conference contributions and publications

Curriculum Vitae

I was born on 24 of Nov 1972 in Lahore Pakistan. I finished my high school education from Azam Garrison Girls College Lahore Cantonment Pakistan. I did bachelors from Lahore College for Women University, Lahore Pakistan in 1992 with Botany, Zoology and Geography. I did Masters in Zoology from University of the Punjab, Lahore Pakistan in 1996. During my masters research I worked on the effect of pesticides on the brain cells of *Musca domestica* and published two articles. After finishing Masters, I worked as a science teacher in Garrison Academy for boys Lahore, Pakistan from 1996-1997. Later on, I joined the Education Department, Govt. of the Punjab, Higher Education wing as a lecturer in Biology in 1997. To carry on PhD research I joined the Department of Integrative Zoology, IBL, Leiden in April 2008 as a PhD student on HEC/NUFFIC scholarship. The funding was provided by my home country through the Higher Education Commission of Pakistan (HEC). In future I intend to carry on working as a researcher in developmental or biomedical field.

Conference contributions

1. *Oral communication*
   1st Meeting on Emerging Technologies in Zebrafish, in Bilbao, Spain, 26th November 2009

2. *Poster Presentation*
   Smart Mix Symposium Leiden, 26th February 2010.

3. *Oral communication*
   Department of Oral Cell Physiology, Vrij Universitiet, Amsterdam, 26th April 2010.

4. *Abstract*
   17 Benelux Conference of Zoology Gent, Belgium, October 2010

5. *Poster presentation*
   Smart Mix symposium Leiden, 16th February 2011

6. *Abstract*
   Smart Mix Symposium Leiden, 16th February 2011

7. *Abstract*
   Plenary Session, Chemistry meeting, Eindhoven, The Netherlands, 15th March 2011

8. *Abstract*
   European Materials Research Society (E-MRS) Nice, France, 13th May 2011

9. *Poster presentation*
   7th European Zebrafish Meeting in Edinburgh, UK, 5th – 9th July 2011

Publications and Manuscripts

1. **Matrix metalloproteinases in osteoclasts of ontogenetic and regenerating zebrafish scales**. de Vrieze, E., Sharif, F., Metz, J.R., Flik, G., Richardson, M.K. *Bone*. **48**: 704-712.

2. **Mesoporous silica nanoparticles as a compound delivery system in zebrafish embryos.** Sharif, F., Porta, F., Meijer, A.H., Kros, A., Richardson, M.K. Submitted to *Nanomedicine* (19 July, 2011).

3. **Acute exposure to dexamethasone in early-life is associated with enduring effects on wound healing in zebrafish larvae**
   Sharif,F., Steenbergen, P.J., Richardson,M.K., Champagne, D.L. Submitted.

4. **Osteoclast-like Cells in Early Zebrafish Embryos**
   Sharif,F., de Bakker,M.A.G., Richardson,M.K. Submitted to *Bone.*

5. Effects of Dichlorovos on the brain and fat body cells of the adult *Musca domestica* (MUSCIDAE: DIPTERA). Sharif, F., Ali, F.A. *Punjab University. J. Zool*. **12**: 97-106 (1997).

6. Cellular components of the brain of *Musca domestica* L. (MUSCIDAE: DIPTERA). Sharif, F., Ali, F.A. *Punjab University. J. Zool*. **11**: 57-66 (1996).